Bleb-driven chemotaxis

in *Dictyostelium discoideum*

Evgeny Zatulovskiy

Gonville and Caius College, University of Cambridge

September 2012

This dissertation is submitted to the University of Cambridge for the degree of

Doctor of Philosophy

Preface

The work described here was undertaken in the Cell Biology Division of the Laboratory of Molecular Biology, Cambridge, from October 2008 to September 2012 and was supported by the Herchel Smith Fellowship.

I hereby declare that this dissertation is my own work and contains nothing that is the outcome of work done in collaboration, except where specifically indicated in the text. This work has not been submitted either as a whole or in part for a degree or qualification at the University of Cambridge or any other institution of higher education. This dissertation does not exceed the length limit specified by the Degree Committee for the Faculty of Biology.

Evgeny Zatulovskiy

Acknowledgements

First of all, I would like to thank my supervisor Rob Kay for introducing to me the exciting “Dicty world” and for his kind assistance during the whole four-year period of my work on this PhD project. I am also very grateful to all members of the Kay lab (past and present) – Louise, David, John, Gareth, Marwah, Pako and Roberto – for their keen help and support, and for creating such a nice and inspiring atmosphere. Also our collaborators – Till Bretschneider and Richard Tyson – contributed significantly to my work, both by their help with experimental data processing and valuable discussions.

An outstanding scientific atmosphere of the MRC Laboratory of Molecular Biology and great historical spirit of the Gonville and Caius College made my PhD experience especially remarkable.

Here I also have to thank all my former lecturers from the St Petersburg State Polytechnical University, as well as my first scientific supervisors – Dr. Abramova, Prof. Pospelov, Dr. Skvortsov, and especially, Prof. Ludmila Puchkova – for teaching me valuable skills and scientific way of thinking, which allowed me to join the University of Cambridge and successfully work here.

I would like to thank my family – my Mom, Dad, my brother Kirill and sister Ekaterina – for their invaluable help and patience. Also I am grateful to all my Russian and Cambridge friends – particularly Denis Rubtsov, Maxim Alekseev, Aleksej Besshaposhnikov, Aleksej Shalygin, and of course, Yulia Vasilenko, whose supported is very much appreciated.

Last but not least, I would like to acknowledge the Herchel Smith Fellowship, which made possible my studies in the University of Cambridge.

Table of Contents

Summary

Evgeny Zatulovskiy: **Bleb-driven chemotaxis in *Dictyostelium discoideum***

Migrating cells have two basic ways of extending their leading edge: by dendritic actin polymerization beneath the membrane, or by fluid pressure, which produces blebs. Most cells are believed to move using actin-driven projections, but in more physiological conditions, blebbing motility is also apparent. It has been shown that certain cells even can switch between these two modes of motility, although it is not known how this switch is triggered. Besides, it is unclear whether blebbing can be regulated by chemotactic stimuli, and generally, how blebbing is controlled in the cell.

In this study I employed a popular model organism – *Dictyostelium discoideum* – to investigate the role of blebbing in chemotaxis. Here I confirm that in standard conditions *Dictyostelium* cells move by a combination of F-actin-driven protrusions and blebs. Blebbing is characterized by the rapid projection of hemispherical patches of plasma membrane at 2-4 times the speed of an actin-driven projection, and leaves transient scars of F-actin marking the original cortex in the base of blebs. I demonstrate that *Dictyostelium* cells can adjust their mode of movement according to the conditions: in a resistive environment they switch almost entirely to "bleb mode".

I show that in chemotaxing cells, blebs are mainly restricted to the leading edge, and they often lead the way when a cell is forced to re-orientate. Bleb location appears to be controlled directly by chemotactic gradients. To investigate how chemoattractant induces blebbing, I have screened signal transduction mutants for altered blebbing. I have found that blebbing is unaffected in many chemotactic mutants, but unexpectedly depends on PI3-kinases and two downstream PIP_3-binding proteins of unknown function – PhdA and CRAC.

I conclude that *Dictyostelium* cells move using a hybrid motor in which hydrostatic pressure-driven bleb formation is as important as F-actin-driven membrane extension, and that cells can change the balance between modes as required. I propose that blebbing motility of *Dictyostelium* cells is a direct response to mechanical resistance of environment. More generally, bleb-driven motility may be a '"high-force" mode of movement that is suited to penetrating tissues. Blebs are chemotactic and their induction may involve branches of the chemotactic signal transduction pathway distinct from F-actin regulation.

CHAPTER 1. Introduction

1.1. Cell movement

In this study our interest is largely focused on the mechanisms of cell motility. The processes of cell movement play an important role throughout the whole lifetime of most organisms. From the early stages of embryogenesis, migration of cells orchestrates tissues formation and morphogenesis (Raz, 2003; Ridley et al., 2003). During gastrulation, for example, large groups of cells migrate collectively as sheets to form the resulting three-layer embryo. Subsequently, cells migrate from various epithelial layers to target locations, where they then differentiate to form the specialized cells that make up different tissues and organs (Solnica-Krezel and Sepich, 2012). Similar migration occurs in the adult organisms too. For instance, during the renewal of skin and intestine, fresh epithelial cells migrate up from the basal layer and the crypts, respectively. Migration is also a prominent component of tissue repair and immune surveillance, in which leukocytes from the circulation migrate into the surrounding tissue to destroy invading microorganisms and infected cells and to clear debris (Luster, 1998). Movement of fibroblasts and vascular endothelial cells is also essential for wound healing. On the other hand, in metastasis, tumor cells migrate from the initial tumor mass into the circulatory system, which they subsequently leave and migrate into a new site to form secondary tumours (Lauffenburger and Horwitz, 1996). So, understanding of cell movement mechanisms presents an important biological problem.

1.1.1. Cell movement cycle

Cell movement is a complex process requiring coordinated activity of different components of the cell, including cytoskeleton reorganisation, membrane trafficking and adhesions contacts formation/disassembly. Hence, these cell processes are accurately orchestrated altogether and operate in a cycle (Lauffenburger and Horwitz, 1996; Mitchison and Cramer, 1996).

Generally, the cell motility cycle can be divided into five consecutive steps:

1. extension of the leading edge;
2. adhesion of the leading edge to an extracellular substrate;
3. contraction of the cell body;
4. disassembly of adhesion contacts at the cell rear;
5. recycling of membrane components from the rear to the front of the cell.

This sequence of events provides the locomotory mechanism where the leading edge of the cell forms a protrusion, which attaches to the extracellular substrate in front of the cells and pulls the whole cell body forward. This mechanism is exploited by the majority of studied motile cells, although some exceptions have also been found.

For example, it has been shown that in some cases cells can move through extracellular matrices in an adhesion-independent manner, simply squeezing through a three-dimensional environment (Malawista et al., 2000; Lammermann et al., 2008). Moreover, there has been demonstrated an example of eukaryotic cells, actively swimming in a fluid environment where no rigid substrate was present at all (Barry and Bretscher, 2010).

The speed of cells migration may vary hugely. For instance, fibroblasts and macrophages normally move at just 1 μm per minute, whereas keratocytes, neutrophils and *Dictyostelium cells* migrate much faster and can reach speeds of between 10 and 40 μm per minute (Abercrombie et al., 1970; Cooper and Schliwa, 1986; Kessin, 2001; Keren et al., 2008).

1.1.2. Mechanisms of leading edge extension

Initial expansion of the leading edge is a key step in cell movement. The first studies describing the process of leading edge projection in motile cells were performed more that 40 years ago by Michael Abercrombie. His experiments accurately established the behaviour of the leading edge of fibroblasts, demonstrating how discrete regions of the pseudopodia undergo repetitive cycles of protrusion and retraction, leading to an overall forward displacement of the cell (Abercrombie et al., 1970; Abercrombie et al., 1977).

Further, it became apparent that different cell types could demonstrate different motile behaviours, although the overall cell motility cycle was usually conserved. Mostly, the difference between various cell types was in the shape and the mechanism of their leading edge projection.

For example, it was found that moving fish epidermal keratocytes have a stable fan-like shape (Euteneuer and Schliwa, 1984), and their migration is very persistent and driven by broad, sheet-like F-actin protrusions called lamellipodia (Pollard and Borisy, 2003).

In contrast with the keratocytes, neutrophils and *Dictyostelium* slime mould cells form narrower and thicker protrusions, named pseudopodia, at the leading edge. Their mode of movement is often referred to as amoeboid, since the shape of the cells continuously changes during migration (Abercrombie et al., 1977). While the overall front-to-back polarization of the cell remains stable, the width and length of the pseudopod, as well as the cell's tail, can vary. Pseudopodia can split or form *de novo* from the sides of the cell (Andrew and Insall, 2007). In amoeboid cells phases of cell migration may alternate with transient pauses accompanied by cell polarisation loss.

More recently, studies on primordial germ cells have begun to shed light on the use of hydrostatic pressure as a force for cell movement, in so called "blebbing motility" (Blaser et al., 2006). It was found that embryonic cells of some organisms (Trinkaus, 1973; Jaglarz and Howard, 1995; Blaser et al., 2006), as well as some cancer cells (Keller and Eggli, 1998; Sahai and Marshall, 2003; Wolf et al., 2003) can migrate by forming F-actin free spherical protrusions, named "blebs", at their leading edge. These projections are driven by cytoplasmic flows created by cell cortex contraction. They form when the intracellular pressure tears the cell membrane away from the underlying cortex, and hyaline blisters form on the surface of the cell (Charras, 2008). Blebs are devoid of F-actin cortex during their expansion phase, but later it gets rebuilt.

An alternative mechanism of cell locomotion has been proposed within the membrane flow model of cell movement (Bretscher, 1976; Bretscher, 1984). The central idea of this model is that membrane endocytosed all over the cell surface is preferentially exocytosed at the front of a migrating cell, thus leading to the extension of the front and a rearward flow of membrane in the fluid lipid

bilayer. This flow would then exert a force against the components of the cell attached to the substratum, driving the cell forward. But so far this model has not received sufficient experimental evidence.

Another model (the cortical relaxation model – *(Bray and White, 1988)*) suggests a mechanism where power for movement is supplied by a uniform contraction of the cortex coupled with a discrete region of cortical relaxation. The net result is a tension in the cortex that drives a retrograde flow of cortical elements from the region of relaxation (the cell front) to the region of highest tension (the rear). Consequently, the actin rich cytoplasm is pushed forward into the pseudopod where it contributes to the generation of new cell cortex. Force is exerted against those components linking the actin cytoskeleton and the substratum in the same way.

1.1.3. Mesenchymal and amoeboid modes of migration

Some authors classify the modes of *in vivo* cell migration as either mesenchymal or amoeboid (Kitzing et al., 2007; Jacobelli et al., 2009; Lorentzen et al., 2011; Petrie et al., 2012). In the mesenchymal mode cells usually demonstrate elongated morphology with a well-defined F-actin-rich leading edge and myosin-rich uropod at the rear. These cells migrate by projecting an F-actin driven protrusion at the front, which forms a continuous contact with the substrate (Jacobelli et al., 2009), pulling the cell forward. The myosin II at the back of the cell helps to destroy the old adhesion contacts and retract the cell rear. Also when migrating *in vivo* through the three-dimensional matrices these cells often secrete metalloproteases to destroy the extra-cellular matrix and free some space for cell progression (Sahai and Marshall, 2003).

In amoeboid-like mode of migration cells usually have more rounded morphology and form plasma membrane blebs instead of F-actin protrusions (Kitzing et al., 2007; Lammermann and Sixt, 2009). These cells are able to squeeze their body through the extracellular matrix instead of destroying it (Wolf et al., 2003). Despite having a less elongated morphology, these cells still can be polarized through the localization of certain cytoskeletal (myosin II,

actin) and membrane-to-cortex linking (ezrin) proteins, as well as lipids ($PI(4,5)P_2$) towards cell's rear in order to squeeze the cell and push its content forward (Lorentzen et al., 2011). In this mode, cells form only temporary, discontinuous adhesion foci with the substrate (Jacobelli et al., 2009).

1.1.4. Actin-driven processes at the leading edge

As mentioned above, there are several different modes of cell migration described so far (Ridley, 2011), but at the moment the most studied is the actin-driven method of cell movement. It is based on extending F-actin-rich protrusions at the front of the cell, forming new attachments and then using myosin-driven contraction to pull up the rear of the cell. Many cells have been shown to use this way of locomotion: from a social amoeba *Dictyostelium discoideum* to mammalian neutrophils and fibroblasts. Many aspects of this mechanism are already well understood, and a lot of proteins involved in the regulation of this processes have been characterized (Insall and Machesky, 2009).

Extension of the actin filaments at the leading edge of motile cells is believed to occur by a Brownian ratchet mechanism, such that thermal fluctuations lead to filament bending that allows the insertion of actin monomers onto the growing barbed ends (Mogilner and Oster, 1996). This allows the filament to grow despite being attached to the surface against which it is pushing.

There are several different types of F-actin rich protrusions that can form at the leading edge of migrating cells. They differ in shape, structure of F-actin fibers and regulatory mechanisms. Many chemotactic cells move by projecting protrusions that are called pseudopodia (Insall, 2010). These protrusions are driven by branched F-actin polymerization that pushes against the plasma membrane causing overall cell displacement (Pollard and Borisy, 2003). The rate-limiting step of actin polymerisation is filament nucleation, and this is performed *in vivo* by actin nucleator proteins. The seven-subunit Arp2/3 complex plays the major role in branched actin polymerization. It contains two

actin-like molecules to which an actin monomer is added in order to begin a new filament. Nucleation by this mechanism occurs on the side of pre-existing filaments, thus creating a branched structure, which leads to the formation of wide F-actin protrusions, such as pseudopodia (Insall and Machesky, 2009). The Arp2/3 complex is regulated through interaction with the activating SCAR/WAVE protein complex. Proteins of the SCAR/WAVE family contain the activating VCA domains that can trigger actin polymerisation and several other domains that participate in the regulation of the protein activity either by themselves or through the interaction with other regulatory subunits of the complex. This allows the integration of different signals to determine when and where actin polymerisation should be initiated (Insall and Machesky, 2009).

Another type of actin-based protrusions – lamellipodia – are similar to pseudopods in that Arp2/3-controlled branched F-actin meshworks drive their expansion. But the difference is that these sheet-like protrusions are much broader and less dynamic in the sense that they usually persist for quite a long time. Thus, cells employing this type of projections – for example, fish epidermal keratocytes – have a characteristic arc shape and long straight paths with a high directional persistence (Mogilner and Keren, 2009).

Filopodia represent another type of F-actin projections. They are thin and consist of long parallel bundles of F-actin filaments that are nucleated by the proteins belonging to the family of formins, and especially mDia formins (Mellor, 2010). Formins bind to the barbed ends of actin filaments, preventing their capping and promoting processive filament extension. Formins are intrinsically active proteins, and their regulation mainly occurs through the auto-inhibition achieved by the formation of homodimers, where GBD-DID domain (G-protein Binding Domain, Diaphanous Inhibition Domain) interacts with the DAD domain (Diaphanous Auto-regulation Domain) of the protein to keep it in the closed conformation (Campellone and Welch, 2010). This inhibition is relieved by the interaction of the GBD domain of formins with activated members of the Rho family of small GTPases, such as RhoA, Cdc42 or Rac, allowing actin nucleation and elongation of existing filaments to proceed.

1.2. Plasma membrane blebs and their properties

1.2.1. Involvement of blebs in cell motility

The involvement of plasma membrane blebbing in cell migration has been widely overlooked for a long time. This could be for a number of reasons. Firstly, since blebs were considered to accompany mostly the pathological states of the cell, the experiments where blebs were observed during the normal physiological processes could have been neglected. Secondly, blebs often have a small radius relative to the cell size and in motile cells they seem to be rather dynamic appearing and retracting on the scale of seconds. And since the F-actin cortex quickly rebuilds in blebs during their retraction phase, they could easily by mistaken for pseudopods or other cell projections. But in recent years there have been published a number of papers describing non-apoptotic blebbing in motile cells, and it became apparent that blebs might play an important role in cell migration and chemotaxis (Charras and Paluch, 2008; Fackler and Grosse, 2008).

There are multiple examples of cells migrating *in vivo* and *in vitro* in a blebbing mode. It was convincingly shown, that germ cells of some organisms migrate through the embryo tissues by expanding large blebs on their surface (Trinkaus, 1973; Jaglarz and Howard, 1995; Blaser et al., 2006; Fink, 2007; Tarbashevich et al., 2011). Inhibition of blebbing causes mismigration of such cells (Tarbashevich et al., 2011).

Moreover, blebs have also been found to drive the movement of certain motile cancer cell lines (Keller and Eggli, 1998; Wolf et al., 2003), especially when these cells are invading into three-dimensional matrices and migrating within the tissues (Sahai and Marshall, 2003; Wolf et al., 2003). Such cells can reversibly change their mode of migration from F-actin- to bleb-driven depending on the properties of their environment (Jay et al., 1995; Kitzing et al., 2007; Lorentzen et al., 2011; Petrie et al., 2012). It was shown that switching to blebbing motility enhances the invasive potential of the cells (Nguyen et al., 2000; Wolf et al., 2003), and therefore some types of metastatic tumour cells can

use blebbing to invade into other tissues (Haston and Shields, 1984; Sahai and Marshall, 2003). Further more, blebbing motility is supposed to act as a potential escape mechanism for invasive tumour cells treated with protease inhibitors. Such treatment inhibits the cells ability to lyse the extracellular matrix required for mesenchymal motility, but cells can switch to a bleb-driven mode of migration in order to simply squeeze through the extracellular matrix (Sahai and Marshall, 2003; Wolf et al., 2003). And this might be the reason for the low efficiency of metalloproteases inhibitors in the treatment of such tumours (Friedl and Wolf, 2003). It was found that combined inhibition of extracellular proteases and blebs suppresses the ability of tumour cells to switch between modes of motility and synergise to prevent tumour cell invasion (Sahai and Marshall, 2003).

Healthy cells of adult organisms also can use plasma membrane blebs for their migration. For example, it was found that during skeletal muscle regeneration, satellite stem cells migrate through the basal lamina to the site of myofiber repair by blebbing (Otto et al., 2011). Interestingly, when these cells move on a myofiber itself or on a planar plastic surface they don't produce blebs and migrate by lamellipodia extension, but when they need to pass through the basal lamina they can switch from lamellipodia-based to bleb-driven migration. Such a switch has been shown to significantly increase the speed of their movement. Primary fibroblasts also have been found to switch from lammelipodia to hydrostatic pressure driven migration when placed into three-dimensional cell-derived matrices or dermal explants (Petrie et al., 2012).

It was shown that cells could also be switched to bleb-driven migration by weakening of their cytoskeleton through partial destabilization of either actin filaments (Lammermann and Sixt, 2009) or microtubules (Takesono et al., 2010). Interference with actin cross-linking proteins also may induce blebbing (Cunningham, 1995).

Besides active participation in cell locomotion, blebs can be also involved in the regulation of plasma membrane tension during cell spreading and migration (Norman et al., 2010).

1.2.2. General features of plasma membrane blebs

Blebs are usually defined as hemispherical protrusions on the cell surface that occur when a patch of plasma membrane detaches from its underlying cortex, and this process is normally dependent on myosin II activity. Blebs seem to have been preserved throughout evolution in a variety of organisms.

Usually the development of a bleb proceeds through three consecutive steps: nucleation, growth and retraction or consolidation (Charras, 2008). The first step – bleb nucleation – results either from delamination of plasma membrane from its supporting cortex (Charras et al., 2005) or from the local rupture or weakening of the actin cortex (Boulbitch et al., 2000; Paluch et al., 2005). This process depends on cortical myosin II activity, and there is a critical cortical tension, below which blebs cannot be induced (Tinevez et al., 2009). Besides intracellular pressure, bleb nucleation also depends on membrane-to-cortex adhesion energy and membrane tension (Charras et al., 2008).

Bleb initiation is followed by the second step – bleb expansion. At this step, the cortex-free membrane, locally detached from the underlying cytoskeleton, is blown outward by the flow of cytoplasm. Expanding blebs are devoid of F-actin, but may contain proteins of the erythrocytic submembranous cytoskeleton (such as protein 4.1 and ankyrin) to protect the cell membrane from rupture (Charras et al., 2006). Total cell volume and surface area remain approximately constant during blebbing (Charras et al., 2005), suggesting that expansion is driven by the flow of fluid within the cell rather than water crossing the plasma membrane. Nevertheless, osmolarity of the medium can seriously affect the blebbiness of some cells (Yoshida and Soldati, 2006).

Bleb expansion causes an increase in membrane tension (Dai and Sheetz, 1999), and since membranes can stretch very little (Mohandas and Evans, 1994), a supply of membrane is required for bleb growth. The plasma membrane for blebs may be provided by unfolding of pre-existing membrane wrinkles, or by exocytic fusion of vesicles in the bleb region, or by the flow of lipids into the bleb through its neck, or by the tearing of plasma membrane from the cortex. And apparently, the latter two mechanisms play the major role: lipid flow supplies membrane for the bleb height growth, whereas membrane tearing

from the surrounding regions of the cortex provides bleb area expansion (Charras et al., 2008).

Both bleb initiation and growth are driven by cytoplasmic pressure, which is created through actomyosin contraction. Increasing the intracellular pressure, as well as weakening of membrane-to-cortex association through the depletion of FERM linker proteins, increases the proportion of blebs and their size in zebrafish mesoderm and endoderm germ layer progenitor cells (Diz-Munoz et al., 2010). Conversely, knock-out or inhibition of myosin II activity has been shown to abolish blebbing (Langridge and Kay, 2006; Yoshida and Soldati, 2006; Takesono et al., 2010). Experiments on bleb initiation by laser ablation of the cortex demonstrated that a bleb's final size and peak speed of expansion positively correlate with the cortical tension, which depends on myosin II activity and properties of the actin cortex (Tinevez et al., 2009). Speed of expansion and the final size of a bleb also positively correlate with each other. And both speed, size and occurrence of blebs negatively correlate with the F-actin content in the cell (Cunningham, 1995).

When bleb expansion ceases, the cortex starts to reassemble under the bleb membrane, and the bleb can be either retracted (Charras et al., 2006) or stabilized through the establishment of adhesion contacts with the substrate (Jay et al., 1995). The temporal sequence of proteins recruitment to the membrane during cortex reassembly has been studied in constitutively blebbing filamin-deficient melanoma cells (Charras et al., 2006). It was shown that as soon as bleb expansion ceased, first, the membrane-to-cortex linking FERM domain protein ezrin was recruited to the cell membrane. This was followed by F-actin polymerization under the membrane. The mechanism of this actin nucleation beneath the membrane of blebs remains unclear, as neither Arp2/3 nor mDia were found to localise to the bleb membrane. Possibly, other formins may be involved in this process. The newly rebuilt F-actin cortex provides resistance to the further expansion of the bleb and can play further roles in bleb retraction through the interaction with myosin II or in bleb consolidation through the formation of adhesion foci. Actin recruitment was followed by actin-bundling proteins that rigidify the F-actin meshwork. Then proteins involved in the control of myosin contractility were recruited to the bleb region. And finally,

myosin II localized to discrete foci on bleb membrane to provide the force required for bleb retraction (Charras et al., 2006). In the melanoma cells studied this sequence of events took about two minutes. In parallel with this process of new cortex formation, the old cortical layer, remaining as a scar in the base of a bleb, starts to gradually disassemble and completely dissolves within a few minutes or faster.

It is still unknown what triggers the re-polymerisation of an actin cortex under the membrane of a newly formed bleb and whether such a trigger exists. Two hypotheses have been suggested: either the cortex assembly is constitutive and blebs are devoid of F-actin because their growth outpaces the constitutive cortical assembly or there exists a signal that detects the separation of membrane from the cortex. This signal could be, for example, the exposure of some membrane lipids or integral proteins released from their cytoskeletal interaction partners, the opening of mechanosensitive ion channels in response to bleb growth, or the presence of active Rho GTPases under the membrane of growing blebs (Charras, 2008).

1.2.3. Regulation of blebbing in migrating cells

For blebs to drive cell migration, their formation must be polarized toward one side of the cell (Charras and Paluch, 2008; Fackler and Grosse, 2008). This might be obtained through the localised changes in the cell, namely either a pressure surge (Charras et al., 2005; Blaser et al., 2006), or weakening of membrane-to-cortex adhesion (Boulbitch et al., 2000; Diz-Munoz et al., 2010; Lorentzen et al., 2011), or cortical rupture (Paluch et al., 2005; Tinevez et al., 2009).

Local rupture of cell cortex might be caused, for example, by local actin depolymerisation or depletion of actin-crosslinking proteins.

The hydrostatic pressure within a cell is raised mainly through the up-regulation of myosin II contractile activity. It was shown that in motile primordial germ cells of zebrafish, blebbing is strongly polarized, and this is mediated by chemoattractant through the local activation of myosin II induced

by Ca^{2+} influx (Blaser et al., 2006). An important role of myosin II activation in the mechanism of bleb induction has been demonstrated in many different cell types – from *Dictyostelium* amoeba to human muscular satellite stem cells (Yoshida and Soldati, 2006; Diz-Munoz et al., 2010; Takesono et al., 2010; Otto et al., 2011).

If critical pressure is created within the whole cell, membrane detachment should occur at the sites, where membrane-to-cortex adhesion is the weakest. Thus, bleb formation can be polarized through the regulation of membrane–cytoskeleton interactions (Fackler and Grosse, 2008). Local weakening of membrane-to-cortex adhesion may be achieved in different ways. For example, it has been shown that in melanoma cells, blebbing can be restricted to the front edge through the reinforcement of the cell rear by enrichment with phosphatidylinositol 4,5-bisphosphate ($PI(4,5)P_2$) lipid and consequent recruitment of protein ezrin, as well as F-actin accumulation (Lorentzen et al., 2011). Ezrin belongs to the family of FERM-domain proteins that have both $PI(4,5)P_2$- and F-actin-binding domains to link the plasma membrane with the actin cortex (Raucher et al., 2000). And hydrolysis of $PI(4,5)P_2$ leads to the release of FERM proteins from the membrane (Hao et al., 2009). There are a number of scientific papers demonstrating that depletion of either $PI(4,5)P_2$ (Sheetz, 2001; Wang et al., 2008) or FERM-domain proteins (Diz-Munoz et al., 2010) can reduce the strength of membrane-to-cortex association and increase plasma membrane blebbing. Depletion of available $PI(4,5)P_2$ pool can occur either due to the hydrolysis (Hao et al., 2009), or as a consequence of phosphorylation/dephosphorylation reactions converting it into $PI(3,4,5)P_3$ or PI(5)P (Niebuhr et al., 2002), or may be caused by the sequestration of $PI(4,5)P_2$ by specific PH-domain containing proteins (Raucher et al., 2000). Therefore, local activation of enzymes and other proteins possessing these activities can cause polarized blebbing and therefore may control bleb-driven migration. In some cell types, capable of moving in the bleb mode, disruption of these proteins has been shown to slow down the migration. For example, inhibition of PI3-kinase (enzyme converting $PI(4,5)P_2$ into $PI(3,4,5)P_3$) in zebrafish primordial germ cells slows down their migration (Dumstrei et al., 2004). In mast cells, PI3-kinase and phospholipase C (enzyme

hydrolyzing PI(4,5)P_2) activities are also required for bleb formation (Yanase et al., 2010).

There are some other signaling pathways that may be involved in the bleb regulation as well. In human skeletal muscle satellite stem cells, nitric oxide (NO) and polar cell polarity (PCP) non-canonical Wnt signaling have been discovered to be involved in blebbing migration (Otto et al., 2011). In antigen-stimulated mast cells, bleb size is regulated by the small GTPase ARF6 (Yanase et al., 2010). There have been also found a formin (FMNL1, (Han et al., 2009)) and a kinesin (KIF13B, (Tarbashevich et al., 2011)) that are also involved in bleb formation.

All the described mechanisms are capable of causing a localized blebbing on cell surface. And if these events are polarized towards one side of the cell then bleb-driven cell movement might act as a real alternative to actin-driven motility. So far there is insufficient data about the mechanisms of bleb-driven migration, and the molecular pathways that control blebbing also remain to be investigated.

1.3. Chemotactic cell movement

1.3.1. Chemotaxis and its physiological roles

Chemotaxis is the process of directed cell movement in a chemical gradient. Chemotaxis plays a key role in a number of important biological processes (Eisenbach and Lengeler, 2004; Rappel and Loomis, 2009; Swaney et al., 2010):

- in embryogenesis, chemotaxis drives primordial cells migration through the embryo, controls cells sorting and patterning and tissue development (Armstrong, 1985; Haas and Gilmour, 2006; Richardson and Lehmann, 2010);
- in neural tissue development, extracellular chemical clues control neurons positioning, axon guidance and formation of

appropriate connections (Tessier-Lavigne and Placzek, 1991; Mortimer et al., 2008);

- in immune response, chemokines attract lymphocytes to the sites of infection (Friedl and Weigelin, 2008; Christensen and Thomsen, 2009);
- in wound healing, chemotaxis towards PDGF released by platelets directs fibroblasts migration into the injured regions (Martin and Parkhurst, 2004; Schneider and Haugh, 2006).

Moreover, chemotaxis is involved in the development of certain pathological conditions in the organism – such as tumours metastasis (Condeelis et al., 2005; Roussos et al., 2011), where cancer cells migrate from their tissue of origin towards other organs, and chronic inflammatory diseases (Luster, 1998), where excessive release of cytokines and other chemoattracrants causes unnecessary recruitment of leukocytes and eosinophils to the tissues leading to the inflammation diseases: asthma, atherosclerosis, atopic dermatitis and others.

That is why understanding of mechanisms underlying cellular ability to sense chemical gradients, become polarised and migrate along these gradients represents a significant biological problem, unsolved so far (Swaney et al., 2010).

1.3.2. Machinery of chemotaxis

Chemotaxis is a directed migration of cells towards (positive chemotaxis) or away from (negative chemotaxis) the source of some diffusible chemical compound, which is called a chemoattractant in the case of positive chemotaxis or a chemorepellent in the case of negative chemotaxis. The mechanism providing cells migration along such chemical gradients is conserved from unicellular amoebae to higher eukaryotes and comprises several consecutive but interrelated stages (Kay et al., 2008; Swaney et al., 2010).

First, cells have to sense the chemical compound and compare its concentration at different parts of the cell surface. This process is referred to as

gradient sensing, and it transforms the extracellular gradient of chemoattractant/chemorepellent concentrations into an intracellular gradient of signalling events. It is initiated by cell surface receptors that bind molecules of chemoattractant/chemorepellent, and further the cell compares the occupancy of these receptors over the cell surface, being able to distinguish the differences in the chemical compound concentration as small as only a few percent over the cell length (Mato et al., 1975; Zigmond, 1977).

Further cells have to amplify the directional signal inside the cell and obtain what is called polarisation, when parts of the cell, differently orientated in the chemoattractant/chemorepellent gradient start demonstrating different morphology and behaviour. As a result, the cell forms front and the rear regions. This process is driven by a well-conserved signaling network downstream of the receptors, leading to the polarization of different molecular components of the cell, including lipids as well as proteins.

The third crucial stage in chemotaxis is cell motility. Some cells obtain motile properties only after the chemoattractant stimulation, whereas others are intrinsically motile, and the chemoattractant/chemorepellent gradient only biases the directionality of their migration (Insall, 2010). The machinery of cell migration is also pretty much conserved throughout the evolution, and we will discuss it in more detains further.

All these three processes are tightly interrelated and interdependent: gradient sensing directs cell polarisation, but at the same time different parts of the polarised cell may differently perceive the extracellular signals; formation of the front and rear edges of the cell is important for cell migration, whereas cell migration might affect the process of polarisation.

1.4. *Dictyostelium discoideum* as a model organism to study chemotaxis

In this study we employ *Dictyostelium discoideum* cells to study the involvement of blebs in chemotactic cell movement. *Dictyostelium* is a

unicellular amoeba that is often used as a convenient model organism for various studies on cell motility and chemotaxis.

1.4.1. Basic biology of the Dictyostelium discoideum

Dictyostelium discoideum is a social amoeba living naturally in the soil of the forests and feeding on bacteria and other microorganisms. *Dictyostelia* form a distinct branch of Eukaryotes, separate from the Opisthokonts (which comprises Animals and Fungi), and are a part of the supergroup Amoebozoa (Schaap, 2011). *Dictyostelium discoideum* has historically been the most widely studied species of *Dictyostelia,*

Dictyostelium discoideum (further referred to simply as *Dictyostelium*) naturally hunts bacteria by sensing the products of their metabolism and tracing them by the means of chemotaxis. *Dictyostelium* digests bacteria by a phagocytosis mechanism that is very similar to the one described in the immune cells of higher eukaryotes.

If the food source gets depleted, *Dictyostelium* cells initiate their developmental programme leading to the aggregation of single cells into multicellular structures that further develop to form an “organism” referred to as a fruiting body – *Figure 1.1* (Kessin, 2001). To do this cells start secreting cyclic-AMP molecules that act as a chemoattractant for other *Dictyostelium* cells.

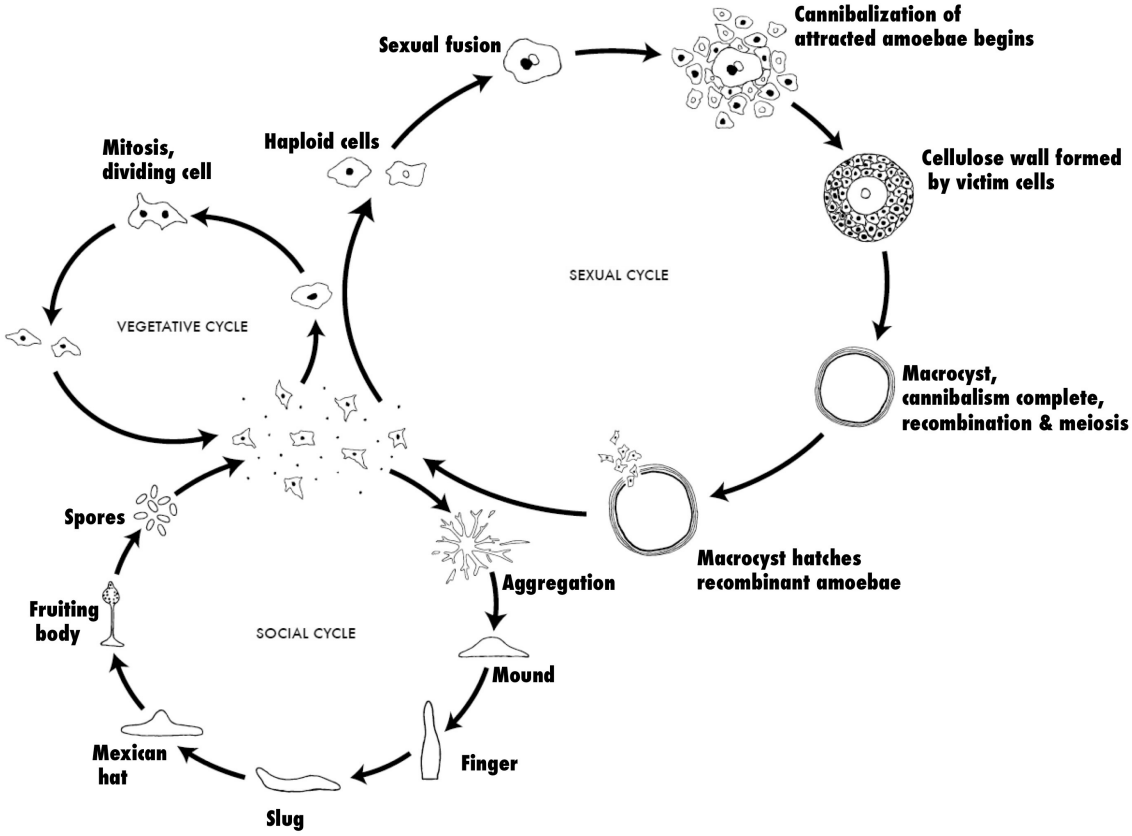

Figure 1.1. **The life cycles of *Dictyostelium discoideum*** (by David Brown and Joan E. Strassmann, image adapted from www.dictybase.org).

In the presence of food source, *Dictyostelium discoideum* exists as haploid amoeba undergoing the vegetative cycle of growth by binary fission. If the food source gets depleted, *Dictyostelium* cells initiate their developmental programme leading to the aggregation of single cells into multicellular structures that further develop into a fruiting body, which consists of stalk and spore cells. During aggregation, the cells attract each other by secreting cyclic-AMP. Alternatively, *Dictyostelium* can also perform a sexual cycle, which begins when two cells of opposite mating types attract each other with cyclic-AMP and fuse to form a diploid zygote. The zygote secretes cyclic-AMP, towards which the surrounding amoebae chemotax and upon arrival become engulfed by the zygote. As a result, macrocyst is formed, which further can hatch and release the progeny of the initial fusion.

So, cells attract each other by producing and sensing the cyclic-AMP gradients. This results in the formation of aggregates containing thousands of *Dictyostelium* cells.

Besides chemotaxis, cyclic-AMP also stimulates transcriptional changes in the cells, and these are required to drive the further developmental program. The aggregates initially form loose mounds, where cells first begin to differentiate. As a result, pre-spore and pre-stalk cells arise within the mound randomly in a characteristic 20:80 ratio. This occurs without any apparent positional information (Kay and Thompson, 2009). Soon after that, cells begin to sort, with pre-stalk cells forming a tip at the top of the mound. Then aggregates progress through several intermediary structures before maturing into a fruiting body. One of the intermediate developmental stages is a multicellular slug that can migrate over long distances in a search for a suitable place to fruit, usually directed by phototaxis and thermotaxis. Triggered by amongst other things, overhead light and a drop in ambient ammonia concentrations, the aggregates become committed to develop into a fruiting body consisting of a large spore head supported by a vacuolated stalk. The stalk is formed by dead cells reinforced with a cellulose wall, and only spores are vital and can give progeny. Therefore, this is a genuine example of altruism demonstrated by cells within a multicellular organism: the pre-stalk cells initiate a cell death program and sacrifice themselves to improve the survival chance of the pre-spore cells (Strassmann et al., 2000). Since spores are resistant to starvation, temperature extremes, desiccation and digestion, the fruiting body provides a temporary solution to the starvation conditions while promoting spore dispersal, prior to the hatching of amoebae and completion of the life cycle. This overall developmental process takes about 24 hours to complete from the onset of starvation.

Besides the described asexual life cycle, *Dictyostelium discoideum* can also perform a sexual cycle that also requires the chemotaxis of cells towards the source of cyclic-AMP (*Figure 1.1*). Each of the *Dictyostelium* cells can belongs to one of the three sexes, referred to as mating types (Bloomfield et al., 2010). The sexual cycle begins when two cells of opposite mating types attract each other with cyclic-AMP and fuse to form a diploid zygote. In a similar manner to asexual

reproduction, the zygote secretes cyclic-AMP towards which the surrounding amoebae chemotax and upon arrival become engulfed by the zygote. Eventually a structure known as a macrocyst is formed, which can remain dormant for many months before an unknown stimulus triggers hatching to take place, releasing the progeny of the initial fusion.

1.4.2. Advantages of Dictyostelium as a model organism

Dictyostelium discoideum is widely used in many laboratories all over the world as a model organism for studying various biological processes (Annesley and Fisher, 2009). While demonstrating many biological features well conserved in higher eukaryotes, *Dictyostelium* cells have some advantageous characteristics making them a convenient model for the research in corresponding fields.

Advantages of *Dictyostelium discoideum* include:

- *Ease of cultivation. Dictyostelium* cells proliferate successfully at room temperature, having an optimum temperature diapason of +21 – +25 °C. They do not require a supply of CO_2 or foetal serum for their growth. Although wild isolates of *Dictyostelium* can grow only in association with bacteria, strains have been isolated in the laboratory that are able to grow in a simple defined media, allowing growth on tissue culture plates, in shaken suspension and on bacterial lawns. Depending on how exactly the cells are grown, doubling times can vary between 4 and 12 hours, allowing large populations of cells to be grown up fairly rapidly. For storage, *Dictyostelium* can either be kept frozen in liquid nitrogen, or spores can be collected and stored in silica gel.
- *Genetic tractability*. The full genome sequencing of *Dictyostelium discoideum* was completed in 2005 and many genes have been annotated (Eichinger et al., 2005). All these resources are now easily accessible through the online

database (*http://www.dictybase.org*). *Dictyostelium* cells have a haploid genome, and therefore genetic manipulations such as gene disruption or replacement can be easily performed by homologous recombination.

- *A set of molecular and cell biological techniques developed for use in Dictyostelium*. These range from restriction enzyme-mediated insertional mutagenesis (REMI) screens (Kuspa, 2006) and expression of tagged proteins using either integrative or replicative plasmids to different microscopy techniques and chemotaxis assays. Cell-type specific, and inducible expression techniques are also all available.
- *Relative simplicity*. Since many key cellular pathways are well conserved in *Dictyostelium,* most (if not all) of their components are present there, but many of them have fewer paralogs in *Dictyostelium*. Furthermore, often there is less redundancy in molecular pathways acting in *Dictyostelium*. And therefore, these two features allow the unwinding of the complex molecular networks present in eukaryotic cells and to define the functions of the proteins involved. Furthermore, responses of *Dictyostelium* cells to various extracellular cues may also be less complicated, and thus environmental conditions and stimuli can be better controlled for these cells and the responses analysed.

These advantages in a combination with unique biological features of *Dictyostelium discoideum*, proved it as a valuable model for research in a diverse range of fields including phagocytosis, cell signalling, DNA-repair, host-pathogen interactions, proteins biosynthesis, development, population evolution, membrane dynamics, self-organisation, vesicle trafficking, and, of course, chemotaxis.

One of the best-explored aspects of *Dictyostelium* biology is its ability to chemotax. In the presence of bacteria, *Dictyostelium* cells live in a vegetative state, and chemotaxis allows them to forage on bacteria by following the gradients of folic acid released by bacterial cells. Upon starvation, *Dictyostelium*

cells become chemotactic to cyclic-AMP. And self-propagating periodic waves of secreted cyclic-AMP allow them to find each other and undergo either sexual or asexual cycle. During their migration, *Dictyostelium* cells can exploit a whole range of possible cell protrusions: lamellipodia (Asano et al., 2004), blebs (Yoshida and Soldati, 2006), pseudopodia and filopodia (Kay et al., 2008). They can favour one or another type of projections depending on their developmental stage and properties of the environment.

At the moment, *Dictyostelium discoideum* remains probably the most popular and powerful model for studying the features and molecular pathways of chemotaxis. It allowed identification of multiple genes involved in the process and improved an overall understanding of organization and features of this phenomenon. In the laboratory, *Dictyostelium* chemotaxis to cyclic-AMP can be studied after making cells aggregation-competent. This is achieved by a combination of starvation in a nutrient-free buffer and periodic pulses with cyclic-AMP, once every six minutes. After four to six hours of pulsing, cells are harvested and their response to chemoattractant can be analysed either by placing them in a gradient of cyclic-AMP, which can be generated in special devices, such as the Dunn chamber, gradient-generating microfluidics device or a micropipette, or by uniformly stimulating the cells with a single dose of chemoattractant.

1.4.3. Chemotactic signalling in Dictyostelium cells

Chemotaxis signaling in *Dictyostelium* is in many aspects similar to certain higher eukaryote cells (e.g. mammalian leukocytes) and represents a network of signaling components that besides linear relations of activation/inhibition also exhibits such complex features as redundancy, crosstalk and feedback regulation – *Figure 1.2* (Swaney et al., 2010).

Chemotactic signalling starts from the binding of the chemoattractant molecule to its receptor on the surface of the cell. *Dictyostelium discoideum* has four cAR receptors (cAR1-4) that interact with cyclic-AMP. The most important

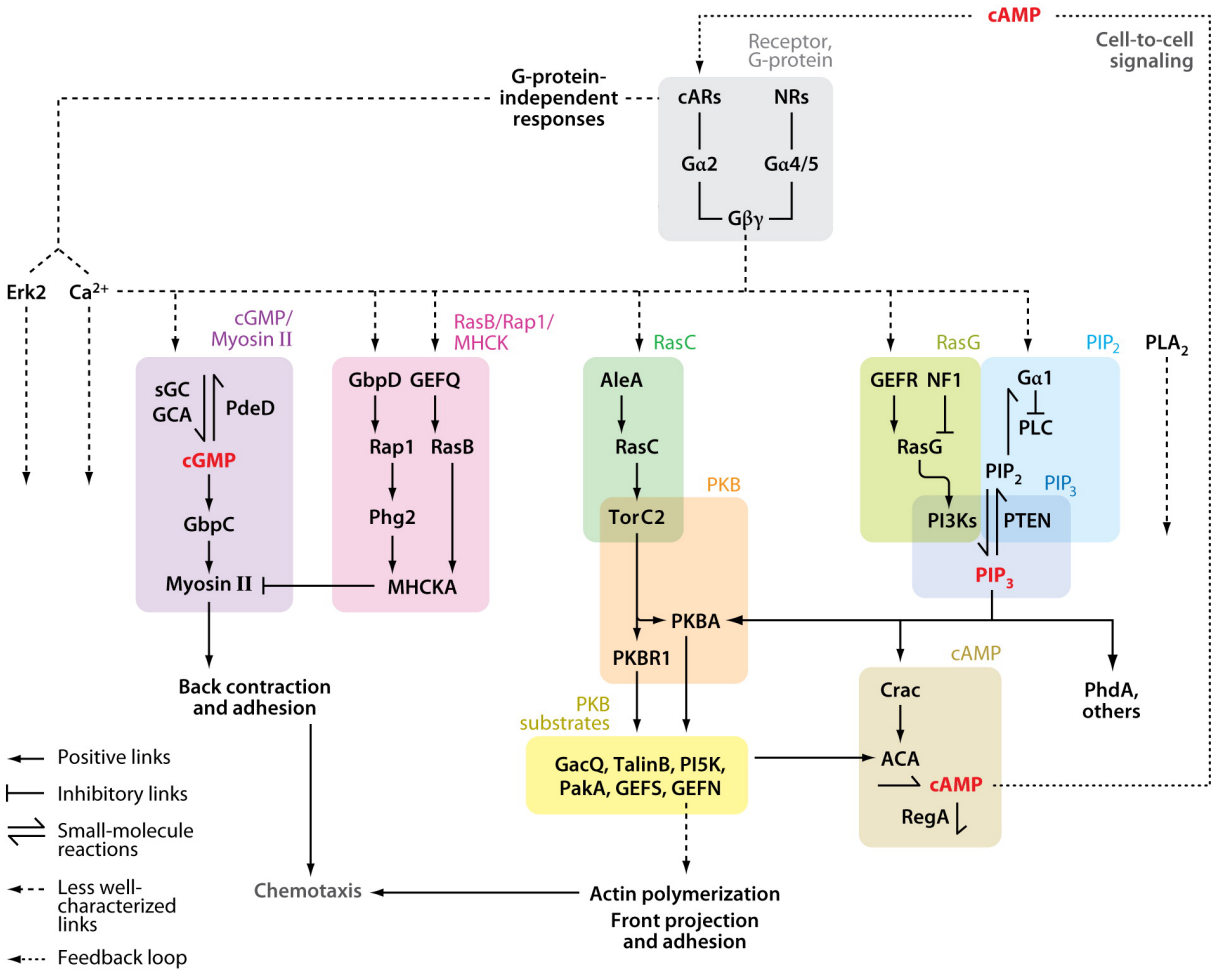

Figure 1.2. **Chemotactic signalling in *Dictyostelium discoideum*** (image adapted from Swaney, Huang et al. 2010).

Chemoattractant cyclic-AMP is perceived by G-protein coupled receptors (cARs) on the cell surface that further activate multiple signalling pathways inside the cell leading to actin polymerisation, myosin contraction and other processes providing overall cell migration.

for chemotactic signalling is the cAR1 receptor. During *Dictyostelium* development its expression peaks at around four hours after the onset of starvation, and the majority of the cyclic-AMP response are mediated by this receptor. Nevertheless, the cAR1 null cells still have some residual response to high doses of cyclic-AMP, and this is believed to be the result of signalling through cAR3, since a double knock-out of both of these proteins causes a complete loss of cyclic-AMP-induced signalling (Insall, Soede, et al., 1994). Cyclic-AMP receptors belong to the class of G-protein coupled receptors. There are 14 Gα subunits in *Dictyostelium,* and only one Gβ and one Gγ. Both cAR1 and cAR3 receptors couple to the same heterotrimeric G protein – Gα2βγ. Deletion of either Gα2 or Gβ, or overexpression of a dominant negative Gγ causes the loss of cyclic-AMP-induced signalling (Kumagai et al., 1991; Wu et al., 1995; Zhang et al., 2001) and consequently a loss of chemotaxis. Binding of cyclic-AMP with its receptor causes the dissociation of Ga2 from Gβγ subunits (Janetopoulos et al., 2001). In gradients of cyclic-AMP, the Gβ subunits form a shallow gradient, concentrating at the leading edge of the cell (Jin et al., 2000). It is supposed that Gβ subunit mediates most of the consequent cyclic-AMP induced events in the cell.

It is usually considered that there are at least four branches of chemotactic signalling downstream of the G-protein (Veltman et al., 2008; Swaney et al., 2010). For a long time it was believed that the main chemotactic compass defining the direction of cell's chemotactic movement is provided by a steep accumulation of $PI(3,4,5)P_3$ lipid at the leading edge. This process is driven by PI3-kinases (PI3Ks) that get activated at the leading edge through RasC-mediated mechanism and convert $PI(4,5)P_2$ into $PI(3,4,5)P_3$, and by PTEN phosphatase that accumulates at the rear part of the cell and performs the reverse reaction (Funamoto et al., 2002; Iijima and Devreotes, 2002). $PI(3,4,5)P_3$ recruits a subset of PH-domain proteins to the leading edge of the cell, and this is somehow involved in the leading edge progression (Zhang et al., 2010).

The production of a mutant in which all five PI3Ks and PTEN had been disrupted gave unexpected results, since it was able to respond to the chemotactic gradients almost as efficiently as wild type cells (Hoeller and Kay,

2007). This discovery suggested that there must exist some other parallel pathways that direct cell migration.

A search for such alternative pathways revealed the phospholipase A_2 (PLA_2) as a possible component complementing the PI3-kinases suppression. It was found that when either PI3Ks or PLA_2 were disrupted alone (genetically or pharmacologically) there was no major chemotactic phenotype, however when disrupted together, cells had severe problems in gradient sensing (Chen et al., 2007). Further pharmacological studies supported this finding, and also suggested that PLA_2 was dependent on calcium signalling via the IP_3 receptor homologue, IplA (van Haastert et al., 2007).

IP_3 can be produced in the cells by another cyclic-AMP activated protein – phospholipase C (PLC) that also affects the phosphoinositides turnover in the cell by hydrolysing $PI(4,5)P_2$ to produce soluble IP_3 and diacyl glycerol (Bominaar et al., 1994). There is only one PLC gene in *Dictyostelium* and the corresponding protein has been shown to be expressed at all stages of development, and its enzymatic activity is activated by chemoattractant (Drayer and van Haastert, 1992).

Another cyclic-AMP activated signalling mechanism discovered in *Dictyostelium* is the TORC2-mediated pathway. TORC2 (TOR-complex 2) is the *Dictyostelium* ortholog of mTORC2. The TOR-complex 2 consists of four proteins: Tor, the ortholog of mTOR; PiaA (or pianissimo), the ortholog of Rictor; RipA, the ortholog of mSin1; and Lst8, whose human ortholog has the same name. The subunits of this complex have all been previously shown to play an important role in chemotaxis (Lee et al., 2005). TORC2 is activated by the small GTPase RasC. TORC2 appears to interact with RasC directly, presumably via the Ras binding domain of the RipA subunit. RasC is activated by a complex that contains two RasGEFs (Aimless and Ras GEFH), protein phosphatase 2A and PHR (a PH domain-containing protein), which are brought together through the interaction with the newly identified scaffolding protein, Sca1. The Sca1 complex translocates to the plasma membrane in a cyclic-AMP dependent manner. When at the membrane, this complex is able to activate RasC and hence initiate downstream signalling via TORC2 and PKB/PKBR1 (Charest et al., 2010).

TORC2 activates the *Dictyostelium* orthologs of the mammalian Protein Kinase B (PKB/Akt) – kinases PKB and PKBR1. *Dictyostelium* PKB contains a PI(3,4,5)P_3-binding PH-domain that provides its recruitment to the leading edge of the cells moving in a gradient of cyclic-AMP (Meili et al., 1999). PKBR1 does not contain a PH-domain but it is myristoylated and therefore constitutively positioned at the plasma membrane (Meili et al., 2000). Therefore, both PI3-kinases and TORC2 are required for the activation of PKB, whereas PKBR1 can be activated solely by TORC2. And overlapping functions of PKB and PKBR1 could partially explain the mild chemotactic phenotype of PI3Ks null cells compared to the PKB/PKBR1 double null strain.

Similarly to mammalian kinase PKB/Akt, *Dictyostelium* orthologs PKB and PKBR1 are activated through the phosphorylations at two key sites: TORC2 phosphorylates their hydrophobic motif, and phosphoinositide-dependent kinases PdkA and PdkB perform the phosphorylation at the activation loop (Kamimura et al., 2008; Kamimura and Devreotes, 2010). Activity of the Pdk kinases is controlled through their recruitment to the plasma membrane by PI(3,4,5)P_3, which leads to their co-localisation with the substrate (Currie et al., 1999). Such relocalisation of both PKB and Pdk proteins to the membrane is induced by the cyclic-AMP signalling.

Activation of the PKB and PKBR1 kinases leads to the phosphorylation of a subset of their substrates, and this seems to up-regulate actin polymerization at the leading edge of chemotaxing cells by some not fully elucidated mechanism, probably through the modulation of SCAR/WAVE complex activity.

Cyclic-AMP stimulation also activates two guanylyl cyclases – one soluble (sGC) and one membrane bound (GCA). These enzymes synthesize cyclic-GMP in a response to chemoattractant stimulation (Roelofs and Van Haastert, 2002). Loss of these proteins causes only a mild chemotactic phenotype, however this phenotype is reported to become more severe when both PLA_2 and PI3K are also inhibited (Veltman et al., 2008), once again confirming the redundancy in the chemotactic signalling.

The main downstream effector of cyclic-GMP is the cyclic-GMP binding protein C (GbpC). GbpC is involved in myosin regulation at the rear part of the cell. Mutants in this gene fail to recruit myosin II to the cortex in response to

cyclic-AMP stimulation and display a similar phenotype to the Myosin II null mutants (Bosgraaf et al., 2005). It seems that GbpC activates myosin II through the phosphorylation of myosin regulatory light chain (MlcE) by MLCK kinase. This branch of signaling acts in the organization of the cell rear. It controls the retraction of the trailing part of the cell and contributes to cell polarization.

1.4.4. Blebbing in the migration of Dictyostelium discoideum and other unicellular amoebae

It has been convincingly shown by Yoshida and Soldati that blebbing can continuously occur at the leading edge of *Dictyostelium* cells moving on a glass surface under a buffer of physiological osmolarity (Yoshida and Soldati, 2006). The authors found that, in migrating cells, blebs always formed at their front side. Intermittent arc-shaped scar structures marking the initial (before membrane detachment) F-actin cortex position were considered as the main signature of blebs. The leading edge of the pseudopods in migrating cells often appeared under the phase-contrast microscope as a hyaline zone devoid of visible membrane organelles. Epifluorescence microscopy of the F-actin marker ABD-GFP showed that multiple successively formed F-actin arcs localized to this hyaline zone. Ageing arcs flowed backwards with respect to the substratum as they disassembled.

Surprisingly, very similar hyaline protrusions have been described in chemotaxing *Dictyostelium* about 30 years ago (Swanson and Taylor, 1982). It was discovered that when developing *Dictyostelium* cells are exposed to strong local gradients of cyclic-AMP, generated by its diffusion from a microneedle, the first response of the cells to such gradients is the local generation of a hyaline pseudopod from the region of the surface nearest the stimulus. These hyaline pseudopods had a smooth surface and did not contain any vesicles, granules or organelles visible under the DIC microscope. These cells often migrated with an anterior edge being rounded and containing hyaline cytoplasm, while the tail

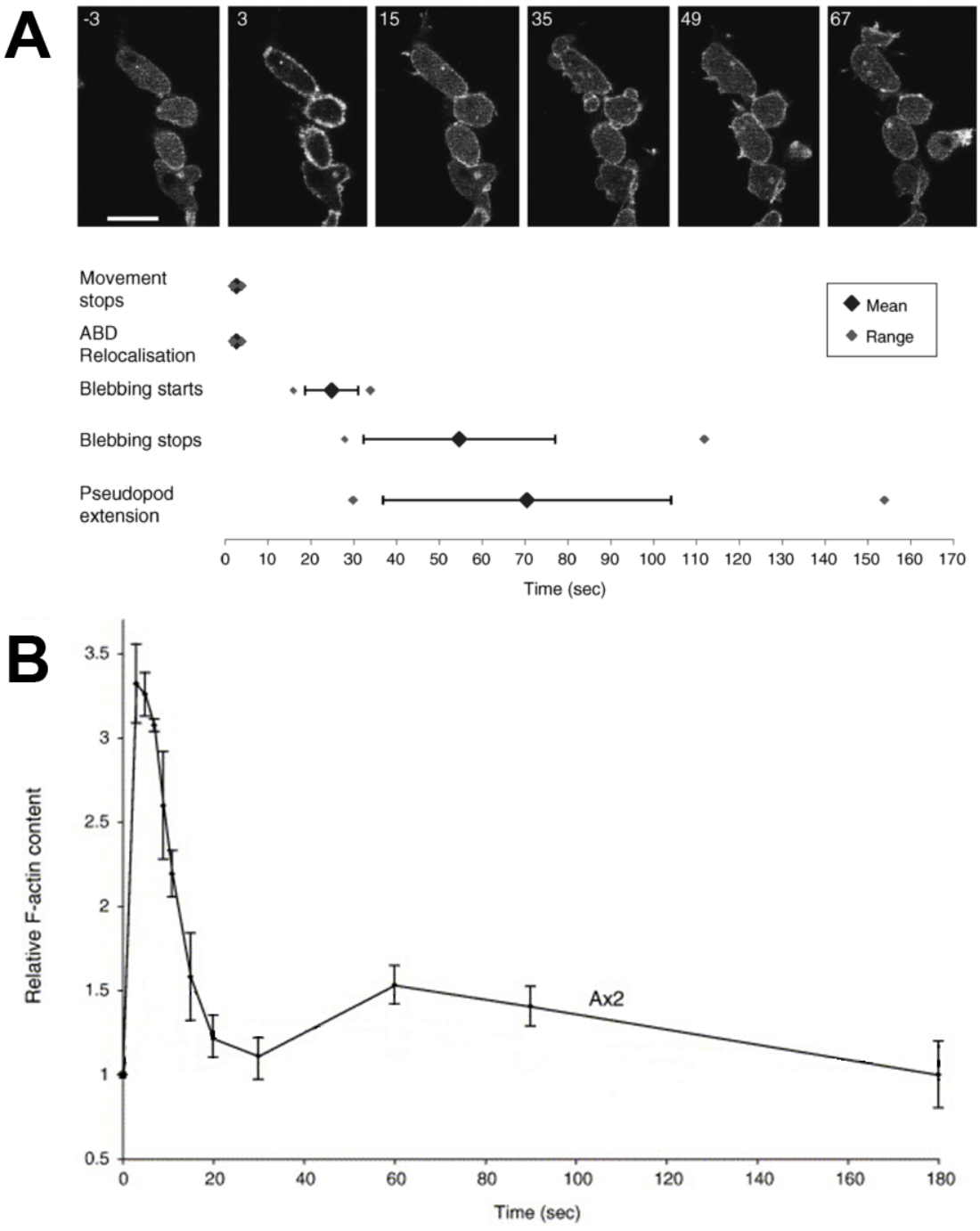

Figure 1.3. **Cyclic-AMP induced blebbing in *Dictyostelium* cells** (image adapted from Langridge and Kay 2006).

Uniform stimulation of *Dictyostelium* cells with chemoattractant cyclic-AMP (1μM) induces massive plasma membrane blebbing (A) that occurs 20-30 seconds after the stimulation, between two phases of F-actin accumulation (B).

was slightly tapered. If the cyclic-AMP filled microneedle was rapidly moved to the tail or the side of the moving cell, the direction of travel could be reversed or changed. The response was always delayed; the amoeba continued awhile in the original direction, without responding to the change in the gradient. After this refractory period a hyaline pseudopod extended from the region of the cell closest to the source of cyclic-AMP. This was later followed by cell re-polarisation and vesicle flow into the pseudopod.

In our laboratory earlier Paul Langridge found that uniform stimulation of *Dictyostelium* cells with the chemoattractant cyclic-AMP induces massive plasma membrane blebbing that occurs 20-30 seconds after the stimulation, between the two phases of increased F-actin content – *Figure 1.3* (Langridge and Kay, 2006). The surface area and volume of cells remained constant during blebbing, suggesting that blebbing is not based on massive exocytosis, but rather relies on redistribution of existing plasma membrane and cytoplasm. It was argued that bleb expansion is not driven by F-actin polymerization, but rather inhibited by preceding F-actin dynamics, since it coincides with the phase of F-actin depolymerisation in cyclic-AMP stimulated cells, and is significantly more pronounced in the cells with partially inactivated Arp2/3 complex, which have lower levels of F-actin polymerisation. Blebbing is rather driven by cortical contraction involving myosin II, since cells lacking myosin II activity completely fail to bleb. Myosin II both induces an increase in hydrostatic pressure within the cell and also increases the availability of membrane excesses caused by cell rounding.

Consistently with this, it was demonstrated that in migrating *Dictyostelium* cells, blebbing also could be inhibited by knock-out or chemical inhibition of the myosin II motor or by the use of high osmolarity buffer (Yoshida and Soldati, 2006). In these cases cells formed exclusively F-actin driven filopodia-lamellipodia protrusions.

It was shown that blebs at the leading edge significantly contribute to *Dictyostelium* cells locomotion: bursts of blebbing correlated with the peaks in cell movement speed; and cells with suppressed blebbing moved nearly twice as slowly as blebbing cells, and their chemotactic index was significantly lowered at a short time range (under 80 seconds after chemotactic gradient application)

but, unlike speed, converges with the speed of blebbing cells at longer time intervals. Pseudopodia extension and cell body retraction was also reduced in these cells. Interestingly, it was found that blebs often appeared between pre-existing or still-growing pseudopodia. And blebbing was often followed by the emergence of F-actin rich filopodia growing from a part of the detached cortical actin layer.

Protrusions similar to blebs in their cytosol-pressure driven nature have been observed in *Dictyostelium* cells treated with quinine (Yoshida and Inouye, 2001). These cells formed rapidly elongating cylindrical protrusions that could drive cell migration. Like blebs, these protrusions were driven not by F-actin polymerization but by cell body contraction through myosin II activity. F-actin was absent in the leading part of these protrusions during the period of their rapid elongation, and got rebuilt during slowing-down or retraction. Similar to bleb extension, formation of these cylindrical protrusions was accompanied by a transient increase in membrane protrusion speed at the site of detachment. The detached F-actin layers also demonstrated some retrograde movement. Interestingly, in the presence of both cytochalasin A and quinine, the protrusions formed were not cylindrical but spherical.

But *Dictyostelium discoideum* is not the only amoeba that has been found to migrate by making hydrostatically driven protrusions. For example, if was shown that *Entamoeba histolytica* also moves by blebbing, and this happens both on two-dimensional surfaces, in three-dimensional tissues and in the liquid environments (Maugis et al., 2010). Interestingly, formation of such cell membrane protrusions that appeared to be blebs was found to correlate with the infectivity of these cells (Coudrier et al., 2005). Another microorganism - *Amoeba proteus* – is also known to migrate by employing cell protrusions driven by the intracellular pressure and cytoplasmic flow, which is caused by cortical contraction (Grebecki, 1994; Yanai et al., 1996).

1.5. Project aims

In this study we use *Dictyostelium discoideum* cells chemotaxing in gradients of cyclic-AMP to study the involvement of blebbing in chemotactic cell

movement. The aim of the project is to investigate whether blebs can be used as a driving force for chemotaxis, alternative to F-actin polymerisation, and to study possible regulatory mechanisms that may control blebbing in *Dictyostelium*.

In the course of this thesis we are trying to address the following questions:

- Does *Dictyostelium discoideum* produce blebs during chemotaxis?
- Can we find a property of the extracellular environment that would switch *Dictyostelium* cells to the blebbing mode of movement?
- Are blebs polarised towards the leading edge of the migrating cells and can blebbing be regulated by the chemoattractant gradient?
- What are the intracellular mechanisms that control blebbing and how are blebs initiated?

By answering these questions we are trying overall to improve the current understanding of the driving mechanisms of eukaryotic cells chemotaxis.

CHAPTER 2. Materials and Methods

2.1. General Materials

Cell culture media, standard buffers and stock solutions were kindly prepared by technicians of the "Media kitchen" within the Cell Biology division at MRC LMB. A list of frequently used solutions and media is provided below. Chemicals and other reagents were obtained from Sigma Aldrich, Invitrogen or BDH unless otherwise stated. Sarstedt, Corning, Becton Dickinson, Sterilin or Starlabs provided consumable sterile cell culture materials. Restriction endonucleases were from New England Biolabs. Oligonucleotides were usually obtained from Sigma.

Frequently used solutions and media:

- *Axenic medium*: HL5 plus glucose medium (Formedium), 200 µg/ml Dihydrostreptomycin
- *SM agar for plates*: 1% peptone (DIFCO), 0.1% yeast extract (DIFCO), 0.22% KH_2PO_4, 0.1% Na_2HPO_4, 1.5% agar, 1% glucose, 8 mM $MgSO_4$
- *KK_2 Buffer*: 16.5 mM KH_2PO_4, 3.9 mM K_2HPO_4, 2 mM $MgSO_4$, 0.1 mM $CaCl_2$, pH 6.1
- *New Salts (NS) Solution*: 20 mM KCl, 20 mM NaCl, 1mM $CaCl_2$

2.2. *Dictyostelium* Methods

In most experiments the axenic strain Ax2 (Kay laboratory strain; DBS0235521 at http://dictybase.org) of *Dictyostelium discoideum* was used as wild type. All experiments were carried out with cells that had been passaged less than 5 times. For the non-Ax2 derived knock-out strains their parental

strain was grown under the same conditions as the mutant and used in experiments as control.

Mutant strains for screening were obtained from the *Dictyostelium* Stock Center (http://dictybase.org/StockCenter/StockCenter.html), or individual donation, as detailed further in *Table 6.1*. Knock-out strains of PhdA (*phdA*-, HM1650) and CRAC (*dagA*-, HM1649) and the double mutant (*phdA*-/*dagA*-, HM1659) were created in strain Ax2 (Kay laboratory) by homologous recombination and recycling of the selective marker (carried out by David Traynor).

2.2.1. Growth and storage of strains

2.2.1.1. Growth in Axenic Medium

Wild type *Dictyostelium* cells and many mutants were grown in axenic medium (see section 2.1) at 22°C, either in shaken suspension (180 rpm) or on tissue culture plates. Reporter strains were grown in axenic media supplemented with G418 antibiotic for selection (10 µg/ml).

2.2.1.2. Bacterial growth

Strains that failed to grow efficiently in axenic medium and those used in parallel experiments with them were grown in association with an overnight culture of *Klebsiella aerogenes* (grown in SM broth at 22°C) on SM agar plates. Short-term stocks of wild type and mutant strains were kept by streaking cells onto a bacterial lawn. But when required for experiments, cells were grown on clearing plates. To set up clearing plates, cells were added to a small volume of a bacterial culture, vortexed to mix and then plated out together on SM agar plates. Amoebae were harvested when the bacterial lawn had begun to look translucent, or was "half-cleared". For a plate to be half cleared in 48 hours, approximately 2 x 10^6 cells of Ax2 would be inoculated onto a plate with 200 µl

of bacteria. In the case of strains that grow more slowly 2.5 x 10^7 would be inoculated per plate. A range of cell densities was always plated to ensure cells at the appropriate stage of growth were available.

2.2.1.3. Strain storage

Strains were stored in liquid nitrogen. In order to freeze down new strains, they were harvested from axenic media or bacterial plates and resuspended into 1.5 ml of freezing medium (Horse serum, 7.5 % DMSO) in a 2 ml cryo-vial (Nunc). This was then chilled on ice before transferring to -80°C in a Cryolite Preservation Module (Stratagene), to prevent cooling at too high a rate. After 24 hours, vials were transferred to a liquid nitrogen storage tank in order to preserve them indefinitely. To rescue strains from liquid nitrogen, cells were scraped onto an SM plate, which had been pre-spread with *K. aerogenes*, and would typically grow up in 3-6 days, depending on the strain.

2.2.2. Transformation of Dictyostelium

For F-actin visualization, *Dictyostelium* cells were transformed with an F-actin reporter construct consisting of GFP fused to the F-actin binding domain of *Dictyostelium* protein ABP-120 (Pang et al., 1998). Transformation was carried out by electroporation (GenepulserXcell, Bio-Rad) as described in (Knecht and Pang, 1995). Briefly, cells were harvested and washed once in ice-cold H50 buffer, resuspended at 4 x 10^7 cells/ml and incubated on ice for at least 5 minutes. 30 µg of plasmid DNA were added to an electroporation cuvette (1 mm gap width, Bio-Rad), to which 100 µl of cell suspension was added and mixed without introducing bubbles. Cells were electroporated with two pulses, 5 seconds apart, of 750 V and 25 µF with no additional resistor. After electroporation, 0.5 ml of axenic media was added to the cuvette, which was then incubated on ice for 5 minutes. The contents of the cuvette were plated out after diluting into axenic medium. Selection was added the next day, generally 10 µg/ml G418 for overexpression constructs.

2.2.3. Preparation of aggregation-competent cells

To prepare aggregation-competent cells, vegetative amoebae were harvested from axenic media or bacterial plates and washed by low speed centrifugation thoroughly in KK_2 buffer (twice in the case of cells grown axenically, four to five times in the case of cells grown in association with bacteria). After washing, cells were counted and resuspended in KK_2 at 2 x 10^7 cells/ml. They were then shaken at 180 rpm at 22°C for one hour before pulsing with 90 nM cyclic-AMP (final concentration) every six minutes for 4.5 hours, using a peristaltic pump (Watson Marlow 505D). RasC-/RasG- double null strain, CRAC null and PhdA/CRAC double null strain cells were pulsed with 400 nM cyclic-AMP as they are defective in cyclic-AMP relay. After this time small clumps of cells start to form and stick to the glass walls of flasks and this was used as morphological check for adequate development. After pulsing and before use in experiments, cells were washed once more in KK_2.

2.3. Biochemical Methods

2.3.1. SDS-PAGE and Western Blotting

Sodium dodecyl sulphate polyacrylamide gel electrophoresis (SDS-PAGE) was used to separate proteins by molecular weight. 4-12% NuPAGE Bis-Tris pre-cast gels (Invitrogen) were used and run using 1x MOPS buffer (Invitrogen). SeeBlue Plus2 Pre-Stained Standard (Invitrogen) was used as molecular weight markers.

Samples were prepared by adding NuPAGE LDS sample buffer (Invitrogen) and β-mercaptoethanol to a final concentration of 1x and 10% respectively to the cell lysates. Samples were then boiled in a water bath for 3 minutes, allowed to cool slightly and centrifuged for a further three minutes in a bench top centrifuge to pellet any debris before loading onto the gel. Gels were

run at 150 V for approximately 90 minutes, or until the ladder showed sufficient separation. For protein staining SimplyBlue (Invitrogen) was used according to manufacturer's recommendations.

For western blotting, proteins separated by SDS-PAGE were transferred to a nitrocelluose membrane (Millipore) using Novex transfer apparatus (Invitrogen). The transfer buffer used comprised: 25 mM Tris-base, 200 mM glycine, 10% methanol, 0.1 mM EDTA. Transfer proceeded at 35 V for 60 minutes.

After transfer, membranes were incubated in a blocking solution (5% non-fat dry milk, TBS-T buffer [150 mM NaCl, 50 mM Tris-HCl pH 7.4, 0.05% Tween-20]) for at least one hour at room temperature before incubating with primary antibodies (in blocking solution) overnight at 4°C.

Blots were then washed three times (10 minutes each time) in TBS-T with gentle rocking. After the third wash, the blot was incubated with HRP-fused secondary antibodies (again, diluted in blocking solution) at room temperature for one hour before repeating washes as before. After washing the membranes, ECL Western Blot Detection Reagent (GE Healthcare) was used to detect protein bands, according to manufacturer's instructions. The blot was then exposed to Fuji Medical X-ray film, and developed using a Kodak X-Omat processor.

The following primary antibodies were used for Western Blotting:

- Anti-CsaA (against Contact Sites A protein): Mouse Monoclonal (№ 123-351-1, from Developmental Studies Hybridoma Bank), dilution 1:250;
- Anti-TalB (against Talin B): Rabbit polyclonal (kindly gifted by Robert Insall's laboratory), dilution 1:1000.

The secondary antibodies used were, respectively:

- Goat-anti-Mouse IgG: BioRad #172-1011, dilution 1:3000;
- Goat-anti-Rabbit IgG: BioRad #172-1019, dilution 1:10000.

2.3.2. Actin polymerisation assay

F-actin content in the cells was determined by extracting the Triton-X

100 insoluble cytoskeleton fraction and staining it with fluorescently labelled phalloidin. This was done to measure the relative changes in F-actin levels over time (Hall et al., 1988).

To perform this experiment, cells were developed to an aggregation-competent state, then washed with KK_2 and resuspended at 1.5 x 10^7 cells/ml in KK_2 with 3 mM caffeine (to inhibit endogenous cyclic-AMP signalling). Then cells were shaken at 180 rpm for another 30 minutes. Afterwards they were washed once again to remove caffeine and continually shaken at 180 rpm for the duration of the experiment.

To study the F-actin polymerisation dynamics, for each time point, 200 µl of cells were added to a 5 µl drop of 41 µM cyclic-AMP to give a final stimulatory concentration of 1 µM. After the appropriate time, 1 ml of 1.2 x fix/stain buffer was added (30 mM PIPES, 6 mM EGTA, 2.4 mM $MgCl_2$, 3% formaldehyde, 0.24 % Triton-X 100, 0.6 mM TRITC-phalloidin), which simultaneously lyses the cells while fixing the insoluble cytoskeleton and staining the F-actin. Samples were taken at 0, 5, 10, 15, 20, 30, 45, 60, 90, 120, 180, 360 and 480 seconds after stimulation with cyclic-AMP (for each time point two samples were prepared, and further their values were averaged to reduce fluctuations). Samples were then rotated at room temperature for 10 minutes before pelleting the insoluble cyoskeleton in a benchtop centrifuge for 2 minutes at maximal speed. After aspirating the supernatant, 1.5 ml of wash buffer was added (25 mM PIPES, 5 mM EGTA, 2 mM $MgCl_2$, 0.1% saponin) and samples were rotated for another 30 minutes at room temperature. The insoluble cyctoskeleton was then pelleted as before and then the TRITC-phalloidin was extracted by adding 1 ml of methanol and agitating (microfuge tube mixer, Model 5432, Eppendorf) for 15 minutes at room temperature. Samples were centrifuged once more to remove debris, and the supernatant was transferred to a clean tube. Fluorescence was measured using a fluorimeter (Perkin Elmer LS50B) with 544nm excitation and 574 nm emission wavelengths. When analyzing data, fluorescence was normalised to the value at t = 0 sec.

Three independent replicates of the experiment have been performed for every strain analysed, and the data are presented for each point as mean value ± standard error of the mean.

2.4. Microscopy Image Collection and Analysis Methods

2.4.1. Confocal microscopy

For microscopy, aggregation competent *Dictyostelium* cells were settled on Lab-Tek chambered microscopy coverslips (Nalge Nunc International, USA). Fluorescence and DIC microscopy data were collected using a Zeiss 710 laser scanning confocal microscope with a 63× oil-immersion objective (Zeiss, Germany) and processed using ImageJ software (NIH, USA; http://rsbweb.nih.gov/ij/). This method allowed time-lapse image collection at frame rates of one or two frames per second. High-speed image collection (4-6 frames per second) was performed using a Perkin-Elmer Ultraview spinning disk confocal microscope with a 100× water objective.

2.4.2. Chemotaxis assays

2.4.2.1. Chemotaxis to the micropipette

Aggregation-competent cells were allowed to settle in a Lab-Tek two-chamber coverslip in KK_2 buffer and then imaged using a laser scanning confocal microscope, as described above. Cells were stimulated using a glass micropipette (Femtotips II, Eppendorf, Germany) filled with 2 μM cyclic-AMP, using a micromanipulator (Eppendorf 5171, Germany). Diffusion from the micropipette created a steep gradient of cyclic-AMP. Images were taken at a rate of one frame per second.

Chemotaxis Index (CI) was calculated for these cells as a ratio between the net distance travelled in the direction of the gradient and the total Euclidean distance (or as a cosine of the angle between the direction of the gradient and the direction of net cell displacement).

Three independent replicates of the experiment have been performed,

and the data are presented as mean value ± standard error of the mean. In each replicate about 50 cells were analysed.

2.4.2.2. Dunn Chamber Chemotaxis

Approximately 3.2 x 10^4 aggregation-competent cells of two different strains (usually Ax2 and a mutant to be tested) were allowed to settle in 40 µl droplets at either end of a haemocytometer coverslip. Once cells had settled, most of the excess buffer was removed and the coverslip was inverted onto a Dunn chamber (Zicha et al., 1991), in which both of the concentric wells had been filled with KK_2. A slight gap was left so that buffer in the outer well could be removed and replaced with KK_2 containing 1 µM cyclic-AMP, creating a linear chemotactic gradient from the inner to the outer well. The gap was then closed by gently sliding the coverslip across, and excess buffer mopped up from around the edges. The assembled Dunn chamber was imaged every 30 seconds for 20 minutes using a 10x phase objective on a Zeiss Axiovert S100 inverted microscope. This had been fitted with a motorized stage (Prior Scientific), which allowed four points on two different Dunn chambers to be imaged simultaneously.

Three independent replicates of the experiment have been performed, and the data are presented as mean value ± standard error of the mean. In each replicate about 50 cells from two different chambers were analyzed.

2.4.2.3. Under-agarose chemotaxis

A modified version of the under-agarose assay method described earlier (Laevsky and Knecht, 2001) was used. A thin layer (750 µl) of 0.5-2.0% SeaKem GTG agarose (Lonza, USA), prepared on KK_2 buffer, was poured into pre-heated, two-chamber Lab-Tek coverslips (surface area of each chamber = 4.2 cm^2) and once the agarose had set, three rectangular troughs cut parallel to each other with 6 mm between them (*Figure 2.1*). The central trough was 4 mm wide and 8 mm long; the side ones 1 x 5 mm. To the central trough, 4 µM cyclic-AMP was added and left in a moist chamber for 30 minutes to allow a gradient to be set up

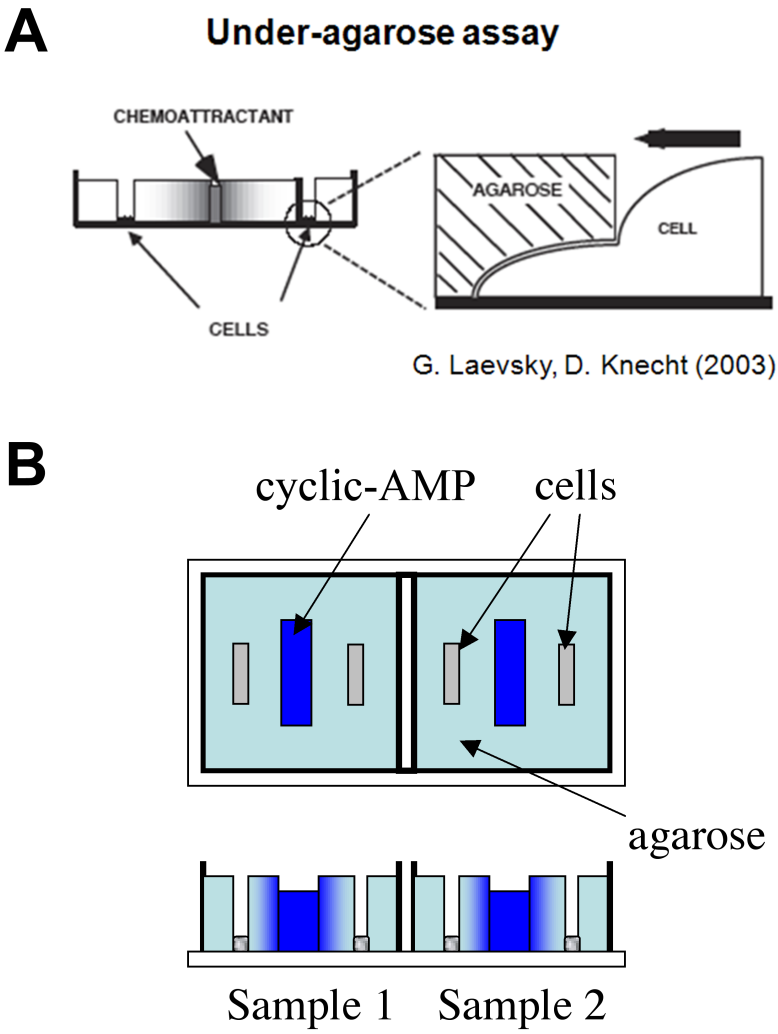

Figure 2.1. **Scheme of the under-agarose assay experiment.**

A modified version of the under-agarose assay method described earlier (Laevsky and Knecht 2001, Laevsky and Knecht 2003)(Laevsky and Knecht, 2001) was used (A).

A thin layer of agarose poured in two-chamber coverslip. After agarose hardening, three parallel rectangle troughs were cut and the pieces of agarose were removed (B). The central one was filled with 4 μM cAMP and left for 30 minutes for gradient to set up. After that, 10^5 aggregation competent cells were placed into the side troughs. Observation was started when the cells began squeezing under the agarose layer.

within the agarose layer, after which 10^5 aggregation competent cells were placed in each side trough and left for another 30 minutes for cells to start moving under the agarose. Further, DIC and fluorescent images were collected using a Zeiss 710 confocal microscope every 500 ms, as described above; this speed was necessary to follow bleb formation. For negative staining, Rhodamine B isothiocyanate - dextran was added to the agarose at 0.5 mg/ml. To estimate the speed of cell migration under agarose, images were collected every 5 seconds for 1 hour using a Zeiss Axiovert S100 microscope (Zeiss, Germany) with 10× objective and a motorised stage. The collective migration speed was calculated as an average displacement (distance from start-point to end-point) of 20 leading cells towards the source of chemoattractant during 1 hour. The experiment was repeated three times, and in each replicate, the speed values from three different coverslips were averaged.

2.4.2.4. Reorientation assay

Cells were settled in a standard Lab-Tek microscopy chamber (Nalge Nunc International, USA) in KK_2 buffer, and a micropipette (Femtotips II, Eppendorf, Germany) loaded with 2 μM cyclic-AMP placed about 40 μm from a cell (observed on Zeiss 710 confocal microscope with 63× oil objective). Once the cell became polarised and started moving towards the micropipette, the micropipette was rapidly moved (in 1-2 seconds) to the middle of the cell's flank at a distance of about 15-20 μm from the cell surface. The process of re-orientation was filmed at one frame per second rate to analyse cell morphology and F-actin distribution dynamics. n=30 cells were analysed.

2.4.3. Cell outline tracking and analysis

Cell outline segmentation and automated membrane protrusions analysis was performed in collaboration with Richard Tyson (University of Warwick) using the QuimP10 software (Warwick Systems Biology Centre, UK;

http://www2.warwick.ac.uk/fac/sci/systemsbiology/staff/bretschneider/quimp/) based on the electrostatic contour migration method (Tyson et al., 2010).

2.4.3.1. Image data collection

For these experiments, the wild-type (Ax2) and a non-blebbing myosin essential light chain null mutant (MlcE-null) strains of *Dictyostelium discoideum,* transformed with an F-actin reporter construct consisting of GFP fused to the F-actin binding domain of *Dictyostelium* protein ABP-120 (Pang et al., 1998), were used. These cells were imaged in the under-agarose assay, as described above, using an agarose concentration of 0.7%, which permits cell to form both blebs and F-actin driven pseudopodia, allowing us to compare these two types of protrusions directly, side by side. To enhance the contrast of the cell outline, samples were negatively stained with Rhodamine B isothiocyanate - dextran (RITC-dextran) added to the agarose at 0.5 mg/ml, and its emission was recorded in a separate fluorescence channel. This stain acts to fluoresce the background while cells appear as shadows.

Images of Ax2 cells were collected using both laser scanning and spinning disk confocal microscopy techniques to provide image sequences at multiple frame rates. Fluorescence and DIC image sequences taken using the Zeiss 710 laser scanning confocal microscope (Zeiss, Germany) with a 63× oil-immersion objective were collected at a frame rate of 2 frames per second, for a period of 100 seconds.

Spinning disk microscopy, carried out on Perkin-Elmer Ultraview microscope with a 100× water objective, was used to capture fluorescence image sequences at speeds in the range of 4-6 frames per second. Laser scanning confocal images taken at 2 frames per second proved insufficient to capture the fastest blebs during extension, hence resulting in an underestimate of the extension speed for the fastest occurring blebs. Additionally, attaining sequences at multiple frame rates allowed us to develop a frame-rate independent method for automated protrusion tracking, eliminating possible side effects of differing frame rates on protrusion analysis.

2.4.3.2. Image pre-processing

Image pre-processing was done using ImageJ macros. Blank sequences of roughly 50 frames (containing no cells in the field of view) were imaged prior to each experiment to capture background illumination. Intensity fluctuations over blanks were removed by equalising the mean intensity at all frames. Average intensity projections were created from the corrected blank frames and Gaussian convolution applied (σ = 1 pixel) to smooth high frequency noise (as provided by ImageJ). Resulting images were used as background masks.

Similarly, image sequences containing cells were processed to remove intensity fluctuations, as described above (sampling of mean intensity was restricted to regions containing no cells). Each frame was then background corrected by dividing image pixels by the corresponding pixels in the background mask. To improve background removal where contrast differed significantly between mask and image, contrast and brightness were matched by manipulating the distribution of pixel intensities. See *Figure 2.2* for an example of background removal.

The Rhodamine B isothiocyanate – dextran (RITC-dextran) fluorescence channel, used for segmentation, was inverted to produce bright cells on a dark background. In cases where background correction was inadequate to achieve an acceptable segmentation, or intracellular structures greatly interfered with the cell edge, the RITC-dextran channel was converted to a binary image using the ImageJ operation "Thresholding". Holes in the binary image were filled using the ImageJ's "Fill Holes" option.

2.4.3.3. Cell outline segmentation and tracking

As mentioned above, automated and semi-automated cell contour tracking was performed using the QuimP10 software, written as a series of plug-ins for the open source image-processing tool, ImageJ. The BOA plug-in provides a supervised image segmentation algorithm, in the form of an active contour, for extracting cell outlines, and is capable of segmenting multiple cells in parallel. The resulting outlines are fed to the ECMM plug-in for boundary tracking. Cortical fluorescence intensities are sampled by the ANA plug-in, in which the user defines a cortex width, and electrostatic contour migration (ECMM)

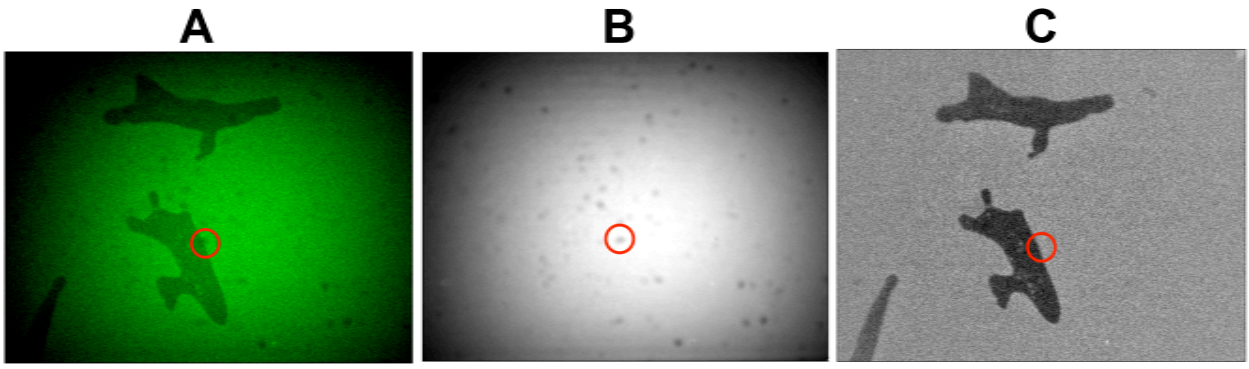

Figure 2.2. **Image pre-processing for automated membrane tracking** (illustration prepared by Dr Richard Tyson)**.**

Dictyostelium cells were imaged under agarose containing RITC-dextran as negative staining (A). Besides, blank sequences of roughly 50 frames (containing no cells in the field of view) were imaged prior to each experiment to capture background illumination. Intensity fluctuations over blanks were removed by equalising the mean intensity at all frames. Average intensity projections were created from the corrected blank frames and Gaussian convolution applied to smooth high frequency noise. Resulting images were used as background masks. (B) Each frame was then background corrected by dividing image pixels by the corresponding pixels in the background mask (C). To improve background removal where contrast differed significantly between mask and image, contrast and brightness were matched by manipulating the distribution of pixel intensities

algorithm is utilised to migrate nodes across the cortex. Finally, the QAnalysis plug-in compiles spatial-temporal maps of motility, fluorescence, convexity and tracking. *Figure 2.3* provides a brief overview of the software pipeline and the data produced at each stage.

The BOA plug-in performs two main functions: cell segmentation and measurement of global cell statistics, such as elongation and displacement. This plug-in can use multiple active contours to provide parallel segmentation of multiple cells. It constructs an outline of a cell as a chain of nodes. The chain is manually initialised around a cell at time point T (which can be any frame within a sequence) ensuring the chain does not overlap any object in the image. The total force vector (depending on the relative positions of the nodes and the gradients of intensity on the image) is then computed for each node, and then positions of the nodes (at sub-pixel resolution) are updated via numerical approximation. As the chain approaches the cell boundary, characterised by high contrast, forces begin to balance, neutralising the internal energy of the chain below a critical threshold, and halting shrinkage of the outline. The process is then repeated at T + 1, the snake is initialised by expanding the solution snake derived at T until it encloses the cell boundary at T + 1. In cases where the object of interest does not leave the bounds of the original, manual initialisation of the chain may be reset to this position at each frame. The result of segmentation is a closed chain of nodes, which is considered further as the cell outline.

Application of ECMM algorithm then replaces nodes of the original segmentation with new nodes based on migrated markers. Marker resolution is pre-set at a density of 0.5 per pixel. Such nodes/markers have associated decimal positions (DPs) encoding their locations on the cell outline at T, and marker origins (MOs), indicating the decimal position from where they originated on the outline at T − 1. Node DP and MO data is used to build, and track through, spatial-temporal maps (STMs). At this point in the analysis, no data is yet collected on fluorescence intensities, but each node has an assigned speed at each time point, computed by ECMM.

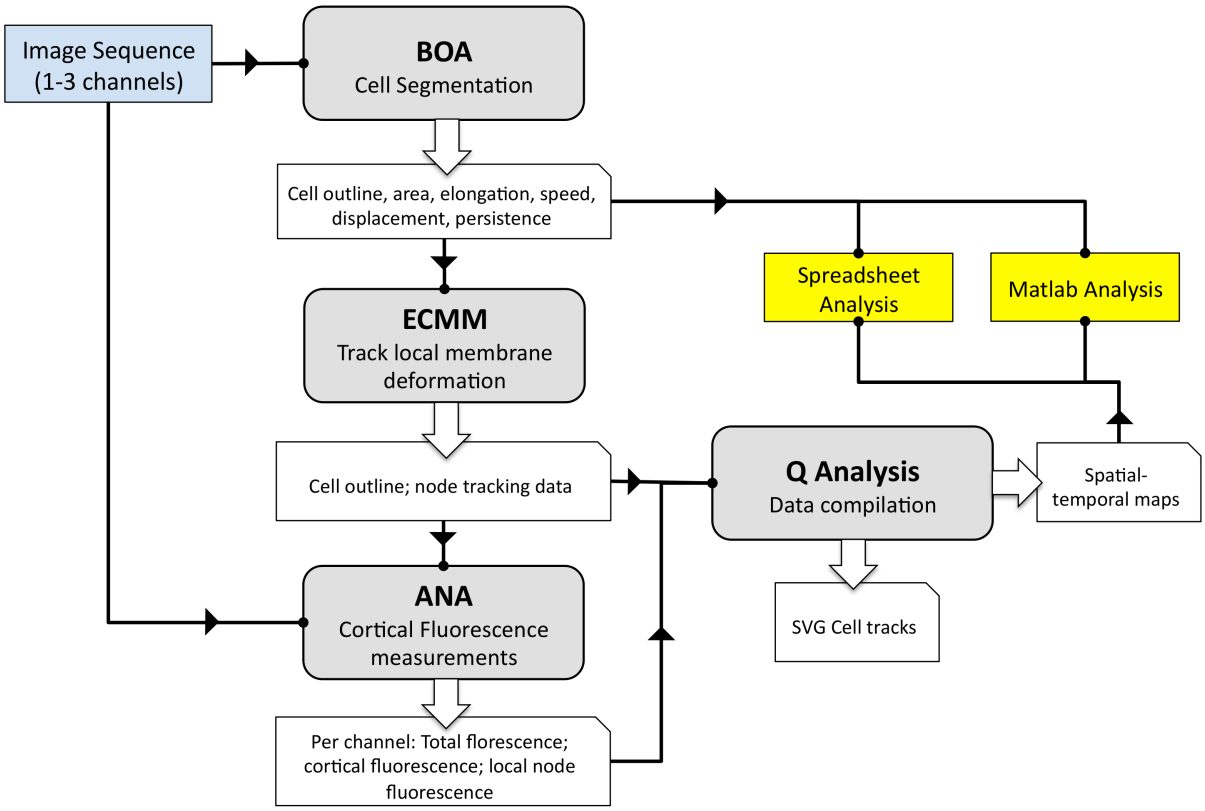

Figure 2.3. **Diagram illustrating the pipeline executed by the QuimP software during cell image analysis** (by Dr Richard Tyson).

The BOA plug-in performs cell segmentation and measurement of global cell statistics, such as elongation and displacement. Application of ECMM algorithm then replaces nodes of the original segmentation with new nodes based on migrated markers. Fluorescence is sampled by the ANA plug-in, assigning fluorescence intensity values to each node. These values are sampled from the local cortical region of a cell, width of which can be set up manually. The QAnalysis plug-in is used for compiling the output from BOA, ECMM and ANA, in order to create visual representation of cell motility and data for analysis.

Fluorescence is sampled by the ANA plug-in, assigning fluorescence intensity values to each node. These values are sampled from the local cortical region of a cell, the width of which can be set up manually. The cortical region is defined as a continuous strip, of uniform thickness (decided upon by the user), located on the immediate underside of the cell outline. In our measurements, the cortex was typically set to a width of 0.7μm. Nodes of the cell outline are migrated across the cortex by ECMM, adapted to simultaneously sample pixel intensities. The maximal sampled intensity is recoded for each node and optionally normalised to the average fluorescence within the cell interior.

Finally, the QAnalysis plug-in was used for compiling the output from BOA, ECMM and ANA, in order to create visual representation of cell motility and data for analysis. This plug-in produces scaleable spatio-temporal maps that contain ECMM measures of membrane speed and fluorescence data in a comparable, consistent format. A spatial-temporal map is a two-dimensional plot, in which the x-axis represents the cell outline, and the y-axis - time (T = 0 being at the top). Values encoded within the plot can represent any desired measure (for example membrane speed, curvature or cortical intensity) at a particular time and location on the cell perimeter. A colour map can be applied to highlight areas of high/low activity, and correlations computed between maps.

2.4.3.4. Analysis of the cell outline tracking data

Information from cell contour segmentation and tracking algorithms was used further for identification and characterization of various cell membrane protrusions. Protrusions were either pointed out manually or identified by the automatic algorithm. Then motility profiles were computed for these protrusions and measurements of peak speed (μm/sec) were performed for them either as the maximum speed within a raw motility profile, or the maximum of a three-frame average, which smooths out the noise. As an alternative to the motility profiles, displacement profiles could be computed for the protrusions by summing over speeds (and scaling by the frame interval). In

this case peak speeds were defined as the maximal gradients on such displacement profiles (See Chapter 4.2 for more details and examples).

Displacement profiles generally assumed the shape of a sigmoid curve, featuring an acceleration phase, a constant speed phase (representative of peak speed), and a deceleration phase. These profiles could be fitted with the generalised logistic sigmoid curve:

$$f(x) = a \cdot \left(1 - e^{-\left(\frac{x}{b}\right)^c}\right) + d$$

This equation allows fitting to negative values during acceleration (resulting from noise, or small contractions) by including the parameter d, and also non-symmetrical acceleration and deceleration. This generalised logistic sigmoid is real-valued and differentiable, therefore the peak speed can be determined from it as a maximal gradient:

$$\frac{d}{dx} f(x) = \frac{a \cdot c \cdot \left(\frac{x}{b}\right)^{c-1}}{b \cdot e^{\left(\frac{x}{b}\right)^c}}$$

Also displacement profiles were used to define the total protrusion displacement (simply as the maximal value in the profile, μm), and protrusion extension duration (as the time taken to reach the maximal displacement, seconds).

Fluorescence and curvature maps could also be computed from the protrusion tracks. Curvature values were calculated for each node of the cell contour as $C_n=(\alpha_n-180°)/180°$, where α_n is the external angle between the edges connecting the node number n with left and right neighbouring nodes, respectively. Normally, curvature values were further averaged across 1 μm windows.

2.4.4. Mutants Screening Methods

To determine proteins, potentially involved in the control of blebbing, about 50 different knock-out strains of *Dictyostelium discoideum* were collected or created in our laboratory as detailed further in the *Table 6.1* (Chapter 6). They were compared to their direct parents in three different assays related to blebbing – 'under buffer': the frequency of blebs compared to actin-driven pseudopodia in randomly moving cells moving on a coverslip under KK_2 buffer; 'under-agarose': the frequency of blebs compared to actin-driven pseudopodia in cells chemotaxing to cyclic-AMP under 0.7% agarose and, in selected cases, the speed of under-agarose chemotaxis determined from time-lapse movies; and 'cyclic-AMP shock': the frequency of blebbing induced by uniform cyclic-AMP stimulation. Detailed descriptions of all of these three experimental approaches are given below. Experiments were carried out with developed cells (after 1 hour starvation and 4.5 hours pulsing with cyclic-AMP). Results from the assays were combined using a scoring system as follows: "0": mutant not distinguishable from its parent; "–" : mutant blebs slightly less well than its parent; "– –" : mutant does not bleb at all, or does very weakly. Similarly, strains that bleb slightly more, and much more than their parent get scores of "+" and "+ +", respectively. The blebbing scores are finally summed for all three assays to give a composite score for each strain.

2.4.4.1. Blebbing during random motility under buffer

For this experiment approximately 2×10^5 aggregation-competent cells in 200 µl of KK_2 buffer were placed into each chamber of a Lab-Tek eight chamber coverslips slide and allowed to settle before imaging. Then images were taken for 2 minutes at a frame rate of 1 frame per second, using the 63x oil immersion objective. For each mutant strain the amount of blebbing during their random (without any stimulation) movement was assessed throughout the experiment in each of the eight chambers and compared to the parental wild-type strain. This experiment was performer in three independent replicates for every strain analysed, and around 50 cells were taken into account in each

replicate.

2.4.4.2. Blebbing in under-agarose assay

For this experiment, a thin layer of 0.7% agarose was poured into pre-heated two-chamber Lab-Tek coverslips, let for about 20 minutes to solidify, and then three parallel rectangular troughs were cut in the agarose, as described above. The central trough was filled with 4 μM cyclic-AMP and left for 30 minutes for gradient to form, and then to one of the side troughs approximately 10^5 aggregation competent cells of the analysed knock-out strain were placed, and the same number of the parental wild-type strain cells were placed to another side trough for reference. Cells were kept on these coverslips in a moist chamber for 1 hour at room temperature before starting the imaging - to let them squeeze and start moving under the agarose. Then two-minute long time-lapse series of the DIC images of the moving cells were collected at a frame rate of one frame per second using a Zeiss 710 confocal microscope with 63× oil-immersion. Further, the amount of blebbing was assessed during the cells migration under agarose and compared to the wild-type strain. For each strain three independent replicates of this experiment have been performed, and in each replicate blebbing was analysed in around 30 cells from three different coverslips.

2.4.4.3. Blebbing after cyclic-AMP shock

"Blebbing assay", developed in our laboratory and described earlier (Langridge and Kay, 2006), was used in order to assess the response of cells to the sudden uniform stimulation with a saturating concentration (1 μM) of cyclic-AMP. Briefly, about 2×10^5 aggregation-competent cells in 210 μl of KK_2 buffer were allowed to settle in 8-chamber Lab-Tek coverslips (number of cells given per well). After that, cyclic-AMP shock was performed by gentle addition of 15 μl of 15 μM cyclic-AMP solution in KK_2 into the chamber. As shown previously, cyclic-AMP instantly mixes with a buffer to form a uniform 1 μM concentration. Imaging of the cells was started about 10 seconds before the stimulation, and

images were taken every second during the following two minutes. In most cases, blebbing occurred between 20 and 50 seconds after cyclic-AMP addition. Blebs were then counted throughout the period of observation and the results of a number of experiments were combined for statistical analysis. The experiment was repeated three independent times for each strain, and within each replicate about 50 cells from eight different chambers were analysed.

2.5. Statistical analysis of the data

Results of the blebbing and under-agarose assays for different strains were compared using unpaired two-tailed Student t-tests. Differences were considered significant at $p<0.05$. Data are shown in the figures as mean ± SEM, and p values are indicated above the error bars for each mutant strain compared to the wild-type parent.

CHAPTER 3. Involvement of blebbing in *Dictyostelium* cell motility

3.1. In standard conditions *Dictyostelium* cells move by a combination of F-actin driven protrusions and blebs.

It is widely believed that *Dictyostelium discoideum* cells migrate by projecting F-actin driven pseudopodia at the leading edge. According to this paradigm, the branched F-actin polymerization at the front edge of the cell builds up a network of F-actin fibres, which pushes the plasma membrane forward and drives cell locomotion (Pollard and Borisy, 2003). At the same time there has been one report in the literature indicating that *Dictyostelium* cells can also produce small, short-lived blebs at their leading edge (Yoshida and Soldati, 2006). These blebs appeared as sudden protrusions, often having a hemispherical shape and a hyaline appearance under the phase-contrast microscope. Epifluorescence microscopy of F-actin marker ABD-GFP revealed intermittent arc-shaped scar structures marking the initial position of F-actin cortex as the main characteristic signature of blebs (Yoshida and Soldati, 2006).

Because there is a considerable genetic variation between laboratory strains of *Dictyostelium* (Bloomfield et al., 2008), I first confirmed the presence of blebs in our standard Ax2 strain (Kay laboratory strain; DBS0235521 in the DictyBase catalogue). I found that blebs are readily apparent at the leading edge of starving cells moving under buffer, provided that movies are taken at a sufficiently high frame rate – at least 1-2 frames per second (*Figure 3.1-A,B*). To visualise blebs in migrating *Dictyostelium* cells I transformed them with an F-actin reporter (a plasmid coding the GFP protein fused with an F-actin binding domain from the *Dictyostelium* protein ABP120 – "ABD-GFP" – (Pang et al., 1998)). In cells moving on a glass coverslip under buffer, blebs could be observed at the leading edge as protrusions different from usual pseudopodia in their hemispherical shape and F-actin scars remaining in the base of these protrusions when cell membrane detaches from its supporting cortex (*Figure 3.1-A*). Blebs were observed in most cells, although their lifetime was quite short (2-5 seconds) and size was small (1 μm or less), and for this

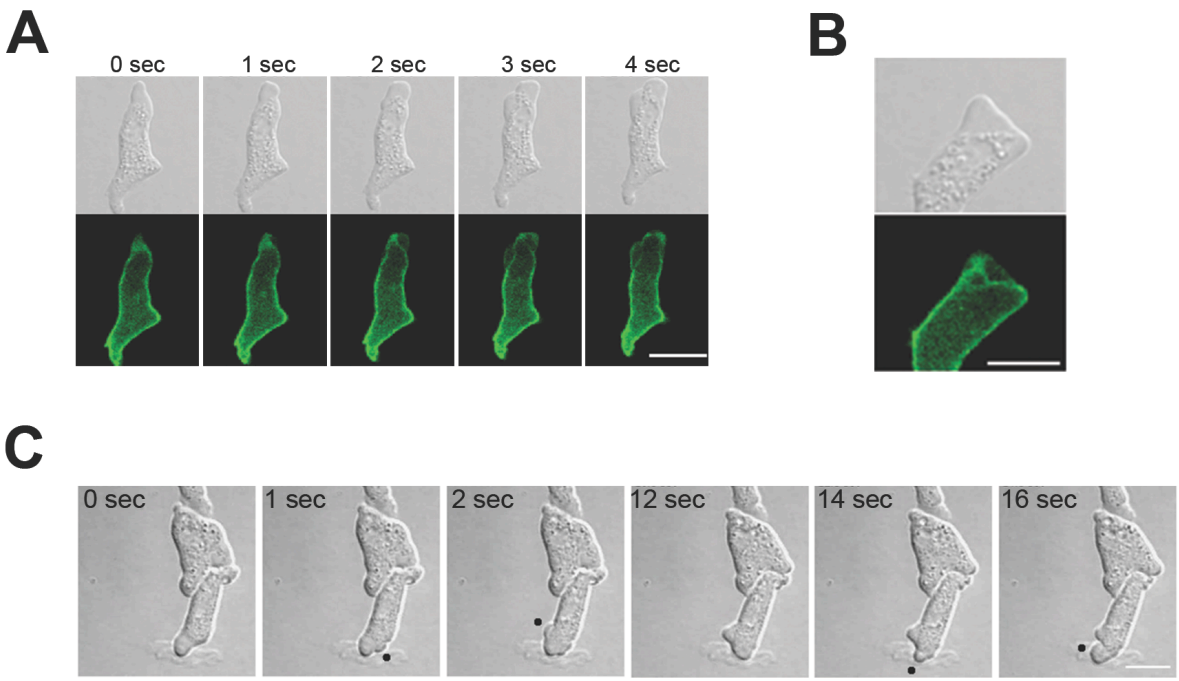

Figure 3.1. **Blebs in *Dictyostelium* cells moving under buffer.**

Figures show Ax2 cells moving on a glass surface under buffer: (A) blebs form at the leading edge of cells - they expand in less than one second, leaving behind an F-actin scar; (B) a hybrid of blebs and F-actin pseudopod; (C) cells in late aggregation readily form head-to-tail streams, the lead cell of which generally moves with blebs (indicated by black spots). Ax2 cells, expressing a reporter for F-actin (ABD-GFP), were starved for 4.5 hr with pulsing by cyclic-AMP. Bar = 10 microns.

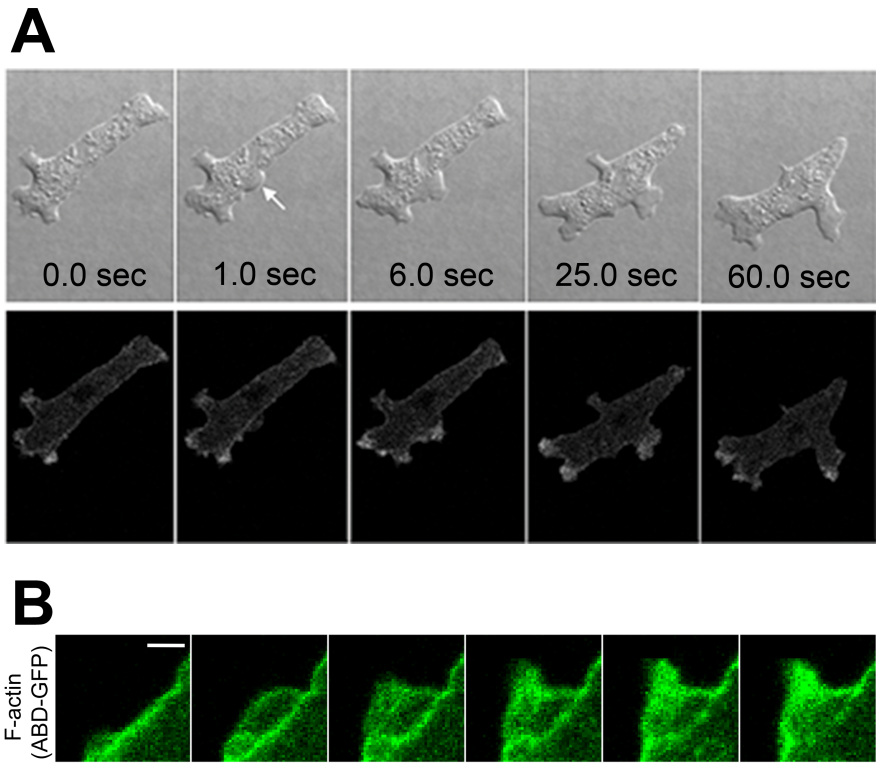

Figure 3.2. **Blebs can give rise to F-actin driven pseudopodia.**

(A) DIC and fluorescence images of a *Dictyostelium* cell moving on a glass surface under buffer: a bleb (indicated by an arrow) is transforming into an F-actin-driven pseudopod by continued actin polymerization; (B) a closer view of a bleb transforming into a pseudopod. Ax2 cells, expressing a reporter for F-actin (ABD-GFP), were starved for 4.5 hr with pulsing by cyclic-AMP. Bar = 1 micron.

reason they require a high speed and high spatial resolution microscopy to detect them.

Blebs in *Dictyostelium* cells grew abruptly and typically completed their expansion in less than a second, were largely F-actin free during this expansion phase, but they left behind an F-actin scar, representing the former position of the cell cortex. Once expansion ceased, the blebs were rapidly re-populated with cortical F-actin and could easily be mistaken for actin-driven projections. Blebs and F-actin-driven projections could co-exist at the leading edge of the same cell and often formed hybrid structures. I found that blebs could transform into actin-driven structures by continued actin polymerization (*Figure 3.2*), and actin-driven processes could spawn blebs at their margins. Therefore, the protrusions that are usually described as F-actin driven pseudopodia actually often have a finer structure and contain multiple blebs stabilised by an F-actin framework (*Figure 3.1-B*) and could be more precisely described as "blebbopodia".

3.2. Blebbing emerges in *Dictyostelium* cells as they progress through the developmental program.

I found out that blebs are rare in growing (vegetative) *Dictyostelium* cells, but become progressively more common after cells are starved and enter their developmental program. Blebs are normally not observed in randomly moving vegetative cells, and stimulation of these cells with a chemoattractant – folate – causes blebbing only in about 5% of cells – *Figure 3.3-C,D*; whereas stimulation of cells after about 5 hours of development with a chemoattractant – cyclic-AMP – induces blebbing in 50-60% of the cells – *Figure 3.3-A,B*. Blebbing becomes more pronounced during development, and by the onset of the multicellular stages of development most cells employ blebbing for their migration. Particularly, for the cells leading small streams, blebbing motility appeared to be more often the rule than the exception (*Figure 3.1-C*).

We hypothesised that at later stages of development cells modify their migration strategy to provide higher locomotory forces, since developing cells

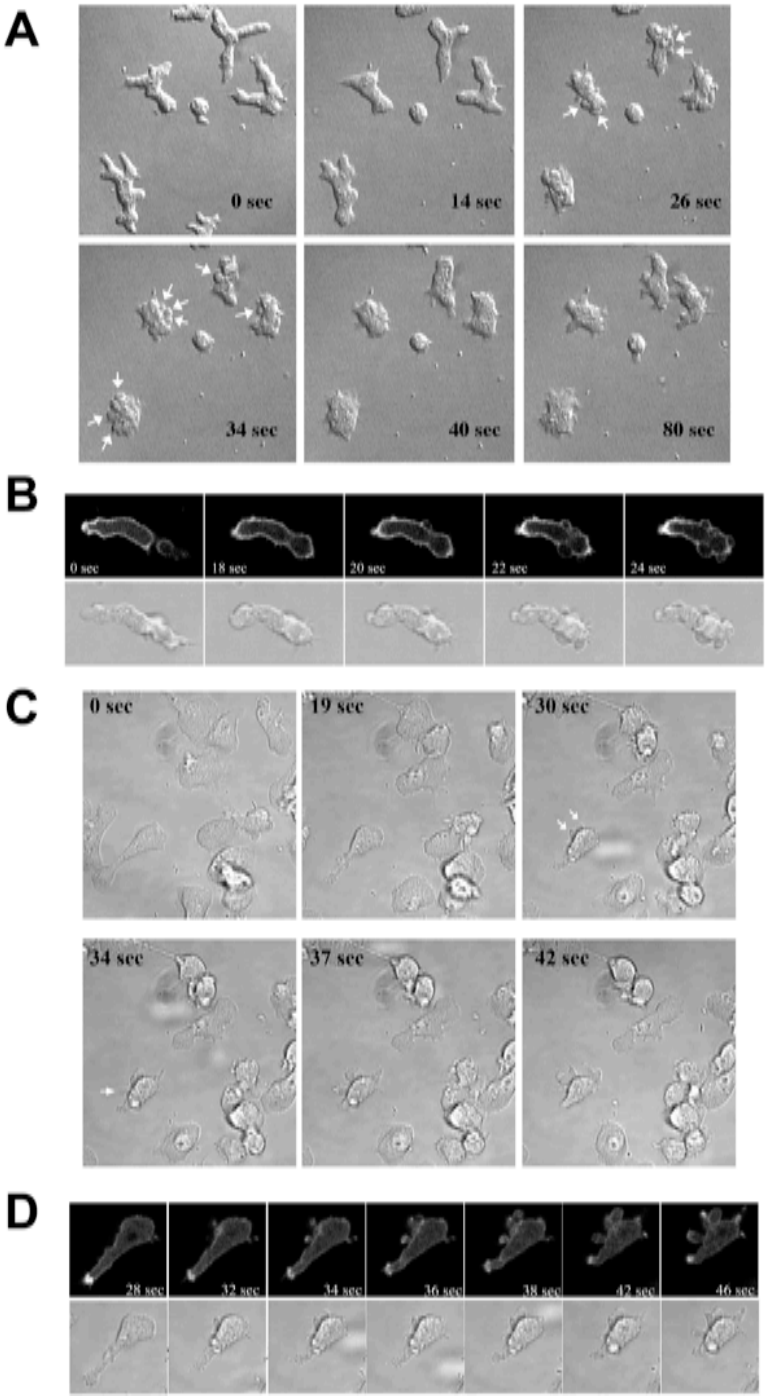

Figure 3.3. **Blebbing in aggregating and vegetative cells.**

(A), (B) – aggregation competent *Dictyostelium* cells stimulated uniformly with chemoattractant cyclic-AMP (1 μM) demonstrate a transient phase of burst-like blebbing (cells were starved for 4.5 hr with pulsing by cyclic-AMP); (C), (D) – only small proportion of vegetative cells produce blebs in response to stimulation with chemoattractant folate (30 μM). (B), (D) – examples of blebby cells (aggregation competent and vegetative, respectively), DIC and fluorescence (ABD-GFP) images.

become more adhesive, often have to take part in a collective migration and later move through the resistive multicellular structures. Blebs might allow cells to employ the hydrostatic pressure of cytoplasm when elastic forces of F-actin branches are not sufficient to drive cell locomotion. Hence, blebbing could provide additional forces for cells migrating in streams and particularly in moving slugs, in a similar way as some motile mammalian cells and invasive tumours switch to a blebbing mode of migration when facing non-degradable three-dimensional matrices (see Chapter 1.2.2). Thus the increase in blebbing during cell development might play a role in preparation for movement within the multicellular structures.

3.3. In resistive environments cells can switch entirely to a "blebbing mode".

Given the above observations, and since blebbing motility is most commonly observed in other cell types when cells migrate through a resistive three-dimensional tissues or matrices (Trinkaus, 1973; Sahai and Marshall, 2003; Wolf et al., 2003; Blaser et al., 2006; Otto et al., 2011), we hypothesised that blebbing-motility might be adopted as a direct response of cells to the mechanical resistance of their environment. To test this idea, we examined *Dictyostelium* cells moving against increased mechanical resistance, which was provided by an agarose overlay (Laevsky and Knecht, 2001). In the conditions of such an under-agarose assay, chemotaxing cells had to resist the pressure of an agarose gel, squeeze their bodies under the agarose layer and to produce high forces in order to deform the agarose and make their track in the direction of a chemoattractant gradient. Agarose in these experiments had a Young's modulus similar to soft tissues (Balgude et al., 2001).

In our experiments, *Dictyostelium* cells, expressing an F-actin reporter ABD-GFP, were plated on plastic coverslips and attracted under agarose overlays of varying stiffness (0.5%-2.5% agarose) by a gradient of cyclic-AMP (see Chapter 2.4.2.3). The effect observed was dramatic: once under the agarose,

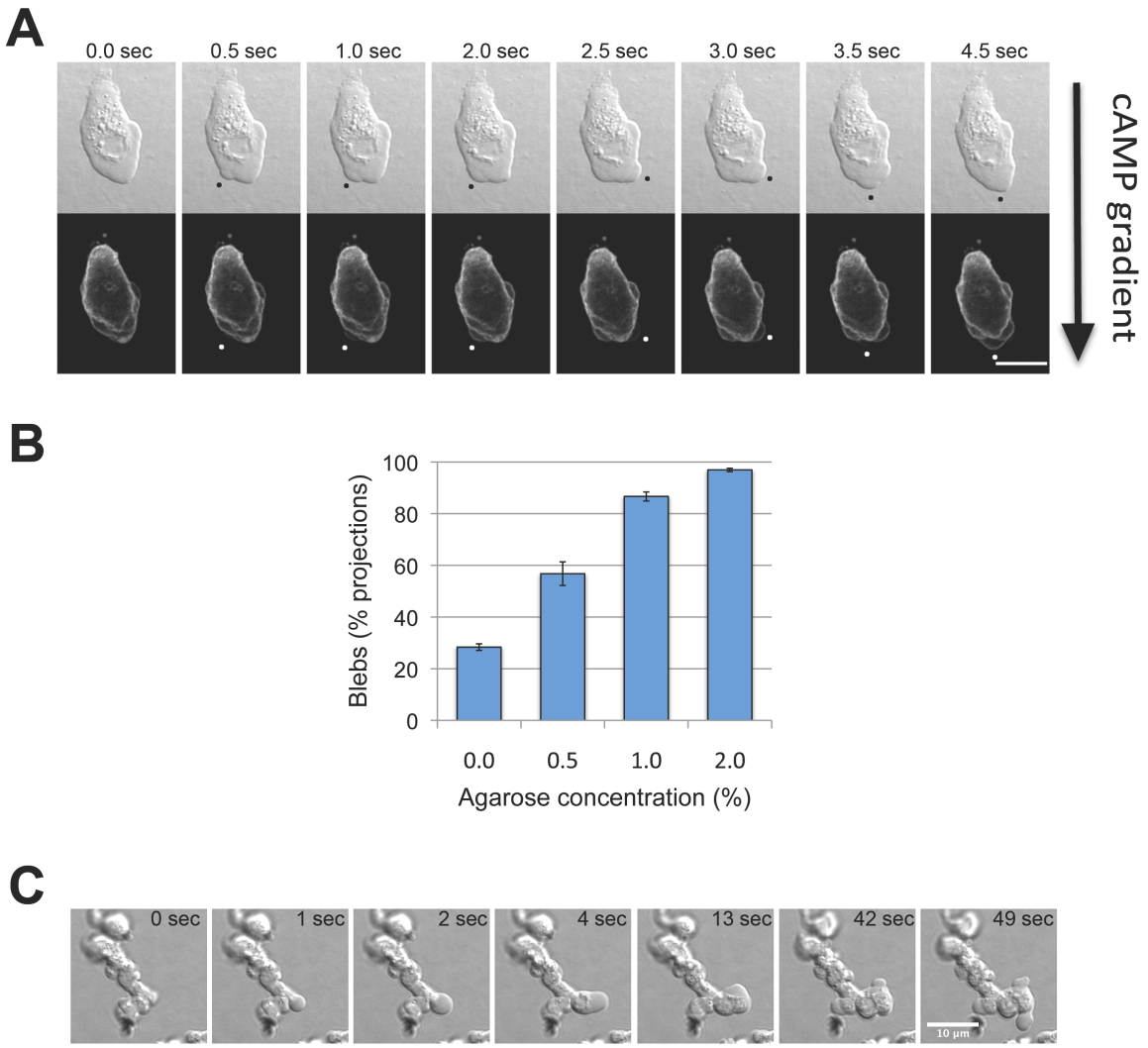

Figure 3.4. **Bleb-driven motility is favoured by mechanical resistance.**

(A) DIC and fluorescence (ABD-GFP reporter for F-actin) images of an Ax2 cell moving on glass under agarose and towards cyclic-AMP: a cell is moving in pure bleb mode under 0.7% agarose; note the rapid expansion of blebs (indicated by black or white spots) and the F-actin scars; (B) cells progressively switch to bleb-driven motility as they encounter increasing mechanical resistance, which is provided by an agarose overlay of increasing strength; (C) Ax2 cells embedded inside 0.5% agarose lattice also move by producing multiple blebs. Ax2 cells were starved for 4.5 hr with pulsing by cyclic-AMP. Bar = 10 microns

cells started moving predominantly using blebs instead of F-actin driven pseudopodia (*Figure 3.4-A*). The balance between F-actin driven projections and blebs shifts towards bleb motility as the stiffness of the agarose increased. And at agarose concentrations above 1% cells move almost entirely in a "blebbing mode" (*Figure 3.4-B*). As controls for chemical specificity, we found that cells moving on top of agarose did not switch to blebbing motility, whereas those moving under a layer of washed polyacrylamide gel did. Cells embedded in agarose lattices likewise moved with blebs, showing that blebbing does not depend on a glass/agarose interface, and any flattening of the cells that may result (*Figure 3.4-C*). Thus *Dictyostelium* cells can readily adapt their movement mode to the environment and adopt an almost pure bleb-driven mode when faced with sufficient mechanical resistance to their movement.

It was previously shown that myosin II activity is required for blebbing in *Dictyostelium* cells (Langridge and Kay, 2006; Yoshida and Soldati, 2006). We have confirmed that cells lacking either of the myosin regulatory (MlcR) or essential (MlcE) light chains or the myosin heavy chain (MhcA) cannot produce blebs in response to a cyclic-AMP shock (where they are suddenly stimulated with a saturating dose of cyclic-AMP; *Figure 3.5-A*). Accordingly, they also cannot make blebs when migrating under buffer, and even in under-agarose conditions they rely on F-actin driven pseudopodia to move, being unable to produce blebs (*Figure 3.5-B*). This is reflected by their low speed of under-agarose migration compared to a wild type (*Figure 3.5-C*). These experiments on under-agarose chemotaxis of myosin II deficient cells show that cells, incapable of myosin contraction and, as shown in blebbing-assay experiments, unable to bleb, migrate slower in resistive environments than cells with a normal myosin function. This result strongly suggests that blebbing not only accompanies under-agarose cell migration but is indeed required for effective cell movement in such resistive environments.

In apparent contradiction to this result, Laevsky and Knecht (Laevsky and Knecht, 2003) did not find any significant difference between the under-agarose movement speeds of normal *Dictyostelium* cells and the myosin II essential light chain null mutant. However, this result can be reconciled with our

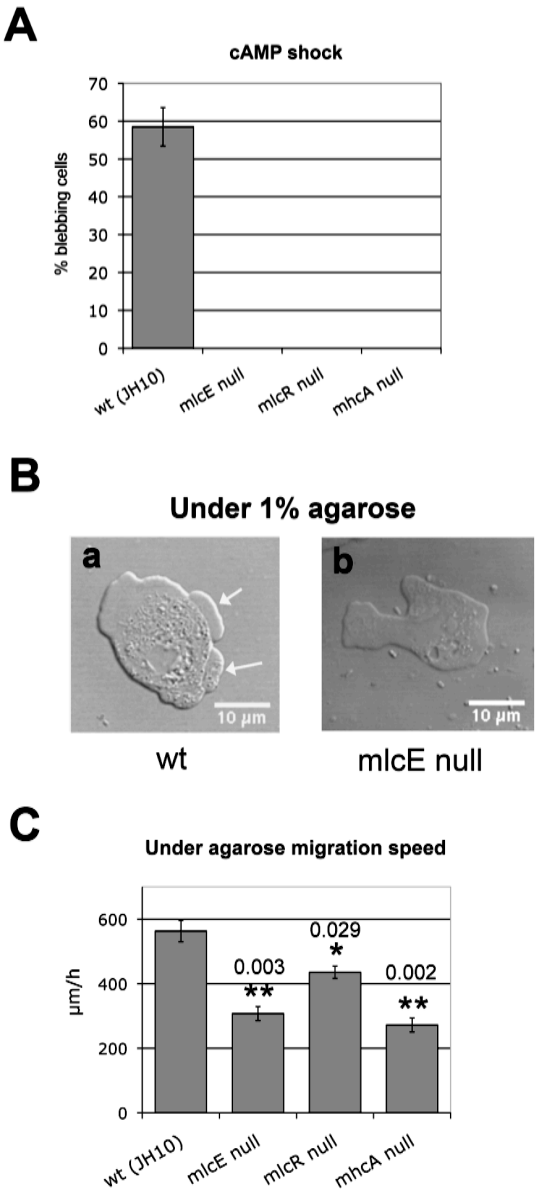

Figure 3.5. **Blebbing is required for efficient cell migration in resistive environments.**

(A) Cells lacking myosin II activity cannot produce blebs. Strains with a knock-out of one of the myosin II chains (essential light chain – *mlcE*, regulatory light chain – *mlcR* or heavy chain – *mhcA*) were stimulated with 1µM cyclic-AMP (cAMP shock), and the proportion of blebbing cells was counted. (B) A representative example of wild type (wt) and *mlcE* null cells migrating under 1% agarose. Cells lacking either of the myosin II chains do not make blebs and migrate by F-actin protrusions, wt cells migrate in a blebbing mode. White arrows indicate blebs. Bars = 10 µm. (C) Cells lacking myosin II activity demonstrate lower speeds of under-agarose chemotaxis. Data are shown as mean ± SEM for three independent replicates. Mutant strains were compared to the wt (p-values are indicated above the bars), * $p<0.05$; ** $p<0.01$.

hypothesis, since these authors studied the migration of vegetative cells in folate gradients. And as described above, blebs are rare in vegetative cells and therefore they could not contribute significantly to cell migration in the Laevsky and Knecht experiments. When these cells chemotax towards folate they migrate exploiting exclusively F-actin driven protrusions, and the absence of active myosin II does not really affect the speed of their migration. As opposed to this, in our aggregation-competent cells, cyclic-AMP induces blebbing, and wild-type cells migrate in a blebbing mode. Thus, in the experiments, performed by Laevsky and Knecht, both normal and myosin II mutant cells were unable to bleb – and as a result there was no difference in their under-agarose speed. But aggregation-competent cells used in our experiments, to the contrary, demonstrated significant difference between non-blebbing myosin mutants and blebbing normal cells. Interestingly, myosin II mutants, which are unable to form blebs, undergo developmental arrest at the tip-less mound stage (Carrin et al., 1996). This may be explained by the described idea that blebbing is required to provide the forces needed for cells to migrate within the multicellular stages formed later in development.

3.4. Blebs can be distinguished from other types of cell projections by a number of objective characteristics.

The above result produces a convenient system to study the properties of blebs: in under-agarose experiments cells form multiple blebs that can be observed with high speed (at least 2 Hz) microscopy using the ABD-GFP reporter to visualise the F-actin scar remaining behind the detached membrane in a bleb (other markers for F-actin – such as LifeAct-GFP (Riedl et al., 2008) – produced similar results, data not shown). We used the spinning-disc confocal microscope for high-speed image acquisition (6 Hz) and added a fluorescent dye (RITC-dextran) to the agarose for negative staining to visualise the cells outlines – *Figure 3.6*. These experiments have shown that bleb expansion phase lasts for only about half a second, and its consolidation or retractions takes only 2-5 seconds. In most cases blebs appeared as spherical caps with a height of 0.93 ± 0.11 μm (average bleb surface area is about 8.3 μm^2,

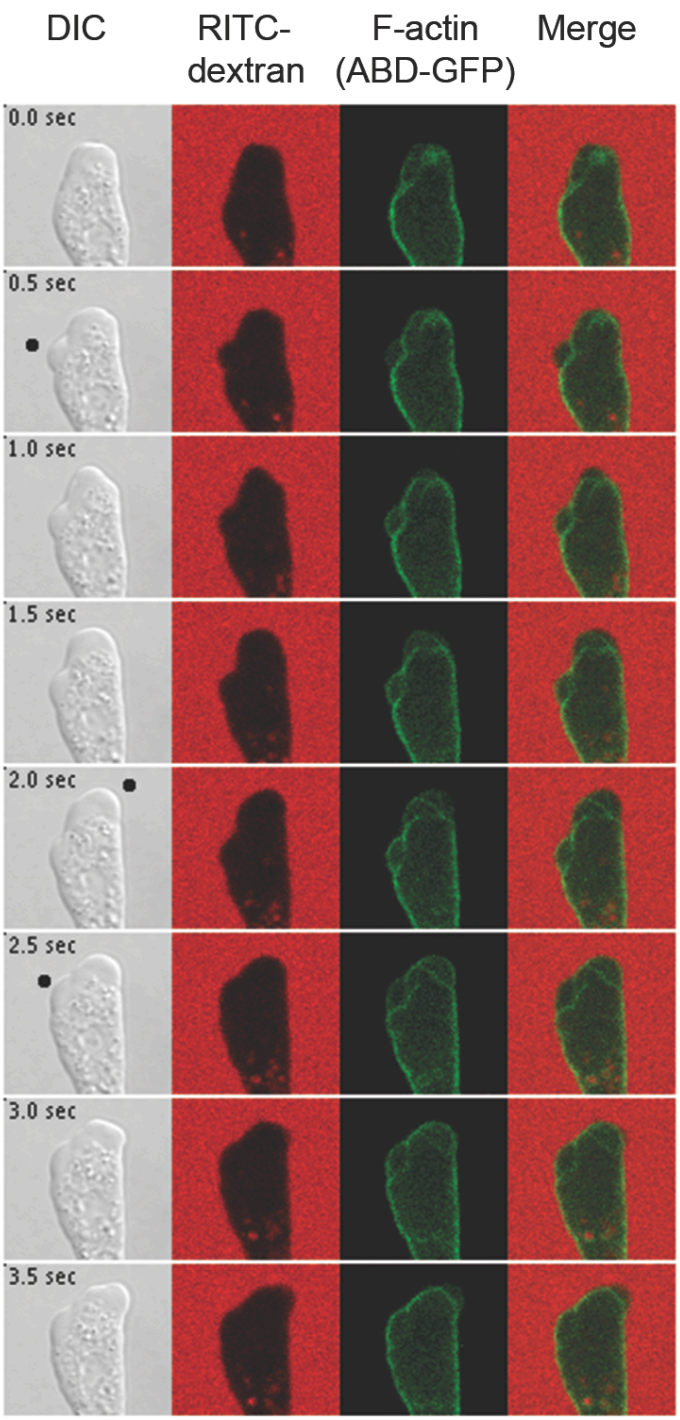

Figure 3.6. **Dynamics of bleb formation under agarose.**

Ax2 cells expressing an F-actin reporter (ABD-GFP) were starved for 4.5 hr with pulsing by cyclic-AMP and then observed under 0.7% agarose containing RITC-dextran florescent dye to reveal the cell outline. Blebs (indicated by black spots) expand in less than half a second, have a smooth surface and leave an F-actin scar at the base.

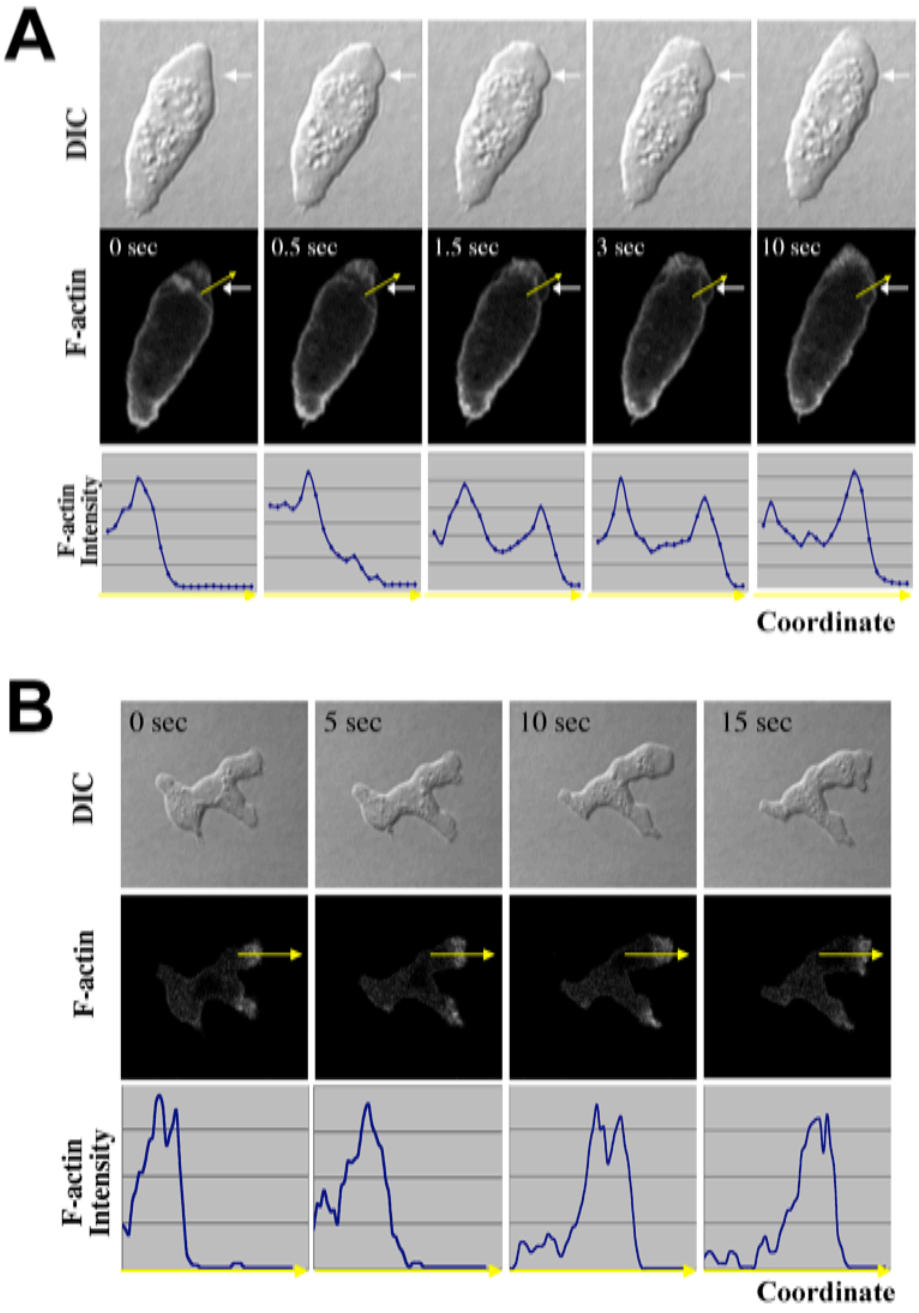

Figure 3.7. **Different F-actin dynamics in blebs and pseudopodia.**

(A), (B): top rows - DIC images of Ax2 cells moving under 0.5% agarose; middle - fluorescence of the ABD-GFP reporter; bottom - F-actin distribution along the line of growth of the protrusion (yellow arrows on middle panels). White arrows on panel (A) indicate the site of bleb formation. During their first moments of existence, blebs lack an F-actin cortex under the membrane. Shortly thereafter, bleb growth ceases and reassembly of the cortex starts apparent as a new layer of F-actin under the membrane. Thus, during bleb formation one can observe the disassembly of an old F-actin layer and the assembly on a new one, whereas during pseudopod growth the same layer of F-actin moves gradually in the direction of pseudopod protrusion.

which is about 1.8% of total cell surface area; and average bleb volume is 3.0 μm^3, which is about 0.5% of total cell volume). Under a DIC microscope the surface of blebs looks smoother compared to other parts of the cell and other protrusions, apparently because the body of the blebs does not contain any F-actin structures, and the F-actin scar remaining at the base of the blebs obstructs the flow of organelles and vesicles into the bleb area (*Figure 3.1-A, 3.6, 3.7-A*).

Manual analysis shows that blebs expand at a speed of about 2 μm/sec (up to a maximum of 5 μm/sec), which is on the average 3-4 times faster than is typical for F-actin driven protrusions. The F-actin dynamics in hydrostatically driven blebs is also very different from F-actin driven protrusions (*Figure 3.7-B*): when the plasma membrane detaches from the cortex, the new cortex starts to re-polymerize at the new position of the membrane, and the old layer of cortex represents a scar that gradually dissolves in about 5 seconds. In contrast, during the growth of F-actin driven protrusions, F-actin is constantly present under the membrane and expands gradually (without disappearance in one place and reappearance in another), often increasing the F-actin layer thickness at the leading edge during the expansion.

Thus, blebs can be readily distinguished from F-actin driven protrusions by objective criteria according to their dynamic properties: high speed and absence of F-actin under the membrane during the expansion phase, as well as smooth surface and often a spherical shape.

Once formed, a bleb can be either retracted through local acto-myosin contraction or stabilised by the newly rebuilt F-actin cortex and rapidly forming adhesion contacts. Visualisation of the cells moving under agarose in a bleb-driven mode using TIRF microscopy with paxillin-GFP as a reporter for adhesion sites showed that rapid phases of cell expansion (bleb formation) are alternated with periods of discontinuous adhesion contacts establishment (*Figure 3.8*). This is similar to the step-wise “walking mode” of amoeboid migration described in the literature (Jacobelli et al., 2009).

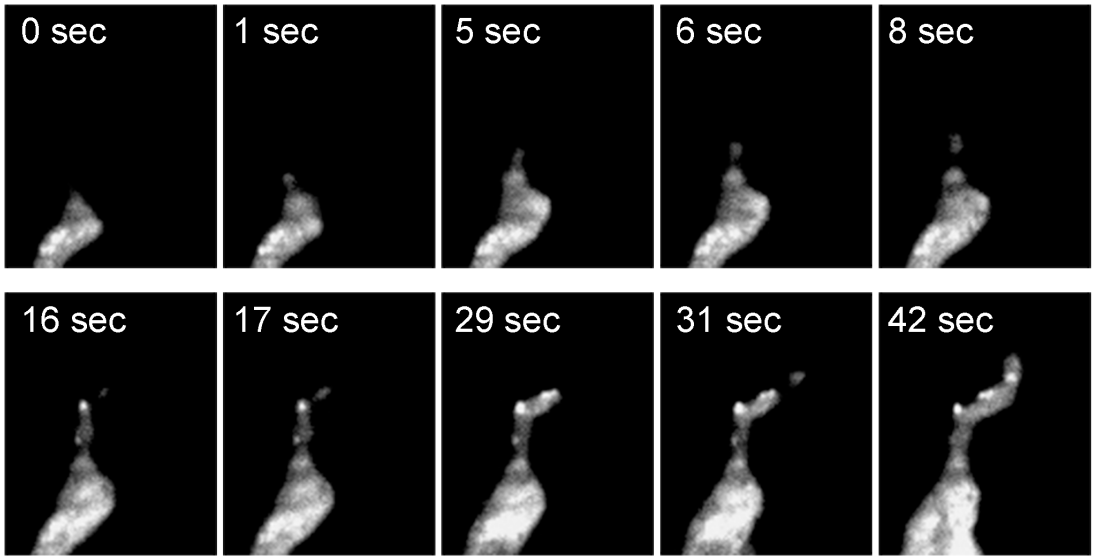

Figure 3.8. **In cells moving under agarose, blebs are stabilised by discontinuous adhesion contacts with the substrate.**

Cells moving along a cyclic-AMP gradient under 1.0% agarose in a bleb-driven mode were visualized using TIRF microscopy with paxillin-GFP as a reporter for adhesion sites. During blebbing movement, rapid phases of cell expansion (blebs growth) are alternated with the periods of discontinuous adhesion contacts formation (bleb stabilization).

CHAPTER 4. Automated analysis of blebs in chemotaxing *Dictyostelium* cells (collaboration with Richard Tyson).

We have utilised the QuimP10 software based on the electrostatic contour migration method (ECMM; (Tyson et al., 2010)) to analyse the fast and small displacements of plasma membrane during blebbing and to describe the F-actin dynamics in these structures (in collaboration with Dr. Richard Tyson and Dr. Till Bretschneider, University of Warwick). In order to minimize the cell outline segmentation noise during the automated image analysis, the time-lapse series of fluorescence images collected using the laser scanning or spinning-disc confocal microscopes were pre-processed to remove fluctuations in intensity over the length of a sequence and to correct uneven illumination see "Materials and Methods", section 2.4.3, *Figure 2.2*). Bleb dynamics were analysed in under-agarose assays using an agarose concentration of 0.7%, which permitted both blebs and actin-driven projections to form. RITC-dextran was added to the agarose for better cell contour detection (*Figure 3.6*).

4.1. Blebs and F-actin driven protrusions have different signatures on motility maps and fluorescence kymographs.

Using the QuimP software for automatic cell outline segmentation and tracking, we created motility maps illustrating the speeds of different membrane protrusions from the cell surface over time, as well as fluorescence kymographs for ABD-GFP showing the amount of F-actin underlying the plasma membrane, and curvature maps (*Figure 4.1-A-C*). On these maps, the horizontal axis represents position on the cell perimeter, and the vertical axis (directed downwards) is time. Speed of projections and fluorescence intensity are illustrated by pseudocolour and the brightness of the corresponding pixels.

In concordance with the previous observations, blebs appear on motility maps as high-speed but short-lifetime projections distinctly standing out against the background (*Fig 4.1-A*, higher magnification – *Figure 4.1-D*). Their speed peaks within less than one second and after that their expansion quickly ceases (*Figure 4.2-A,B*). F-actin driven pseudopodia have a clearly different appearance on these maps – they propagate for longer periods of time and have lower

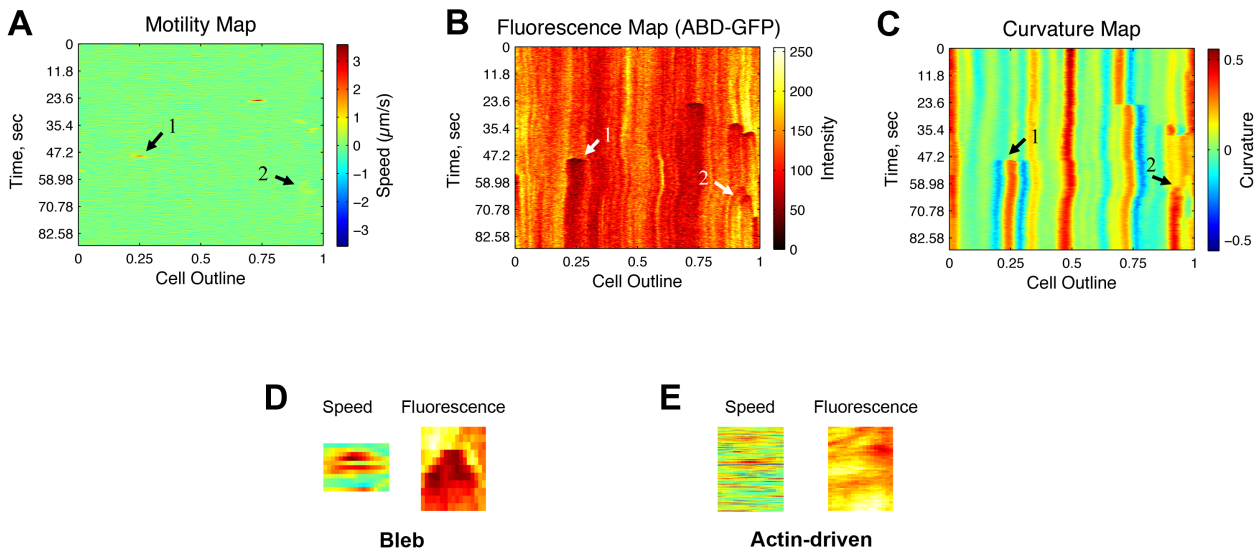

Figure 4.1. **Motility, fluorescence and curvature maps for different cell protrusions.**

(A) Motility map illustrates the speeds of membrane displacement at different points around the cell perimeter; (B) Fluorescence map shows the amount of F-actin reporter ABD-GFP at the membrane; (C) Curvature map demonstrates the concavity (negative curvature) or convexity (positive curvature) of different regions of the cell membrane. Arrow with the number "1" indicates a bleb formation. It is characterised by high speed and short lifetime on motility map, loss of F-actin at the membrane on fluorescence map and positive curvature on top of the protrusion and negative - on the sides on curvature map. Arrow number "2" indicates a pseudopod growth. It is a long-living, low-speed protrusion enriched with F-actin and characterised by positive curvature. (D), (E) – higher magnification motility and fluorescence maps for a bleb (D) and a pseudopod (E). Ax2 cells transformed with F-actin reporter ABD-GFP were starved, imaged under 0.7% agarose containing RITC-dextran, and the images analysed using QuimP software for cell outline segmentation, tracking and analysis.

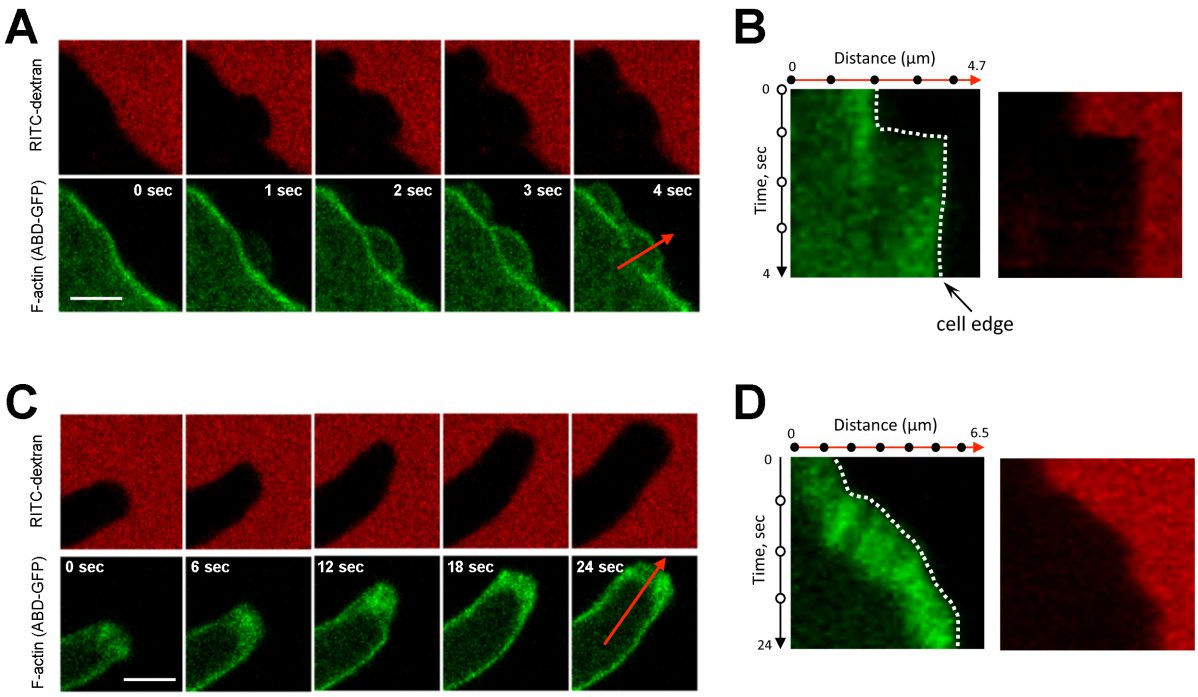

Figure 4.2. **Blebs and pseudopodia growth under agarose.**

(A), (C) – image series illustrating a bleb and a pseudopod growth under agarose, respectively. (B), (D) – space-time plots (kymographs) illustrating F-actin dynamics in the growing bleb and the pseudopod, respectively. Distribution of ABD-GFP (green) and RITC-dextran (red) are shown along the line, normal to the surface of the protrusion and shown as the red arrow on panels (A) and (B), respectively. Ax2 cells expressing an F-actin reporter (ABD-GFP) were starved for 4.5 hr with pulsing by cyclic-AMP and then attracted with cyclic-AMP under 0.7% agarose containing RITC-dextran for cell outline visualization. Bar = 1 μm.

speeds that are harder to distinguish from the background segmentation noise (*Figure 4.1-A,E* and *4.2-C,D*). Despite image pre-processing, motility maps still contain significant noise, which sometimes can obscure the profiles of pseudopodia extension.

Since blebs are F-actin free during their expansion phase, they appear on ABD-GFP fluorescence maps as arc-shaped dark streaks corresponding to their location (*Figure 4.1-B,D*). As opposed to blebs, F-actin driven protrusions have bright traces running a long way diagonally on fluorescence kymographs.

4.2. Speed and magnitude of membrane displacement in blebs and pseudopodia.

In trying to automatically measure the speed of membrane protrusion in blebs and pseudopodia, we faced certain difficulties. Basically, the problem was to develop a universal approach that would be suitable for different types of projections, very diverse in their speed. So, highly dynamic blebs require membrane tracking from image sequences taken at a frequency of at least 2-3 frames per second. At the same time, F-actin driven pseudopodia progress several times slower than blebs, and therefore, trying to track them from high frame rate image sequences would produce a significant error, because the membrane displacement between frames would be comparable with membrane fluctuations and the noise produced by cell outline segmentation algorithm.

Figure 4.3-A shows an example of automatic speed measurements for a bleb and an F-actin driven pseudopod from a time-lapse image sequence taken at 4.5 frames per second. We have determined the peak speed of protrusions either as the maximum speed within a raw motility profile, or the maximum of a 3-frame average. One can see from this example that noise from high frame rate image tracking artificially leads to an overestimation of peak speeds for F-actin driven projections, whereas smoothing on the other hand blurs true peaks present in blebbing.

Trying to overcome these difficulties, we decided to analyse displacement profiles of the observed protrusions (by summing membrane displacements

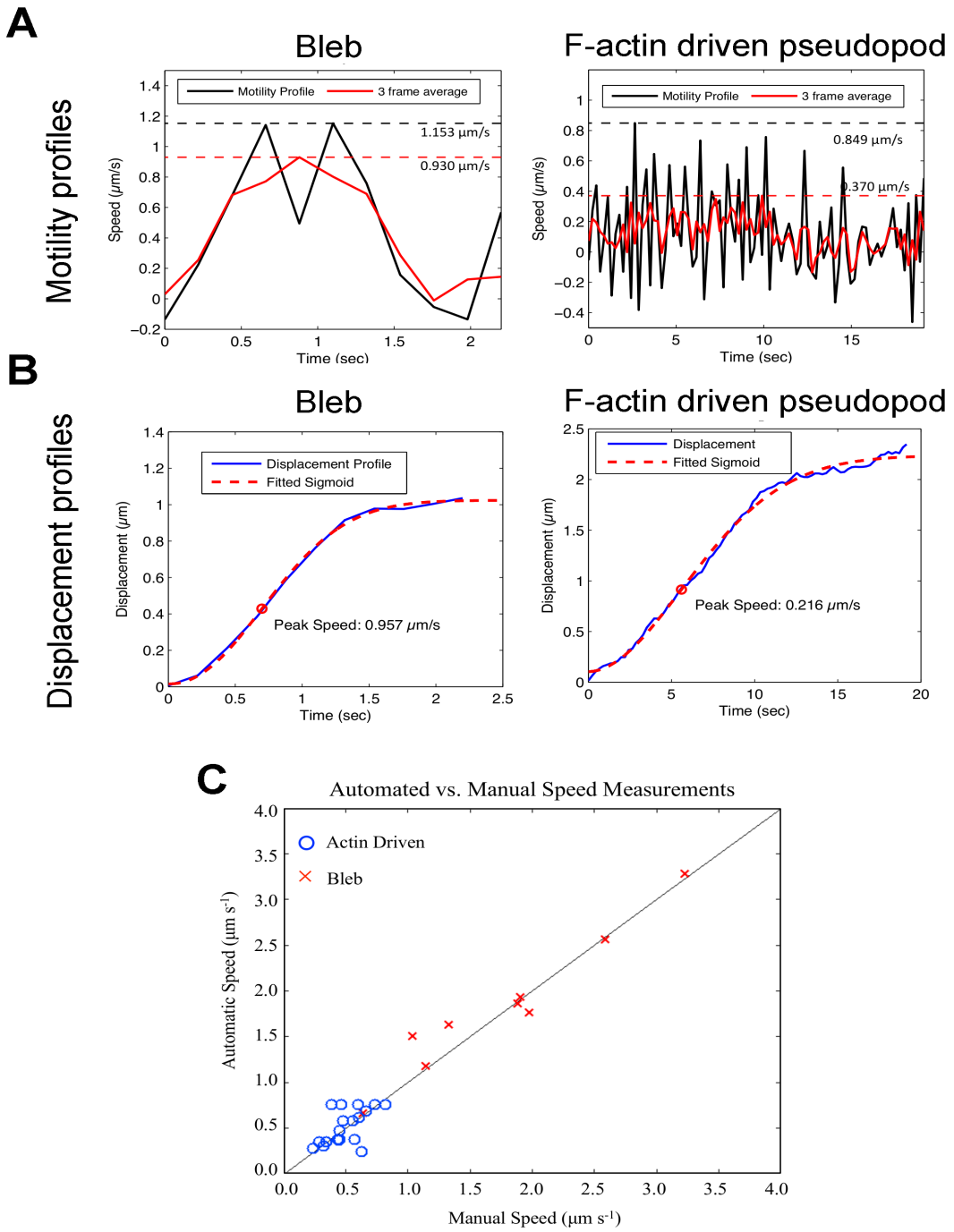

Figure 4.3. **Measurements of the protrusions peak speeds.**

(A) Peak speeds for a bleb and a pseudopod were determined from 4.5 fps image sequences as the maximum values within the raw motility profiles, or the maximum of a 3-frame average. Noise from high frame rate image tracking leads to an overestimation of peak speeds for F-actin driven projections, whereas smoothing blurs true peaks for blebs. (B) Displacement profiles of the observed protrusions fitted with generalized logistic sigmoid curves, and the peak speeds defined as the maximal gradients of these curve. This algorithm produced peak speed values similar to those obtained by manual measurements for a control set of protrusions (C).

over time during protrusion growth) instead of their speed profiles. We fitted the displacement profiles with generalized logistic sigmoid curves, which include an acceleration phase, a steady speed phase, and a deceleration phase, and defined peak speeds as the maximal gradient of this curve (*Figure 4.3-B*). This algorithm produced peak speed values similar to those obtained by manual measurements for a control set of protrusions (*Figure 4.3-C*), thus proving this approach as reliable.

We applied this strategy to compare average speeds of blebs and F-actin driven projections. The measured peak speed of blebs appeared to be 1.78 ± 0.74 μm/sec (mean ± SD, n=37) with the maximal measured value of 4.93 μm/sec. For F-actin driven protrusions the speed is 0.59 ± 0.23 μm/sec (n=88), the fastest one being 1.15 μm/sec. Thus, in most cases these two types of membrane protrusions are objectively distinguishable by their speed.

An additional objective criterion that can be used to automatically distinguish between blebs and pseudopodia is total membrane displacement: blebs are small protrusions that have a short expansion phase, whereas F-actin driven pseudopodia expand for several seconds and produce continuous membrane displacement to distances significantly exceeding bleb sizes. We used the displacement profiles described above to estimate the total membrane displacement (as the maximal value in the displacement profile) and track duration (as the time taken to reach the maximal displacement). We have plotted all identified cell protrusions onto 2D maps showing their speed versus total displacement (*Figure 4.4-A*). It can be clearly seen that blebs and F-actin driven protrusions form two separable regions on this scatter plot: blebs have higher speed but small length of membrane displacement, whereas F-actin driven structures expand more slowly but cover longer distances. Interestingly, for blebs there is a positive correlation between their size and speed. This can probably be explained by the mechanics of bleb formation: the higher the force that induces bleb formation, the faster bleb expands and the larger size it reaches before the force is equilibrated.

As a control for our mapping strategy, we analysed in a similar way the MlcE null strain of *Dictyostelium*, which lacks the essential myosin light chain gene (*mlcE*), and compared it to the wild-type Ax2 strain. The MlcE null cells lack

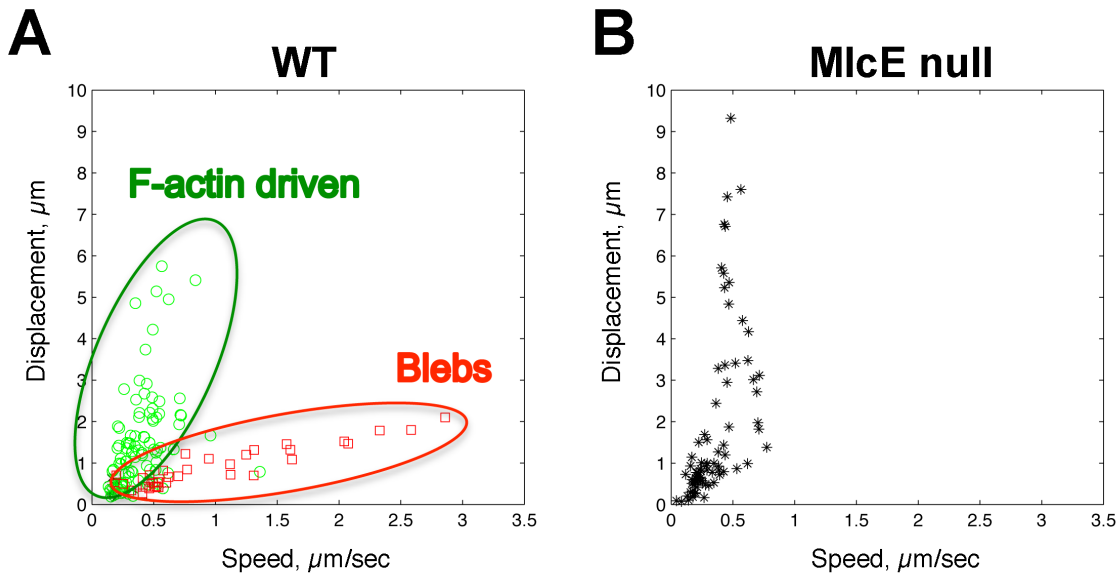

Figure 4.4. **"Speed vs Displacement" distribution of blebs and actin-driven protrusions.**

(A) In the wild-type strain of *Dictyostelium* (Ax2), blebs and F-actin driven protrusions form two separable regions on the scatter plot: blebs are characterized by higher speeds but small magnitudes of membrane displacement, whereas F-actin driven structures expand more slowly but cover longer distances. Protrusions speeds and displacements were measured automatically by the QuimP software. Classification of the protrusions was done manually and independently from the automated characterisation. (B) The MlcE null cells lack myosin II contractile activity and cannot produce blebs under the experimental conditions utilized. Accordingly, all protrusions identified in these cells by the automatic tracking algorithm, grouped on the scatter plots in the area corresponding to the F-actin driven protrusions, and no points were found in the high-speed region of the map, where blebs lie in the wild-type strain.

myosin II contractile activity and cannot produce blebs under the experimental conditions utilized. Accordingly, all protrusions identified in these cells by the automatic tracking algorithm, grouped on the scatter plots in the area corresponding to the F-actin driven protrusions, and no points were found in the high-speed region of the map, where blebs lie in the wild-type strain (*Figure 4.4-B*). Importantly, in MlcE null cells, even projections that were identified as F-actin driven had a speed of expansion significantly lower than the same type of protrusions in the wild-type strain (average values: 0.49 μm/sec in MlcE null versus 0.67 μm/sec in the wild-type). This supports the idea that pseudopodia are normally driven by a hybrid motor that involves intracellular hydrostatic pressure as well as F-actin polymerization.

4.3. F-actin dynamics in blebs.

An important feature distinguishing blebs from other cell protrusions is the absence of F-actin during their expansion phase. Therefore, we used the QuimP membrane tracking software to analyse the amount of F-actin underlying the plasma membrane (using the confocal images of F-actin reporter ABD-GFP). ABD-GFP fluorescence drop should be a reliable criterion allowing a bleb to be distinguished from an F-actin driven pseudopod. We estimated the percentage fluorescence drop by comparing the ABD-GFP level at the membrane just before the protrusion starts to expand and the minimal fluorescence level during first 2 seconds of expansion. An interval of 2 seconds was chosen to allow plasma membrane to separate completely from underlying cortex (since the utilized software measures the maximum intensity values within a set membrane width, a drop in ABD-GFP intensity will not be apparent until a bleb membrane has displaced sufficiently to escape the F-actin scar remaining behind).

The analysis has revealed a 78.0 ± 6.3 % fluorescence drop of ABG-GFP in expanding blebs, and only 15.5 ± 16.7 % in pseudopodia. This observation provides a clear segregation between these two types of protrusions, which is confirmed by “Speed vs. F-actin drop” scatter plots – *Figure 4.6-A*. In these plots, blebs and pseudopodia form two separable groups of points: high-speed blebs

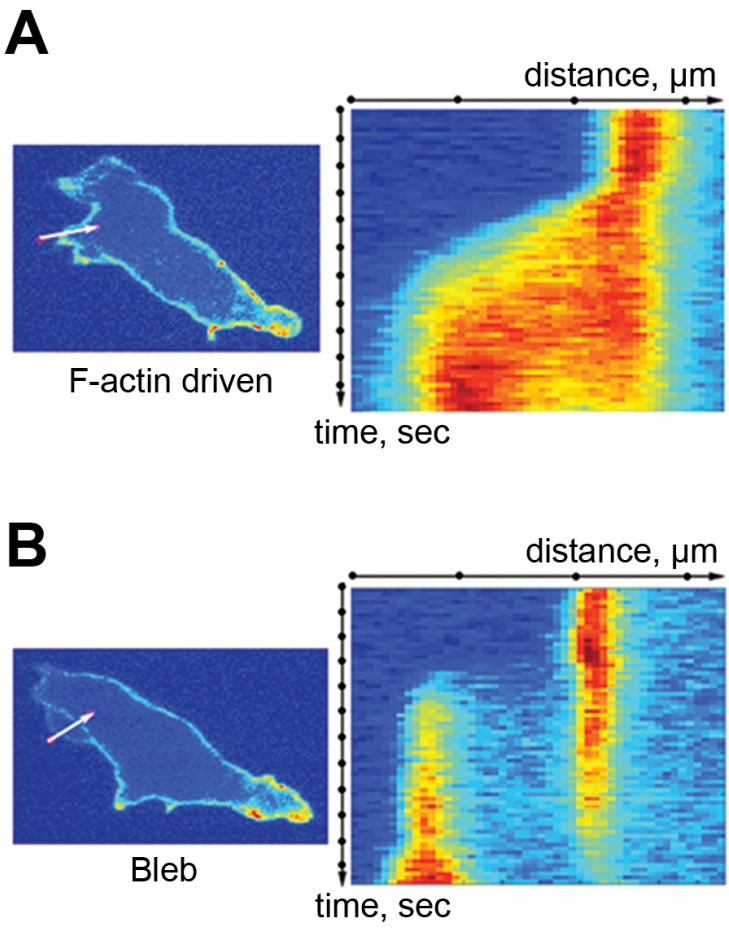

Figure 4.5. **Space-time plots comparing an F-actin driven process with a bleb.**

The fluorescence intensity of an F-actin reporter was measured along the protrusion paths (arrowed lines). It is apparent that F-actin is present continuously at the membrane of an F-actin driven projection (A) but not a bleb, where the F-actin scar is readily apparent (B). Ax2 cells expressing an F-actin reporter (ABD-GFP) were starved for 4.5 hr with pulsing by cyclic-AMP. They were observed under 0.7% agarose containing florescent dye to reveal the cell outline and analysed using the QuimP software.

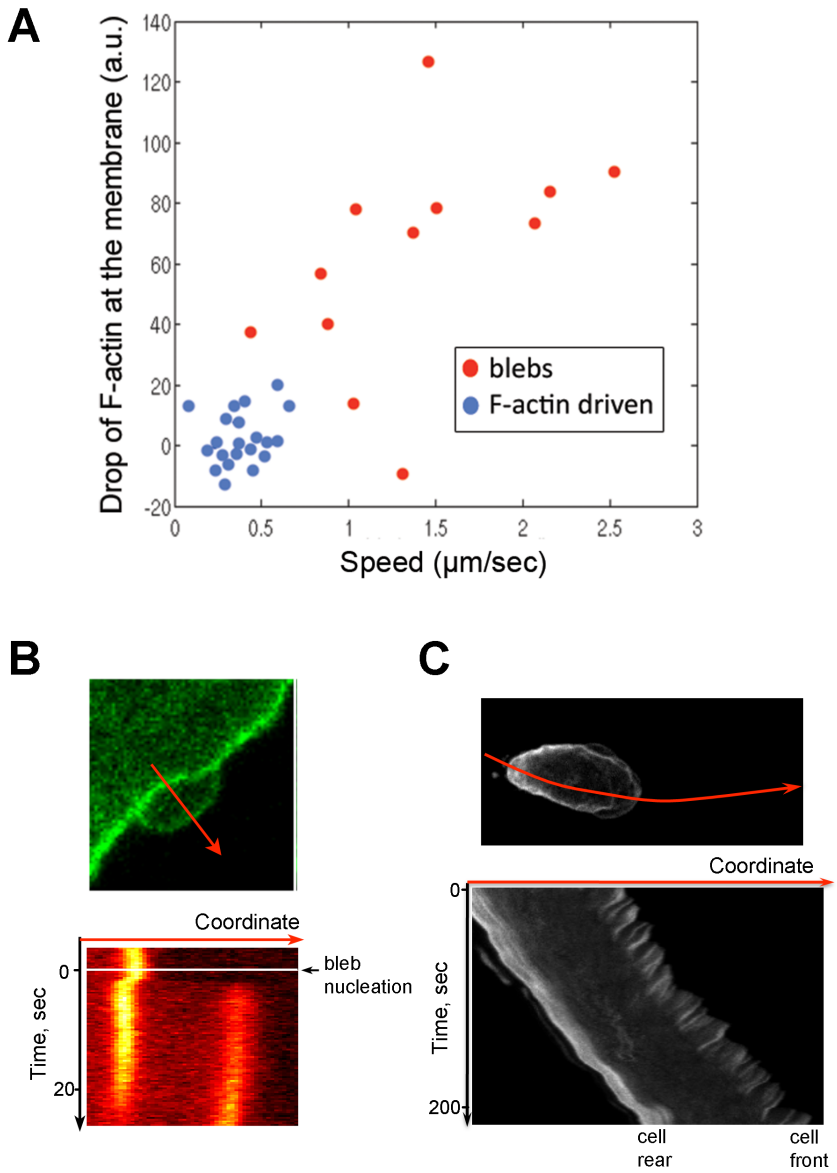

Figure 4.6. **F-actin dynamics in the blebs.**

(A) Blebs and pseudopods were identified by eye, and their speed of projection and the drop in membrane-associated F-actin content at the time of projection compared. It is apparent that blebs are projected 3-4 times faster than F-actin driven pseudopods (blebs: 1.5 mm/sec; F-actin driven pseudopods: 0.4 mm/sec) and that there is nearly always a large drop in F-actin at the membrane when they are projected. (B) A space-time plot showing F-actin distribution across the bleb (along the red arrow): a fast retrograde movement of the actin scar can often be observed at the moment of bleb formation. (C) A space-time plot of F-actin distribution along the cell path (red arrow): gradually dissolving actin scar demonstrates further flow towards the interior of the cell but with a lower speed. Ax2 cells expressing an F-actin reporter (ABD-GFP) were starved for 4.5 hr with pulsing by cyclic-AMP. They were observed under 0.7% agarose.

are characterized by a large drop in F-actin reporter fluorescence, whereas slow pseudopodia demonstrate a small, if any, ABD-GFP decrease.

Kymographs of ABD-GFP distribution along a line normal to the membrane demonstrate that during the phase of rapid expansion blebs don't contain detectable F-actin. When the expansion ceases a new cortex is rebuilt at the new position of the plasma membrane, whereas the old layer of F-actin remains in the base of the bleb as a scar, which after a certain delay (2-5 seconds) starts to disassemble (*Figure 4.5-B, 4.6*). The time of disassembly varies greatly from bleb to bleb – between 3 and 45 seconds, and has non-linear dynamics. Interestingly, in most cases there is a fast retrograde shift of the F-actin scar during the short period of bleb expansion (*Figure 4.6-B*), followed by a slower retrograde flow during the disassembly phase (*Figure 4.6-C*).

4.4. Blebs preferentially form in concave regions of the cell surface.

Besides membrane motility and fluorescence maps we also used the QuimP software to produce curvature maps of the cell surface. We performed the averaging of cell surface curvature over 1 μm windows and represented it as normalised values in the range [−1, 1] (negative curvature values corresponding to concave regions) – *Figure 4.1-C*. Formation of either blebs or F-actin protrusions locally increased the membrane curvature by the values of about 0.3 ± 0.1. Both these types of cell projections have positive values of membrane curvature on their tops but blebs often have small regions of negative curvature on their sides.

Further analysis has shown that blebs preferentially form in the concave regions of the cell surface: an average curvature in the areas of bleb formation is –0.124 ± 0.104 (mean ± SD). For F-actin driven projections this value is +0.100 ± 0.100. Examination of the "Speed vs. Curvature" scatter plots (*Figure 4.7-A*) reveals that for blebs there is a correlation between these two parameters: higher speed blebs emanate from the areas with higher concavity. These observations suggest that the strain caused by curvature in the plasma membrane contributes to the forces that initiate and drive bleb expansion.

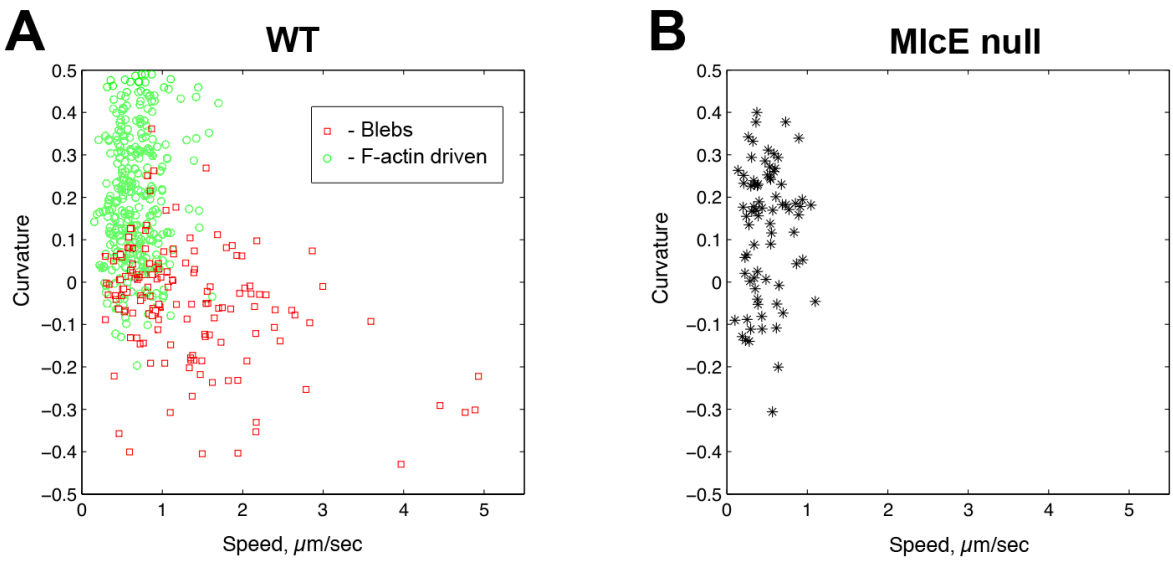

Figure 4.7. **"Speed vs Curvature" distribution of blebs and actin-driven protrusions.**

(A) Automated protrusions analysis in the wild-type cells reveals that blebs preferentially form in the concave regions of the cell surface (where curvature values are negative). Furthermore, higher speed blebs usually emanate from the areas with higher concavity. (B) In the MlcE null cells, where blebbing is suppressed, most projections form in the cell regions of positive or zero membrane curvature. Scatter plot, showing membrane protrusions produced by these cells, lacks the group of points lying in the negative curvature area, which corresponds to blebs in the wild-type strain plots.

In the MlcE null cells, where blebbing is absent, most projections form in the regions of positive or zero membrane curvature. “Speed vs. Curvature” scatter plots, showing membrane protrusions produced by these cells, lack the group of points lying in the negative curvature area that normally corresponds to blebs in the wild-type strain plots (*Figure 4.7-B*).

4.5. Discussion: Blebs and F-actin driven protrusions present two different types of chemotactic cell projections.

For a long time blebbing had been overlooked in migrating cells. Only recently did it became evident that blebs may be as important for cell movement as F-actin driven pseudopodia and lamellipodia. Partially this oversight may be due to the fact that until recent time cell motility had been mainly studied on flat solid surfaces, whereas blebs seem to be favoured by migration through three-dimensional elastic lattices. Moreover, as evidenced by the *Dictyostelium* example, blebs are very dynamic structures: the phase of their F-actin free expansion in motile cells may last for less that half a second, and immediately after that they rapidly get re-populated with F-actin. And since in many chemotactic studies cell images are acquired with a frequency of one frame per 5-20 seconds, blebs easily could be missed or mistakenly considered as F-actin driven protrusions. One would often need a high-speed microscopy with a good enough spatial resolution in order to identify such non-apoptotic blebs.

Furthermore, as we found in our experiments, in such dynamic cells as *Dictyostelium*, blebs can appear in various shapes depending on the local membrane configuration. And therefore one would need some expertise to be able to identify these blebs, since they sometimes look different from stereotypic spherical protrusions. Generally, here we consider plasma membrane blebs in their broader definition, as cell projections that occur when plasma membrane transiently delaminates locally from the cortex and that are driven by cytosolic pressure and therefore require actomyosin contractility (Charras, 2008).

Accordingly, the main criterion that we used for identifying blebs (especially in the beginning of this study) was the presence of arc-shaped F-actin

scars, marking the pre-bleb position of the cortex, below the newly formed cortical layer. Further we noticed that such protrusions usually expand suddenly and have a hyaline appearance and smooth surface under the DIC microscope. All these features combined allow blebs to be identified with great confidence.

And the automated cell protrusions analysis most convincingly proved that there are two different types of protrusions produced by chemotactic cells. Manual validation of the software-based protrusions sorting results confirmed that these two "populations" of cell projections – blebs and F-actin driven pseudopodia – are clearly distinguishable by a number of objective criteria. Blebs are characterized by a short and rapid expansion phase during which the membrane is depleted of F-actin. Whereas, F-actin driven protrusions, on the contrary, take many seconds to expand, are rich in F-actin and progress, on average, several times slower than blebs.

Hence, results obtained in this study demonstrate that *Dictyostelium* cells have two motors for chemotactic movement – actin polymerization and fluid pressure leading to blebs. This redundancy of motors gives migrating cells a functional robustness and great flexibility to move in different environments.

CHAPTER 5. Chemotactic regulation of blebbing

5.1. Blebs occur preferentially on the up-gradient part of the cell

It was discovered earlier that global stimulation of *Dictyostelium* cells with the chemoattractant cyclic-AMP within 20-30 seconds induces multiple plasma membrane blebbing (Langridge and Kay, 2006), suggesting that blebs themselves might be chemotactic.

We therefore decided to analyse bleb orientation in the cells moving steadily under agarose towards a source of cyclic-AMP. As we have described earlier, such cells switch their mode of movement and produce multiple blebs in the course of under-agarose migration. Analysis of the distribution of such blebs around cell surface revealed a clear and strong chemotactic orientation of blebbing (*Figure 5.1*). Most blebs formed at the front edge of the cell and almost none of them appeared at the rear.

This strongly indicates that blebbing might be regulated by the chemoattractant gradient. But even so, it might be argued that the polarization of blebbing in these cells is a consequence of their stable polarization and is only indirectly controlled by the chemotactic signaling.

5.2. Blebs lead the way during forced cell reorientation

To address the above issue, we performed a reorientation experiment to follow blebbing in the cells that are forced to quickly change their direction due to a rapid change in the chemoattractant gradient (*Figure 5.2-A*). Cells under buffer were attracted towards a micropipette releasing cyclic-AMP, and once they had become elongated and started moving towards this source of chemoattractant, the micropipette was quickly moved to the flank of the cell, inducing the cells to turn (Swanson and Taylor, 1982) – *Figure 5.2-A*. These experiments allowed me to observe blebs in cells that are not strongly pre-polarised in the direction of the chemoattractant gradient.

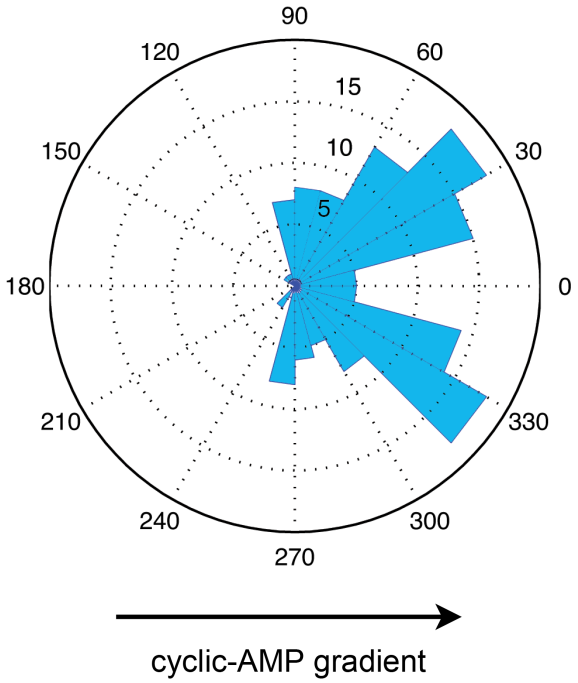

Figure 5.1. **Chemotactic orientation of blebs in the under-agarose assay.**

Directionality plot demonstrates the chemotactic orientation of blebs in *Dictyostelium* cells steadily chemotaxing under 0.7% agarose towards cyclic-AMP. Most blebs form at the front edge of the cell and almost none of them appear at the rear. n = 144 blebs have been analysed; the numbers next to the concentric circles indicate the numbers of blebs in each angular sector.

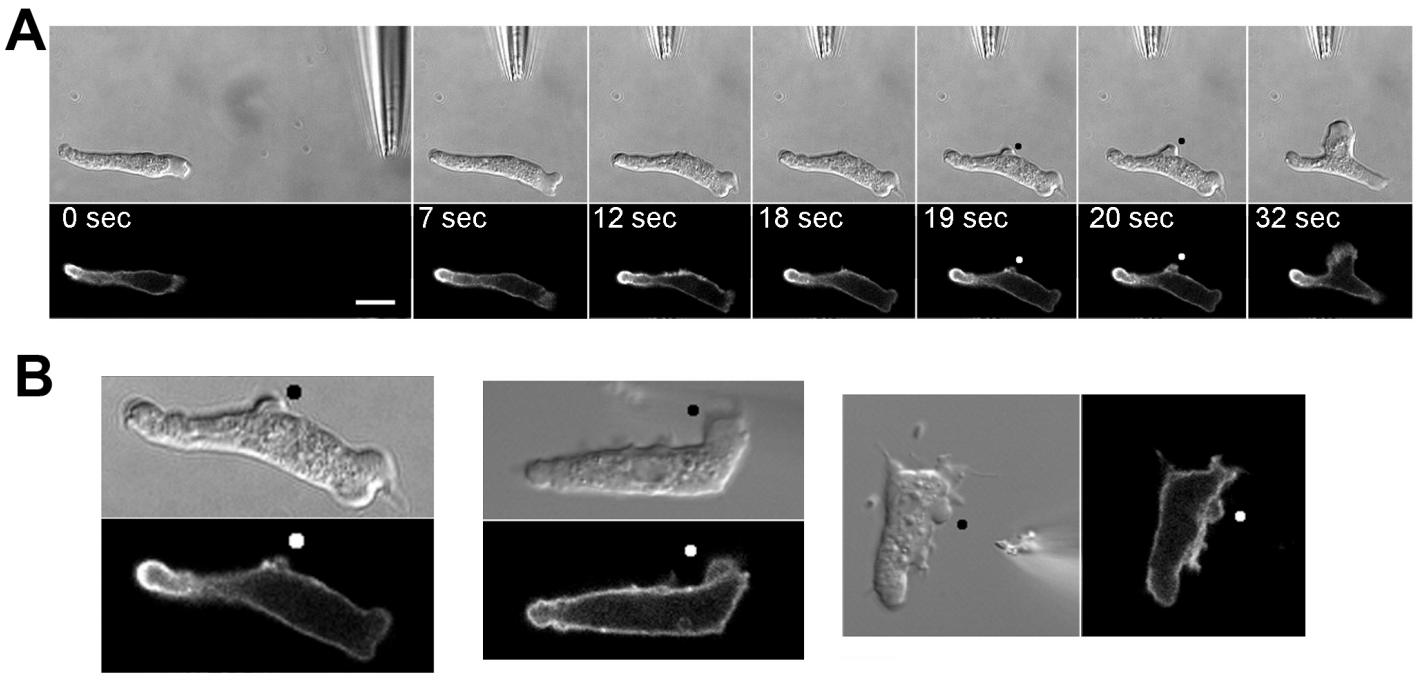

Figure 5.2. **Blebs are chemotactic to cyclic-AMP in reorientation experiments.**

In reorientation experiments a cell under buffer was induced to turn by moving a micropipette releasing cyclic-AMP. (A) Once the micropipette has moved, a bleb forms on the flank of the cell and then evolves into an F-actin pseudopod as the cell moves in the new direction. (B) Examples of reorientating cells: during this process, blebs can be observed on the side of the cells closest to the source of chemoattractant. Ax2 cells expressing an F-actin reporter (ABD-GFP) were starved for 4.5 hr with pulsing by cyclic-AMP and then attracted with cyclic-AMP filled micropipette. Bar = 10 μm.

The micropipette produces strong gradients, which can be calculated as corresponding to a change in the concentration of cyclic-AMP of 1.3-2.0 fold across a 10 μm cell (Postma and van Haastert, 2009). In these gradients cells turn abruptly, behaving differently from ones in shallow gradients (Andrew and Insall, 2007), in that they often formed *de novo* cell protrusions rather than split the pre-existing ones.

I performed the reorientation experiment in two slightly different formats, where the micropipette was moved to either about 45˚ or about 90˚ from the initial cell orientation (*Figure 5.3-A*). In the first format, where the degree of reorientation was smaller, most cells (about 73%) changed their direction by turning or splitting a pre-existing pseudopod (*Figure 5.3-D*), although some of them formed a new pseudopod (*Figure 5.3-E*). Interestingly, blebs were observed during both of these processes (*Figure 5.3-C*). In the second format, where the direction of the gradient changed more substantially, only about 34% of cells turned by splitting and redirecting the existing pseudopodia, whereas the rest of the cells formed an alternative pseudopod on their flank *de novo*, and this evolved into the new leading edge (*Figure 5.3-B*). For convenience, I decided to focus on the latter, more extreme, situation to study the role of blebs in the reorientation process.

As mentioned, around one third of cells in this experiment turned while maintaining their leading edge, and these were not analysed in detail, although blebs often led the way. In the remaining cases, the cells produced a new leading edge from their flank, and blebs frequently formed in the new direction of travel within 30 seconds of moving the needle, well before the overall polarized shape of the cell was lost (*Figures 5.2-A,B, 5.3-B,E*). Bleb formation was part of a more complex process of reorientation, which stereotypically consisted of first, the formation of F-actin microspikes in the new direction of travel, then of blebs, and only later of an F-actin filled pseudopod that caused overall cell re-polarisation. There was some variation in this pattern and, sometimes blebs did not form at all, but when they did, they always preceded F-actin filled pseudopodia, and surprisingly, often gave rise to them by continued actin polymerization (*Figure 5.4*). This strictly temporal sequence of events

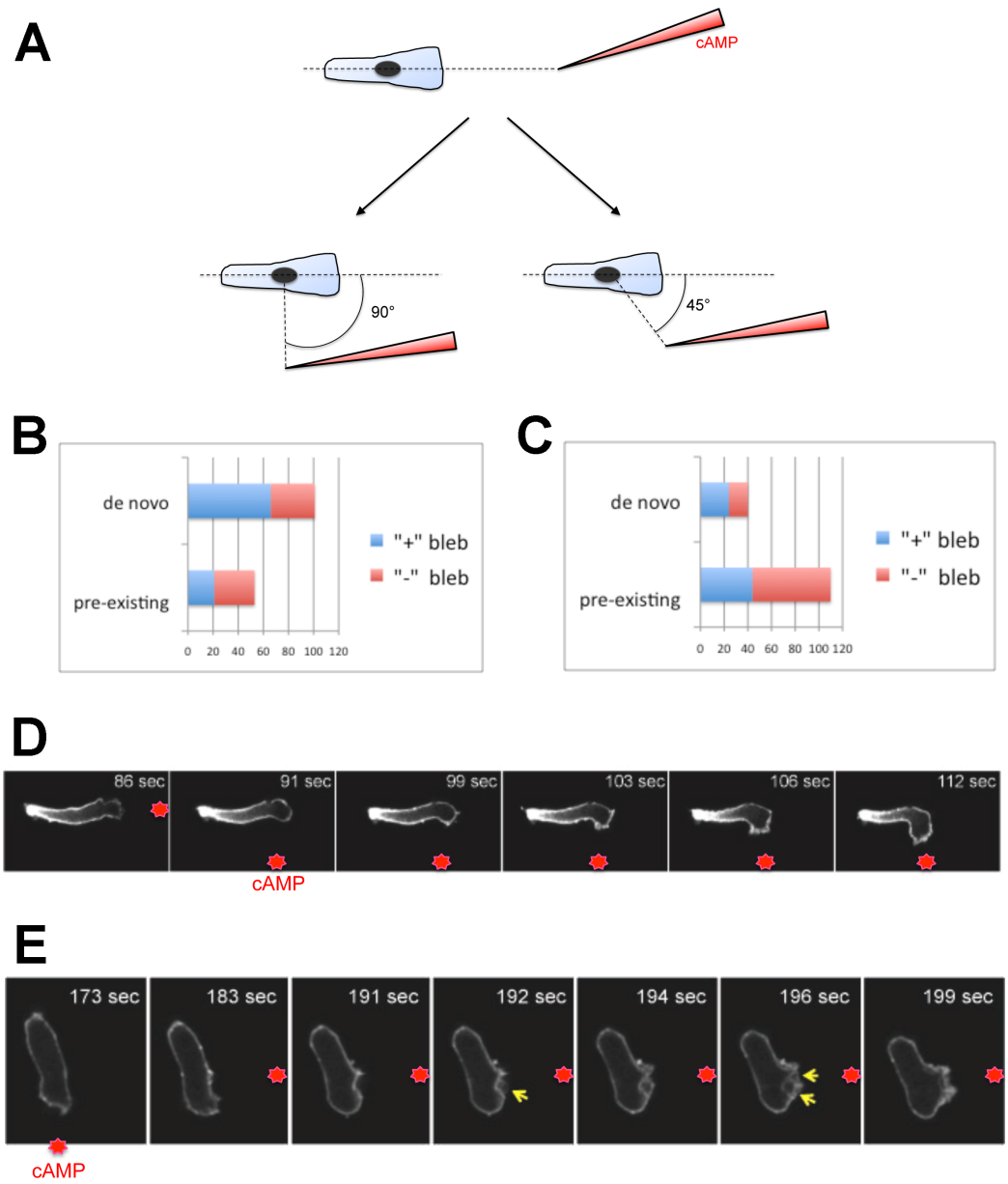

Figure 5.3. **Different ways of cell reorientation.**

(A) The reorientation experiment was performed in two slightly different formats: the micropipette was moved to either about 90˚ or about 45˚ from the initial cell orientation. (B) In the first format, only about 34% of cells turned by splitting and redirecting the existing pseudopodia, whereas the rest of the cells formed an alternative pseudopod on their flank *de novo*, and this evolved into the new leading edge. (C) In the second format, most cells (73%) changed their direction by turning or splitting a pre-existing pseudopod, although some of them formed a new pseudopod. Blebs were observed during both of these processes. Abscissa – number of cells. (D) A cell reorientating by turning a pre-existing pseudopod. (E) A cell reorientating by projecting *de novo* pseudopod on its flank. In (D) and (E) the ABD-GFP fluorescence images of chemotaxing Ax2 cells are shown.

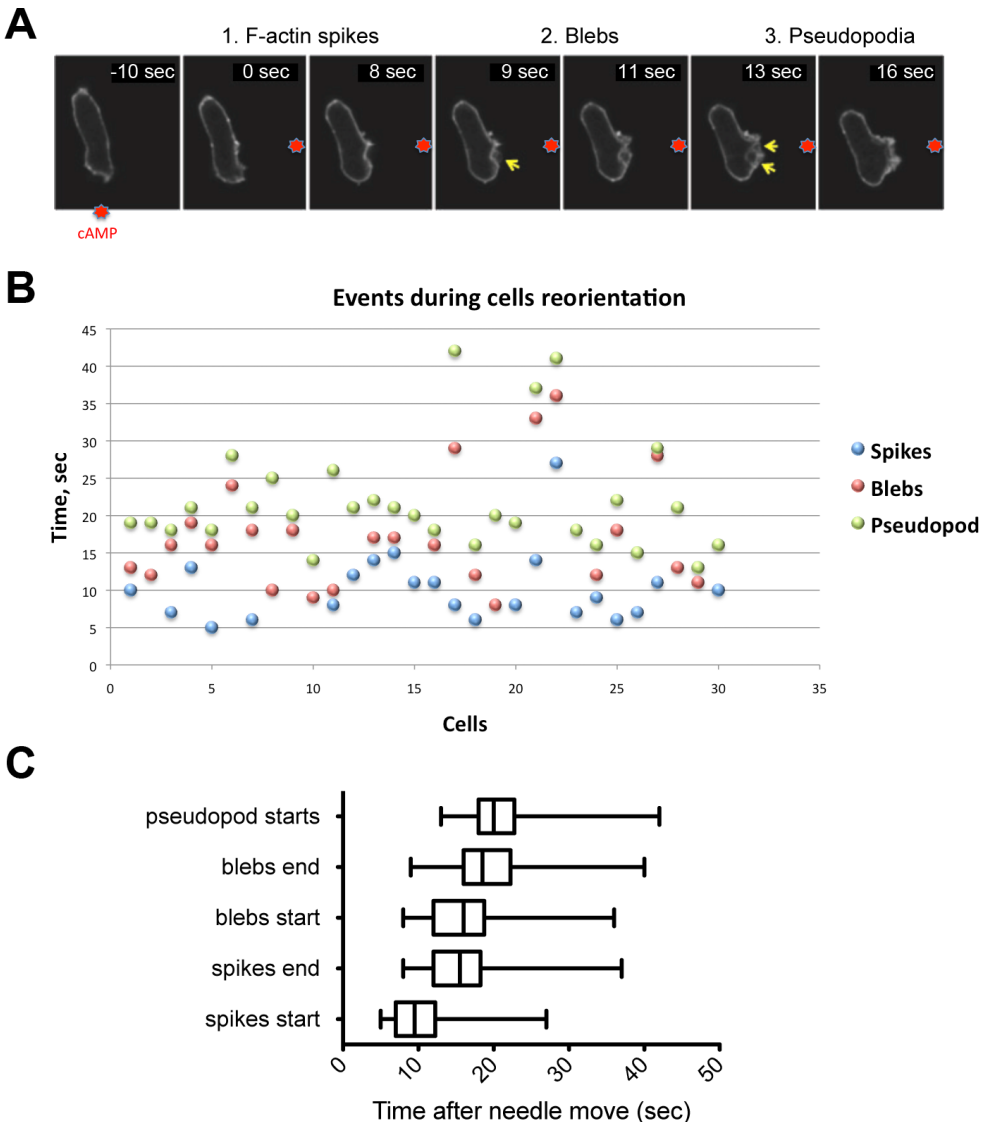

Figure 5.4. **Time course of cell reorientation.**

(A) An example of a cell reorientating by forming a new pseudopod from its flank. ABD-GFP fluorescence images are shown. (B) Reorientation was studied in n=30 *Dictyostelium* Ax2 cells. Each cell is indicated on the plot by a number on the horizontal axis. The sequence of events – formation of microspikes, blebs and pseudopodia – is plotted against the vertical "time" axis. These cells produced a new leading edge from their flank, and blebs frequently formed in the new direction of travel within 30 seconds of moving the needle, well before the overall polarized shape of the cell was lost. Bleb formation was part of a more complex process of reorientation, which stereotypically consisted of first, the formation of F-actin microspikes in the new direction of travel, then of blebs, and only later of an F-actin filled pseudopod that caused overall cell re-polarisation. (C) Time course of reorientation, showing the sequence of events after the needle is moved (at t = 0 sec) for the analysed sampling of 30 cells.

provokes the speculation that there may be a mechanistic link between the successive structures, in which microspikes could trigger blebs, and blebs initiated F-actin-driven pseudopodia (see Discussion section 7.5.3). Interestingly, blebs could often induce pseudopodia growth not only in reorientation experiments but also even in randomly moving cells (*Figure 3.2*).

The sequence of events during reorientation is very similar to that described following the uniform stimulation of *Dictyostelium* cells with cyclic-AMP: a biphasic activation of F-actin polymerisation with a drop of F-actin and increased blebbing in between the two peaks (Langridge and Kay, 2006) – compare *Figure 5.4-A,C* with *Figure 1.3* of the Introduction. Although in the case of micropipette experiments all these events occur locally, on the side of the cell closest to the source of chemoattractant.

5.3. Chemoattractant-induced blebbing might require a global intracellular pressure increase and local membrane modifications.

It had been shown that chemoattractant stimulation is able to induce blebbing in *Dictyostelium* cells, and the reorientation experiments demonstrate that chemotactic gradients can control where exactly blebs form around the cell perimeter. As the mechanism responsible for the chemotactic orientation of blebbing in *Dictyostelium* is completely unknown, I first decided to compare blebbing induced by two stimuli, one chemotactic and the other not.

As described above, cyclic-AMP gradients can induce orientated blebbing. On the other hand, in unpublished work, Dr David Traynor of this laboratory has found that ATP can induce vigorous blebbing when presented as a uniform stimulus (just like cyclic-AMP), but does not act as a chemoattractant and cannot induce localized blebbing.

I therefore compared blebbing induced by saturating, uniform stimulation of aggregation competent cells with cyclic-AMP (1 μM) and ATP (100 μM). I found genetically that myosin II activity is necessary for both cyclic-AMP and ATP induced bleb formation (*Figures 3.5-A* and *5.5*), and disruption of

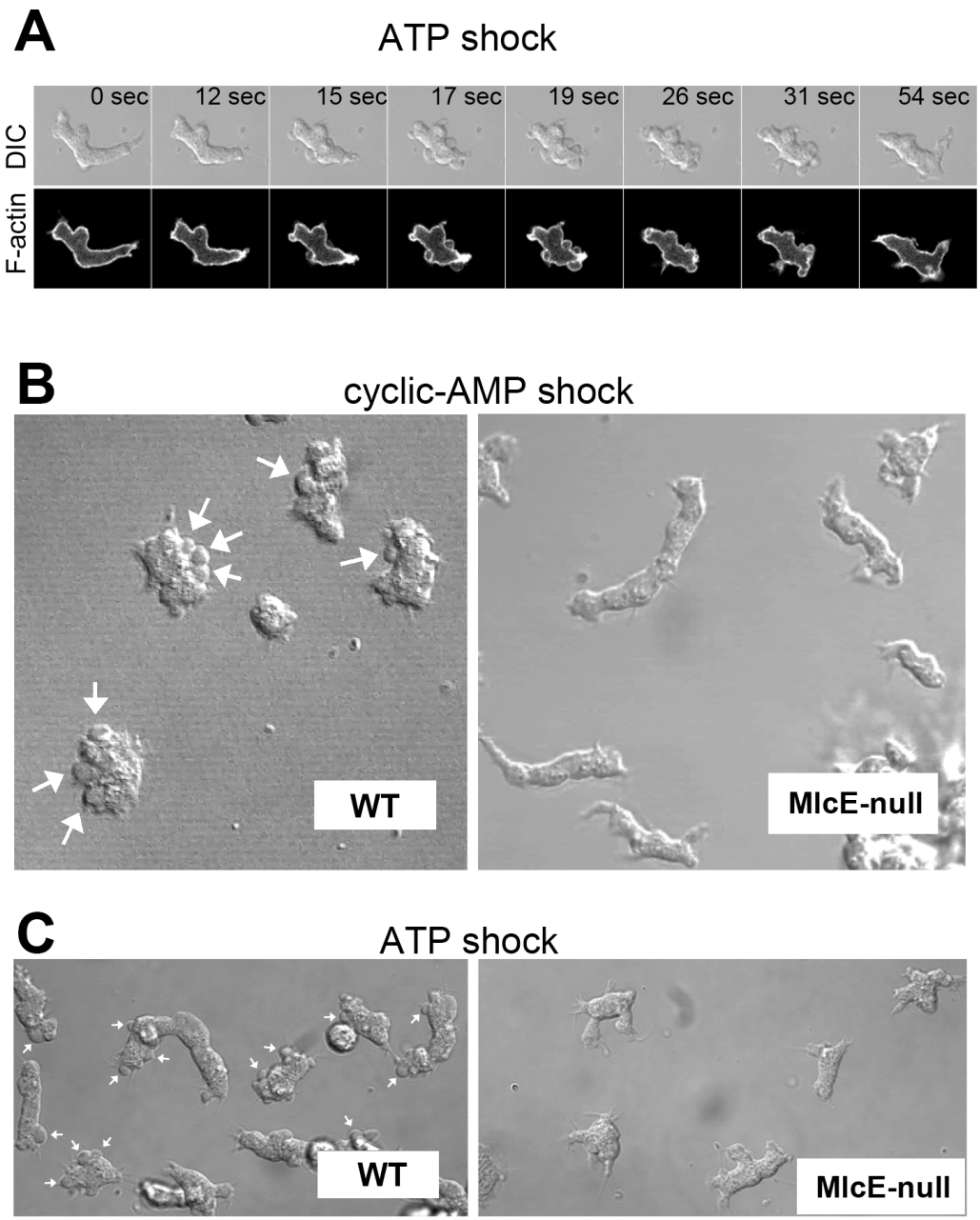

Figure 5.5. **Bleb induction in *Dictyostelium* cells requires myosin II activity.**

(A) Uniform stimulation of *Dictyostelium* cells with ATP (100 μM) can induce vigorous blebbing (similarly to cyclic-AMP stimulation). DIC and ABD-GFP fluorescence images of a cell stimulated with ATP is shown as a representative example. (B) Myosin essential light chain (MlcE) null cells do not bleb in response to cyclic-AMP. (C) ATP cannot induce blebbing in the MlcE null cells either.

any of the myosin II chains completely suppresses blebbing in both cases. Presumably, myosin II contraction is required to produce sufficient intracellular hydrostatic pressure, which pushes the plasma membrane outwards and causes its detachment from underlying cortex to initiate blebs formation. Most likely during movement, this pressure is transmitted within the cell according to Pascal's law, since the contractile acto-myosin network is localized at the rear of cells migrating under agarose (Laevsky and Knecht, 2003), whereas blebs appear mainly at the front edge, although the formal possibility of local myosin II activation through the phosphorylation of its regulatory chain cannot be eliminated (De la Roche et al., 2002; Charras et al., 2005).

This argument suggests that a mechanism might operate during chemotaxis that controls the position of bleb initiation on the cell surface. The most obvious mechanism is by control of membrane-to-cortex adhesion, with blebs forming where this interaction is weakened. Such a weakening may be provided by local membrane or cortex modifications caused by chemoattractant-sensitive signalling pathways. And since ATP does not act as a chemoattractant and cannot cause localized blebbing, ATP should not activate these pathways.

It is known that cyclic-AMP activates G-coupled receptors on the surface of *Dictyostelium* cells, which leads to the activation of RasC and RasG small GTPases and the recruitment of PI3-kinases to the plasma membrane (Parent and Devreotes, 1996), which convert $PI(4,5)P_2$ lipid into $PI(3,4,5)P_3$. Thus, a gradient of cyclic-AMP causes a gradient of these events along the plasma membrane leading to a steep accumulation of $PI(3,4,5)P_3$ at the front edge of the cell (Funamoto et al., 2002). To test whether this process is relevant to chemotactic bleb induction I examined relevant fluorescent reporters during blebbing: RBD-GFP, which binds to activated Ras proteins, and PH^{phdA}-GFP, which contains the PH-domain from the PhdA protein and interacts with $PI(3,4,5)P_3$ in the plasma membrane.

The uniform stimulation experiments confirm that cyclic-AMP does indeed cause Ras activation and $PI(3,4,5)P_3$ accumulation at the plasma membrane (Sasaki et al., 2004), and show that this precedes bleb formation (*Figure 5.6-A,B*). However, neither RBD-GFP nor PH^{phdA}-GFP

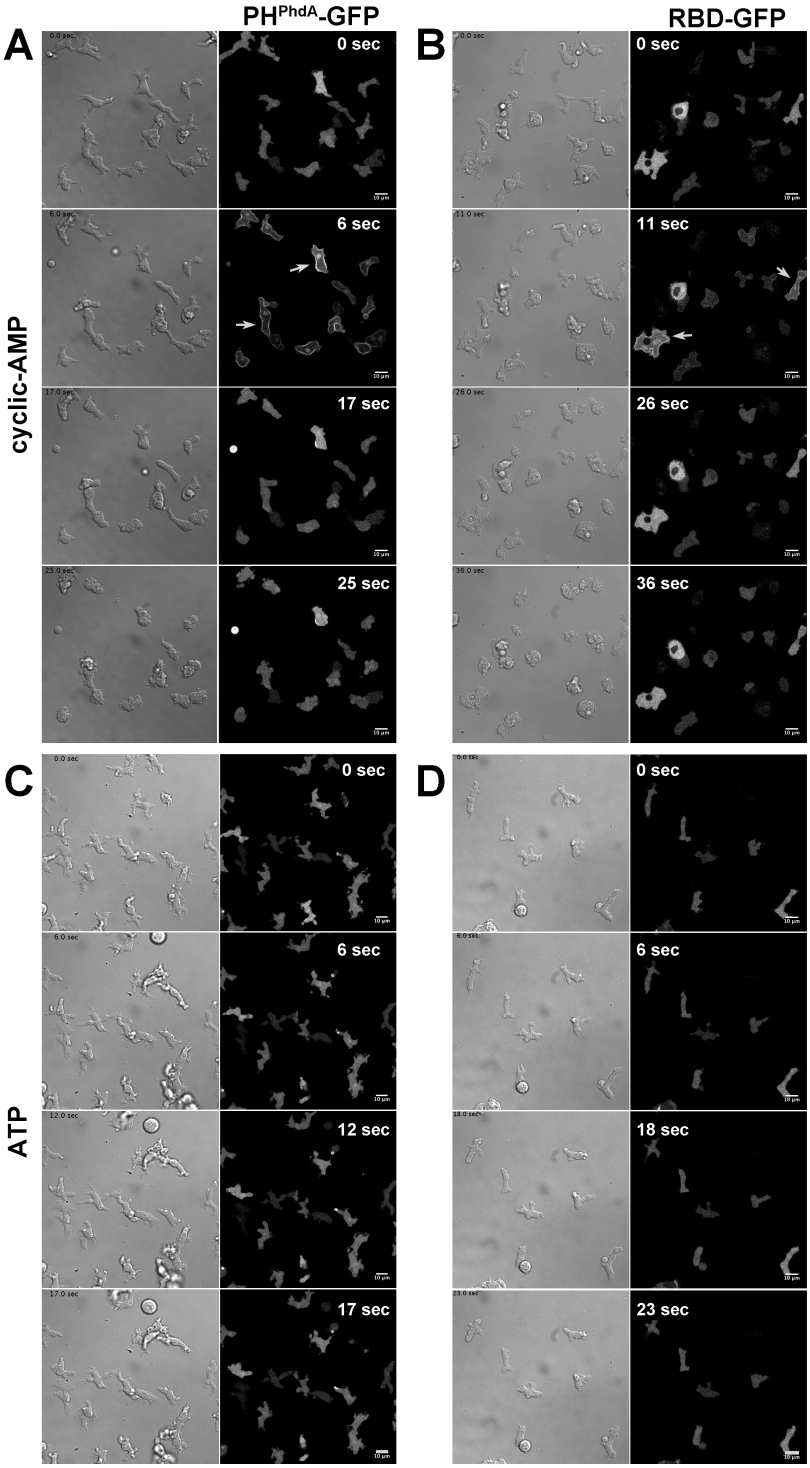

Figure 5.6. **Chemotactic stimulus activates Ras GTases and induces PI(3,4,5)P_3 accumulation in the plasma membrane.**

(A), (B) – Cells stimulated with 1 μM cyclic-AMP. (C), (D) – Cells stimulated with 100 μM ATP. (A), (C) – DIC and PH^{phdA}-GFP fluorescence images of the cells. (B), (D) – DIC and RBD-GFP fluorescence images. Cyclic-AMP stimulation causes transient accumulation of RBD-GFP and PH^{phdA}-GFP at the membrane, while ATP stimulation does not. Bar = 10 μm.

recruitment to the plasma membrane is observed after ATP stimulation (*Figure 5.6-C.D*), thus supporting the assumption that the ability of cyclic-AMP to determine the site of bleb formation might be mediated through these chemotactic pathways, which cause local lipid and protein modifications. Further, local $PI(3,4,5)P_3$ accumulation is observed in micropipette stimulation experiments. When a cell is attracted by the micropipette releasing cyclic-AMP, a patch of $PI(3,4,5)P_3$ forms in region of plasma membrane closest to the micropipette, often preceding a bleb formation and cell polarisation in this direction (*Figure 5.7*). Because of the relatively low signal-to-noise ratio of the $PI(3,4,5)P_3$ reporter PH^{phdA}-GFP and gradual accumulation of $PI(3,4,5)P_3$ in the plasma membrane, such local enrichment of $PI(3,4,5)P_3$ on the sites of bleb formation could be reliably identified only in about 20% of bleb initiation events, whereas in most of the remaining cases the gradient of $PI(3,4,5)P_3$ became evident during or shortly after bleb formation.

Concerning ATP stimulation, there is data in the literature indicating that in certain types of mammalian cells, ATP also can cause blebbing; and this process depends, on the one hand, on myosin II activation through ROCK kinase modulation and calcium influx (Morelli et al., 2003; Roger et al., 2008; Hwang et al., 2009), and on the other hand, on membrane modifications by phospholipases PLD and PLA_2 (Panupinthu et al., 2007). ATP-induced activation of these two enzymes leads to production of lysophosphatidic acid (LPA). And LPA itself has been shown to cause dynamic blebbing in osteoblasts even with a knocked-out ATP receptor. Interestingly, it has been reported earlier that LPA can act as chemoattractant for *Dictyostelium* cells (Jalink et al., 1993). Therefore, I tested whether LPA can cause blebbing in *Dictyostelium* and found that the uniform stimulation of these cells with 1 μM LPA causes the same affect as 100 μM ATP stimulation: the cells demonstrated a rapid and transient burst of blebbing. Moreover, I also found that ATP-induced blebbing is seriously suppressed in the PLA_2 null *Dictyostelium* cells, therefore suggesting that ATP-induced blebbing, similarly to cyclic-AMP-induced, requires both myosin II activation and plasma membrane modifications.

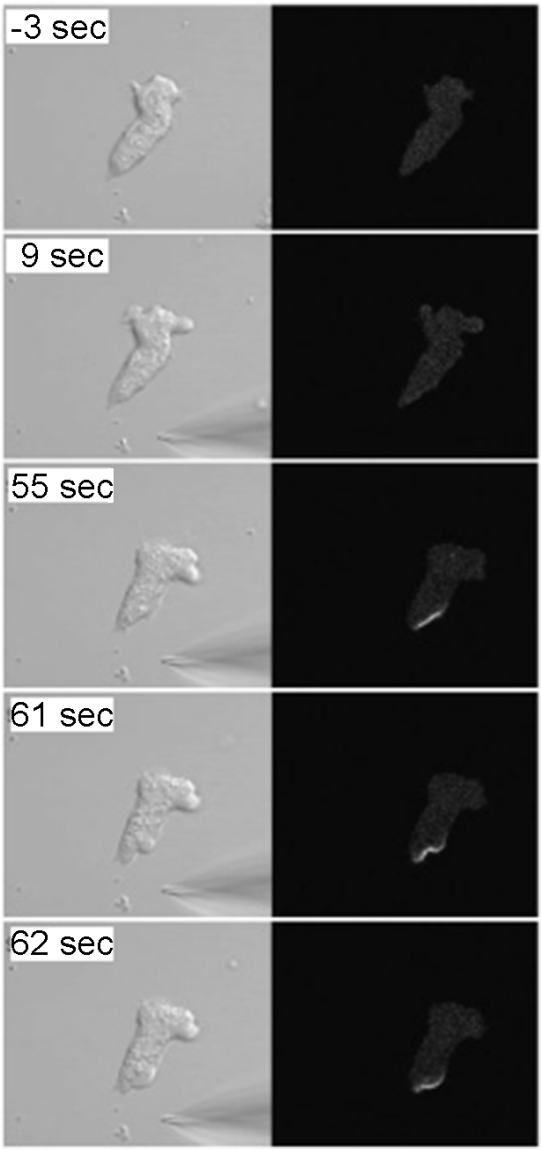

Figure 5.7. **Chemotactic bleb formation is preceded by local PI(3,4,5)P_3 accumulation.**

When a cell is attracted by a micropipette releasing cyclic-AMP, a patch of PI(3,4,5)P_3 forms in the plasma membrane at the site closest to the micropipette. This event often precedes bleb formation at this site and further cell re-polarisation. Ax2 cells, expressing a reporter for PI(3,4,5)P_3 (PH^{phdA}-GFP), were starved for 4.5 hr with pulsing by cyclic-AMP.

5.4. Chemotactic blebbing does not require the Talin B cleavage.

I also tested another hypothesis concerning the membrane-to-cortex linkers, which was inspired by experiments on global phosphoproteome analysis of cyclic-AMP stimulated *Dictyostelium* cells (John Nichols, unpublished data). In particular, SILAC mass-spectroscopy experiments showed a significant increase in phosphorylation of protein TalinB and calpain-like protein CplA (Huang et al., 2003) in *Dictyostelium* cells after uniform cyclic-AMP stimulation at time points coinciding with blebbing. It is known that talin cleavage by calpain protease can modulate cell contractility (Kotecki et al., 2010) and adhesion (Franco et al., 2004), improve cell motility and invasiveness and modulate F-actin organisation (Calle et al., 2006). I supposed that in our case, cleavage of talinB by CplA protease could weaken membrane-to-cortex interaction and induce chemoattractant-dependent blebbing.

Experimental data disproved this hypothesis, since I did not found any cleavage of TalinB after cyclic-AMP stimulation of cells (*Figure 5.8*), and chemical inhibition of cell proteases by an inhibitor cocktail did not result in any change in blebbing (data not shown).

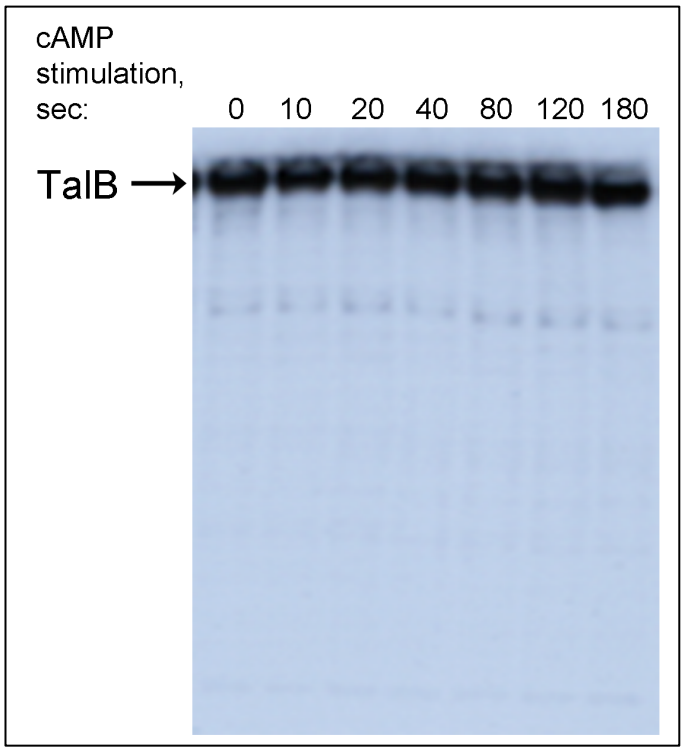

Figure 5.8. **Cyclic-AMP stimulation does not cause talin B cleavage in *Dictyostelium* cells.**

Western blotting with antibodies against talin B does not reveal any changes in *Dictyostelium* cells stimulated with 1 μM cyclic-AMP. Ax2 cells were starved for 4.5 hr with pulsing by cyclic-AMP, then washed and shaken with caffeine for 30 min to stop cyclic-AMP secretion. After that cells were stimulated with cyclic-AMP and then after the indicated times, the reaction was stopped and cells were lysed to prepare samples for electrophoresis.

CHAPTER 6. Targeted genetic screen for genes involved in the control of blebbing

In order to further investigate the chemotactic pathways that regulate blebbing, I employed a targeted genetic screen of key chemotactic mutants to obtain leads and limit possibilities concerning the control mechanisms of blebbing.

Around 50 cytoskeletal and signal transduction mutants (Swaney et al., 2010), created in the *Dictyostelium* community by gene knock-out, were screened for their ability to bleb using three different assays (as described in the Materials and Methods, Chapter 2.4.4):

- cyclic-AMP shock, where blebs are counted after cells are exposed to a sudden, uniform cyclic-AMP stimulus ("blebbing assay", (Langridge and Kay, 2006));
- random cells movement on a flat surface under buffer, where the proportion of blebs to total projections is estimated by eye;
- chemotaxis under 0.7% agarose, where the intensity of blebbing was assessed in cells chemotaxing through a resistive environment along a gradient of cyclic-AMP.

The assays were carried out on cells competent to respond to cyclic-AMP and each of the knock-out strains was compared to its direct wild-type parent, to minimize strain to strain variability. The use of such reference strains allowed us to identify genes, which when disrupted, suppress blebbing and others which, to the contrary, make cells more blebby.

Results from all the assays were assessed using a scoring system as follows: the strain was given a score "0" if this mutant was not distinguishable from its parent in this particular assay; a score "–" was given to a mutant that blebs slightly less well than its parent; and "– –" if a mutant does not bleb at all, or does so very weakly. Similarly, strains that bleb slightly more, and much more than their parent get scores of "+" and "+ +", respectively. The blebbing scores are finally summed for all three assays to give a composite score for each strain.

All the described experiments were carried out in a triplicate. And every time for each strain 30-50 cells from several different microscopy chambers were analysed for each set of experimental conditions.

These experiments confirmed that all the wild-type strains used – Ax2 (from different laboratories), Ax3, JH10, DH1, NC4A2, kAx3 – demonstrate a similar degree of blebbing under the conditions utilized, and also that this is similar to a wild isolate of *Dictyostelium discoideum* – NC4, demonstrating that blebbing observed during cell migration is not simply an artifact of certain laboratory strains.

The results are mapped onto a scheme showing our current understanding of the chemotactic signal transduction network (Swaney et al., 2010) – *Figure 6.1* (details are summarized in *Table 6.1*). In what follows, I consider in detail the results in terms of the mechanics of blebbing and the signal transduction pathways controlling it.

6.1. Myosin II activity is required for blebbing.

As expected, and mentioned earlier in this Thesis, mechanically, bleb formation absolutely depends on myosin II contractility. Consistent with previous data, null mutants of myosin II heavy chain (MhcA), its essential light chain (MlcE) or regulatory light chain (MlcR) are unable to bleb in a cyclic-AMP shock, random motility or under-agarose assay. Analysis of time-lapse movies also shows that they move significantly more slowly under agarose than wild-type cells.

Myosin II activity is regulated in *Dictyostelium* largely through its regulatory light chain phosphorylation by the kinase MlckA, which is activated in response to cyclic-AMP signalling downstream of guanylyl-cyclases (soluble sGC and membrane-anchored GCA) and cyclic-GMP-binding proteins GbpC and GbpD (Bosgraaf et al., 2002; Bosgraaf et al., 2005). As expected, elimination of this cyclic-GMP-mediated signalling impairs blebbing. However, the effect is not as dramatic as in myosin II knock-outs. This suggests that either the basal activity of myosin II is sufficient to create a critical pressure for bleb nucleation, or other mechanisms of myosin II activation may be involved. The first possibility looks more probable, because the effect of Gpbc/GbpD and sGC/GCA disruption appears mostly in the cyclic-AMP stimulation experiments,

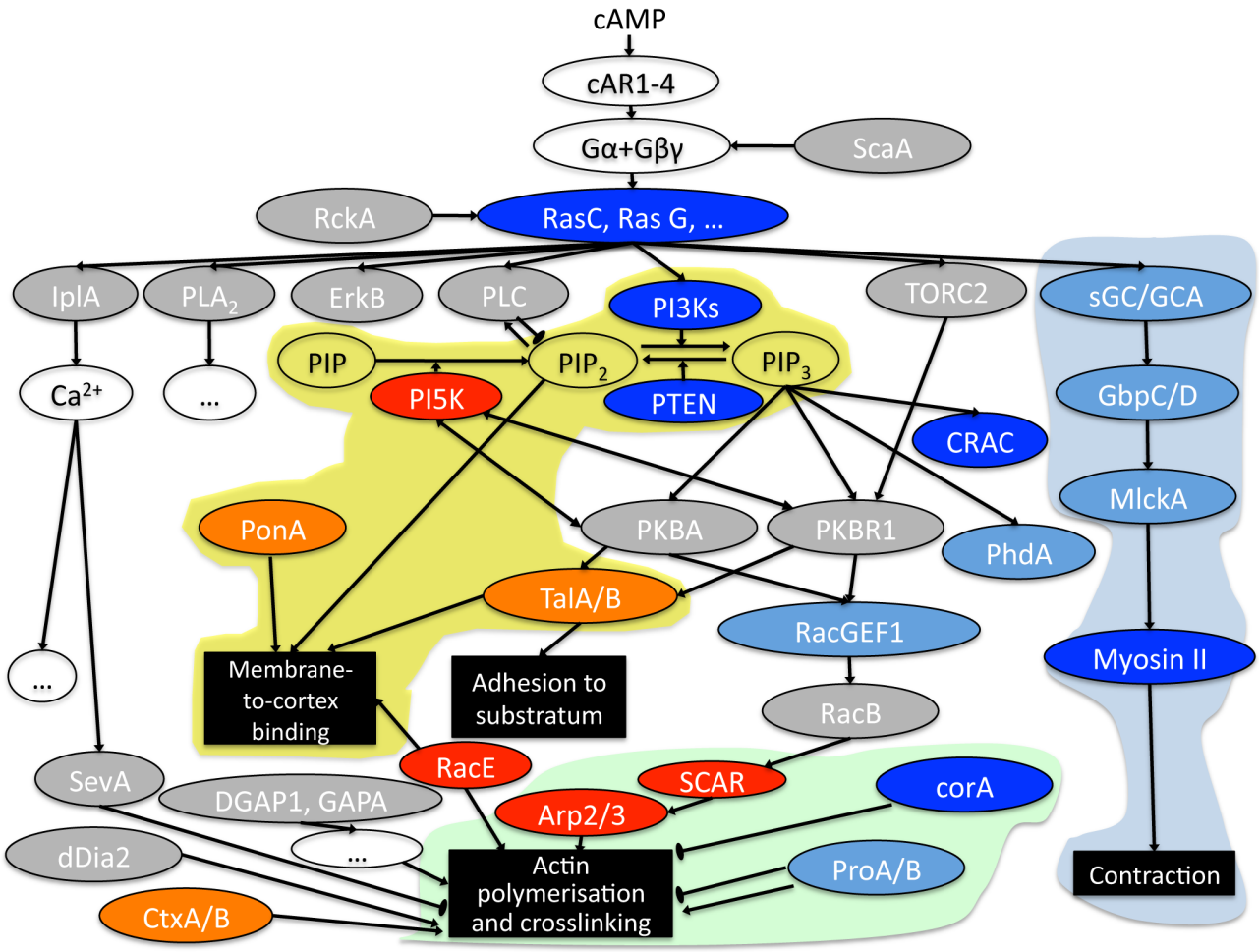

Figure 6.1. **Summary of the genetic screen for blebbing mutants.**

The results of the screen are superimposed on a scheme summarizing current understanding of chemotactic signal transduction. Colour code: grey – no effect; orange – modest stimulation of blebbing; red – strong stimulation; pale blue – modest inhibition; blue – strong inhibition. The results of three assays related to blebbing (blebbing in response to cyclic-AMP; bleb frequency during movement under buffer; and bleb frequency under agarose) are combined; further details in Table 6.1.

Table 6.1. ***Screen for mutants with altered blebbing and bleb-driven motility.***

Blue colours represent reduced blebbing in each assay and yellow/red, increased blebbing.

* Strain numbers starting with "DBS" refer to the Dicty Stock Center (http://dictybase.org); numbers starting with "HM" refer to the MRC LMB collection.

№	Protein knocked out	Strain*	Source	Description	Blebbing activity			Bleb. score
					under buffer	under agarose	cAMP shock	
1	**MlcE**	DBS0236566 (HM1519)	Stock Center (R.Chisholm)	myosin essential light chain	- -	- -	- -	-6
2	**MlcR**	DBS0236567 (HM1520)	Stock Center (R.Chisholm)	myosin regulatory light chain	- -	- -	- -	-6
3	**MhcA**	HS2206	J.Spudich	myosin II heavy chain	- -	- -	- -	-6
4	**PI3K1-5**	HM1200	Kay lab	PI3-kinases	- -	-	- -	-5
5	**PTEN**	HM1289	Kay lab	PI(3,4,5)P_3-phosphatase	- -	-	-	-4
6	**PI3K1-5+ PTEN**	HM1295	Kay lab	See above	-	-	-	-3
7	**PLC**	HM1308	A. Harwood	Phospholipase C	0	0	0	0
8	**PI3K1-5 + PLC**	HM1475	Kay lab	See above	- -	-	-	-4
9	**PLA_2**	HM1378	Kay lab	Phospholipase A2	0	0	0	0
10	**PI3K1-5 + PLA_2**	HM1369	Kay lab	See above	- -	-	- -	-5
11	**PKB**	HM1519	P. Devreotes	Protein kinase B, target of PI3Ks	0	0	0	0
12	**PKBR1**	HM1520	P. Devreotes	Related to PKB	0	0	0	0
13	**PKB + PKBR1**	HM1521	P. Devreotes	See above	+	0	+	+2

№	Protein knocked out	Strain*	Source	Description	Blebbing activity			Bleb. score
					under buffer	under agarose	cAMP shock	
14	**RacB**	HM1568	R. Firtel	Rho GTPase	**0**	**0**	**0**	**0**
15	**RacGEF1**	HM1569	R. Firtel	Rac GEF factor A	**0**	**0**	**-**	**-1**
16	**GAPA**	HM1544	H. Faix	Ras GTPase-activating protein (IQGAP-related)	**0**	**0**	**0**	**0**
17	**DGAP1**	HM1143	J. Faix	Ras GTPase-activating protein (IQGAP-related)	**0**	**0**	**0**	**0**
18	**ScaA**	HM1567	R. Firtel	Scaffold protein	**0**	**0**	**0**	**0**
19	**RckA**	DBS0236880 (HM1564)	Stock Center (R.Firtel)	Regulator of G protein Signaling, tyrosine kinase-like protein	**0**	**0**	**0**	**0**
20	**PakB + PakC**	DBS0236715 (HM1563)	Stock Center (R.Firtel)	Myosin I heavy chain protein kinase, p21-activated kinase	**0**	**0**	**0**	**0**
21	**PonA**	DBS0236821 (HM1565)	Stock Center (E.Luna)	Ponticulin, anchors actin cytoskeleton to plasma membrane	**0**	**0**	**+ +**	**+2**
22	**TalB**	HM1387	K. Inouye	Talin, FERM-domain protein	**0**	**-**	**+**	**0**
23	**TalA + TalB**	HM1554	M. Tsuijioka	Talins, F-actin-binding FERM-domain proteins	**+**	**ND**	**ND**	**+1**
24	**CorA**	DBS0236172 (HM1561, HG1569)	Stock Center (G. Gerisch)	Coronin, actin binding protein inhibiting actin nucleation	**- -**	**-**	**-**	**-4**
25	**ProA + ProB**	DBS0236827 (HM1562)	Stock Center (M. Schleicher)	Profilins, G-actin binding, PIP_2-binding proteins involved in F-actin regulation	**-**	**0**	**-**	**-2**
26	**SevA**	DBS0236166 (HM1566, HG1132)	Stock Center (G. Gerisch)	Severin, Ca^{2+}-dependent F-actin fragmenting protein	**0**	**0**	**0**	**0**

№	Protein knocked out	Strain*	Source	Description	Blebbing activity			Bleb. score
					under buffer	under agarose	cAMP shock	
27	**dDia2**	HM1583	J. Faix	Diaphanous-related formin	0	+	-	0
28	**ArcB**	HM2245	Kay lab	Actin related protein 2/3 complex subunit 2, involved in F-actin nucleation	+ +	+	+ +	+5
29	**Arp2 (GFP KI)**	HM2191	Kay lab	actin related protein 2, component of Arp2/3 complex	+	0	+	+2
30	**Nap**	IR57	R. Insall	Component of SCAR complex, regulates actin polymerisation	0	0	0	0
31	**Pir**	SB16	R. Insall	Component of SCAR complex, regulates actin polymerisation	+ +	+	+	+4
32	**Abi**	AP3	R. Insall	Component of SCAR complex, regulates actin polymerisation	+	0	+ +	+3
33	**HSPC300**	AP2	R. Insall	Component of SCAR complex, regulates actin polymerisation	+	0	+	+2
34	**SCAR1**	IR48 (received from R.Insall)	R. Insall	Component of SCAR complex, regulates actin polymerisation	+	0	+	+2
35	**PikI**	HM1513	Kay lab	PI(4)P-5-kinase	+ +	0	+	+3
36	**IplA**	HM1486	Kay lab	Inositol 1,4,5-trisphosphate receptor-like protein, Ca2+ channel	0	0	0	0
37	**Gca + SgcA** (in DH1)	DBS0236000 (HM1581)	Stock Center (P. van Haastert)	Guanylyl cyclases	0	0	-	-1
38	**Gca + SgcA** (in Ax3)	HM1585	P. van Haastert	Guanylyl cyclases	0	-	-	-2
39	**GbpC**	HM1582	P. van Haastert	Cyclic GMP-binding protein, with RasGEF domain-	0	-	-	-2
40	**GbpC + GbpD**	DBS0235996 (HM1580)	Stock Center (P. van Haastert)	Cyclic GMP-binding protein, with RasGEF domain-	0	0	-	-1

№	Protein knocked out	Strain*	Source	Description	Blebbing activity			Bleb. score
					under buffer	under agarose	cAMP shock	
41	**MlckA**	DBS0236386 (HM1586, HS183)	Stock Center	Myosin light chain kinase (activates myo II)	-	0	-	-2
42	**PhdA**	HM1587	R. Firtel	PIP_3-binding protein, PH-domain protein	+	0	- -	-1
43	**CRAC**	DBS0235559 (HM1596)	Stock Center (P.Devreotes)	Cytosolic regulator of adenylyl cyclase, PH-domain protein	-	-	-	-3
44	**PhdA**	HM1650	Kay lab	PIP_3-binding protein, PH-domain protein	0	0	- -	-2
45	**CRAC**	HM1648	Kay lab	cytosolic regulator of adenylyl cyclase, PH-domain protein	-	-	-	-3
46	**PhdA + CRAC**	HM1669	Kay lab	see above	-	- -	- -	-5
47	**Pia**	HM1461	Kay lab	Component of TOR complex 2	0	0	0	0
48	**Lst8**	HM1415	Kay lab	Component of TOR complex 2	0	-	+	0
49	**ErkB**	HS175	M.Maeda	extracellular response kinase from MAP kinase family	+	0	-	0
50	**RasC**	HM1505	Kay lab	Ras family small GTPase responsible for chemotaxis	0	-	-	-2
51	**RasG**	HM1497	Kay lab	Ras family small GTPase responsible for chemotaxis	-	0	0	-1
52	**RasC + RasG**	HM1429	G.Weeks	Ras family small GTPases	0	-	- -	-3
53	**RacE**	HM1604 (originally 24EH6)	D.Robinson	Rho GTPase	+ +	+ +	+	+5
54	**CtxA + CtxB**	DBS0235599 (HM1605)	Stock Center (J.Faix)	Cortexillins, member of the alpha-actinin/spectrin superfamily of F-actin-binding proteins	+	0	+	+2

whereas during random cell motility under buffer the disruptants behave very similarly to wild-type cells (see *Table 6.1*).

6.2. Blebbing is regulated reciprocally to actin polymerisation.

Impairing actin polymerization has an opposite effect on blebbing to myosin II disruption. I found that blebbing is increased in null mutants of different components (Abi, Nap, Pir, HSPC300, Scar1) of the SCAR/WAVE complex (Blagg et al., 2003) and in the Arp2/3 complex mutants with reduced actin-polymerising activity (ArcB knock-in with 6 amino acid changes, Arp2-GFP knock-in strains – (Langridge and Kay, 2006)).

Conversely, disruption of coronin (CorA; (Shina et al., 2011)) and profilins (ProA and ProB; (Haugwitz et al., 1994)) – proteins that inhibit actin nucleation and polymerisation – reduces blebbing. For example, coroninA null cells move almost exclusively by F-actin driven lamellipodia – both in buffer and under agarose. And even cyclic-AMP shock induces only very few blebs in these cells. Profillin null cells also rarely bleb in response to the uniform cyclic-AMP stimulation. They experience difficulties getting under agarose and often appear in a flattened, poorly polarised shape with multiple filopodia and, occasionally, lamellipodia-like structures.

Apparently, it is not only the absolute amount of F-actin that defines a cell's propensity to bleb, but F-actin organization also plays a role. We have found that knock-out of the cortexillins (CtxA and CtxB; (Shu et al., 2012)) – F-actin binding proteins from the alfa-actinin/spectrin superfamily – makes cells more blebby. Especially after cyclic-AMP shock, these cells form extended blebs whose growth they have difficulty in arresting.

Similarly, elimination of RacE protein produces a strong blebby phenotype. It was shown earlier that RacE plays an essential role in the organization of the cortical cytoskeleton and is required to maintain proper cortical integrity (Gerald et al., 1998). We find that RacE null cells are characterized by multiple constitutive blebbing when observed under standard

conditions in a buffer. And they produce even more blebs when stimulated with cyclic-AMP or placed under the agarose layer.

6.3. Interference with membrane-to-cortex binding proteins enhances blebbing.

Elimination of both talins in a double mutant (TalA and TalB; (Tsujioka et al., 2008)) or ponticulin (PonA; (Hitt et al., 1994)), all of which link the actin cytoskeleton to the cell membrane, increased blebbing, presumably as a result of decreased membrane-to-cortex adhesion. These knock-out strains are also less adhesive to the extracellular substrate, which may contribute to their blebbing phenotype. TalA/TalB double null cells have a spherical morphology with only a minimal contact with the substrate and easily get detached. Therefore, it was impossible to perform the cyclic-AMP shock experiment on these cells, since they immediately got washed away when cyclic-AMP was added. Also in the under-agarose assay, they were unable to escape from the loading well and could not get under the agarose. Under buffer they were quite immotile and produced multiple blebs around their surface.

A single TalB knock-out allowed cells to establish better adhesion with the substrate but they still experienced difficulties squeezing under agarose. Those cells that managed to get under agarose migrated slowly, and similarly to ones in the under-buffer conditions, formed multiple elongated balloon-like protrusions all-around cell surface. After a cyclic-AMP shock they produced more blebs than wild-type cells.

Ponticulin null cells demonstrated the greatest difference from wild type in the cyclic-AMP shock assay. They produced a huge number of blebs that were smaller in size that the wild-type ones. Also the ponticulin null cells adhered more weakly to the substratum, similarly to the talin disruptants.

6.4. Chemotactic signalling pathways in the regulation of blebbing

As already described (Chapter 1.3.3), *Dictyostelium* cells perceive cyclic-AMP signals using a typical G-protein coupled receptor, which, through intermediate steps, activates Ras GTPases and multiple downstream effectors, such as the TORC2 complex, phospholipases PLA_2 and PLC, PI3-kinases and PKB, and some others (Swaney et al., 2010). Surprisingly, my genetic screen reveals that elimination of many proteins considered central to chemotaxis has no effect on blebbing.

Although it was shown in the literature that in zebrafish germ cells calcium signalling is important for blebbing motility, eliminating chemotactic calcium signalling in *Dictyostelium* by knock-out of the presumed IP_3 receptor, IplA (Traynor et al., 2000), had no discernable effect on blebbing. Likewise, mutation of the phospholipases PLA_2 and PLC, the MAP kinase ERK2, and components of the TORC2 complex did not detectably affect blebbing.

In contrast, I obtained clear evidence that PI3-kinase signalling plays a crucial role in *Dictyostelium* cell blebbing (*Figures 6.1, 6.2-A-C*), and therefore investigated this area in more detail.

6.5. Blebbing is regulated by PI3-kinases but not through the PKB/PKBR1 activation.

PI3-kinase signalling is abolished in a strain where all five receptor-linked PI3-kinases in the genome are knocked-out, and previous work has shown that this strain has only a minimal chemotactic defect when moving in strong cyclic-AMP gradients under buffer (Hoeller and Kay, 2007). However, I found that the same strain is severely impaired in blebbing: mutant cells make only a small fraction of the number of blebs of the wild-type in response to a cyclic-AMP shock and are slower-moving in the more challenging under-agarose conditions (*Figure 6.2-A,C*). Confirming this, acute treatment of wild-type cells with the PI3-kinase inhibitor, LY-294002, also inhibits blebbing in the cyclic-AMP shock assay.

PI3-kinases produce $PI(3,4,5)P_3$ in the plasma membrane, which serves as a docking site for downstream effector proteins. Three such proteins, each

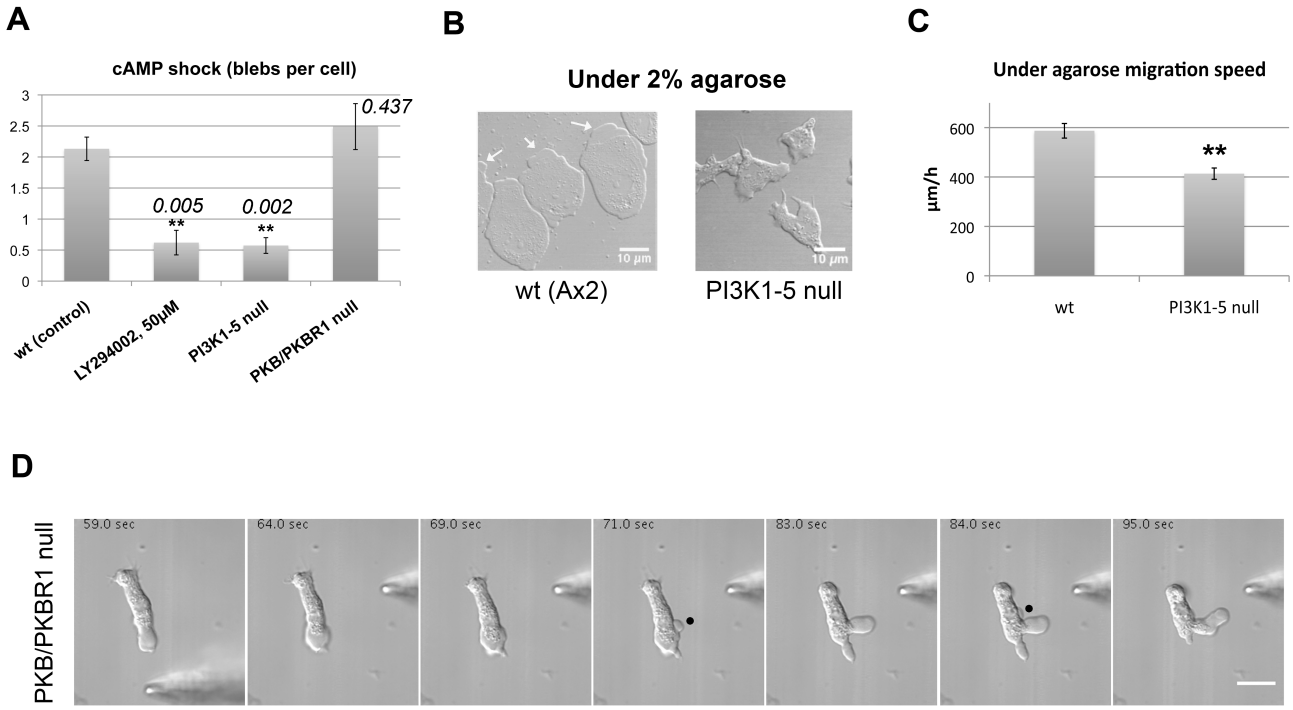

Figure 6.2. **Blebbing is regulated by PI3-kinases but not through the PKB.**

(A) Blebbing in response to uniform stimulation with 1 μM cyclic-AMP. It is apparent that blebbing is greatly reduced in a PI3-kinase quintuple mutant, and in wild-type cells treated with LY294002, an inhibitor of PI3-kinases. Of the downstream, PI(3,4,5)P_3-binding proteins, elimination of PKB (in a double mutant with its membrane bound homologue, PKBR1) has little effect on blebbing, (B) Morphology of cells chemotaxing under 2% agarose: wild-type cells move with rounded blebs, whereas the PI3-kinase quintuple mutant has a spikey morphology with very few blebs. (C) Speed of movement of mutant cells chemotaxing towards cyclic-AMP under 2.0% agarose; again a PI3-kinase mutant is severely affected. (D) PKB/PKBR1 null cells are able to produce blebs (indicated by black spots) in the direction of the cyclic-AMP gradient in the micropipette experiments. Bar = 10 μm.

carrying a PH-domain, are known to be relevant to *Dictyostelium* chemotaxis: the protein kinase PKB/AKT (Meili et al., 1999), and two less well-characterised proteins, CRAC (Insall, Kuspa, et al., 1994; Parent et al., 1998; Comer et al., 2005) and PhdA (Funamoto et al., 2001). I therefore tested mutants in each of these proteins (*Figures 6.1; 6.2-A; 6-3-A,B; Table 6.1*).

A double mutant of PKB and its membrane-anchored homologue, PKBR1, is known to be severely impaired in chemotaxis in standard conditions (Kamimura et al., 2008). But surprisingly, I found that blebbing in these cells is not affected as judged by our assays (*Figures 6.1 and 6.2-A*). Moreover the PKB/PKBR1 null cells appeared to be able to produce blebs in the direction of the cyclic-AMP gradient in the micropipette experiments (*Figure 6.2-D*). This proved that the PI3-kinases dependent control of blebbing is not mediated by PKB and PKBR1.

6.6. PI3-kinases can control blebbing by recruiting PH-domain containing proteins PhdA and CRAC.

Since the PKB/PKBR1 pathway appeared to be unimportant for PI3-kinase dependent regulation of blebbing, this left CRAC and PhdA as possible effectors. My assays show that elimination of either of these proteins significantly impairs blebbing (*Figure 6.1; Table 6.1*).

CRAC and PhdA are both soluble proteins with similar $PI(3,4,5)P_3$-binding PH-domains at their N-termini. Their expression increases strongly in early development (Parikh et al., 2010) as cells become competent for chemotaxis to cyclic-AMP. Null mutants of both genes have chemotactic defects, and CRAC is additionally required to couple the cyclic-AMP receptor to activation of adenylyl cyclase.

We re-created the single mutants of CRAC and PhdA in our laboratory strain by homologous recombination (knock-outs carried out by David Traynor), and also made a double mutant with both genes knocked out. As expected, all

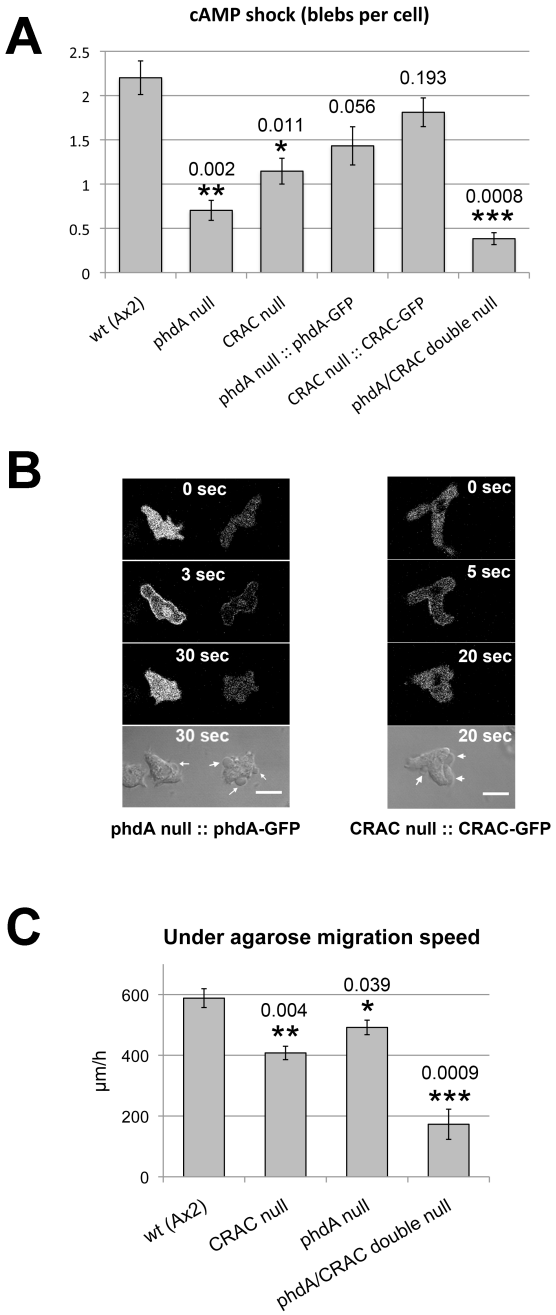

Figure 6.3. **PH-domain proteins PhdA and CRAC are required for cell blebbing.**

(A) Elimination of CRAC and PhdA reduces blebbing in cyclic-AMP shock assay, with a very strong phenotype when both are eliminated. (B) Response to the uniform cyclic-AMP stimulation can be substantially rescued by over-expressing the PhdA or CRAC GFP-fusion protein. (C) Speed of movement of mutant cells chemotaxing towards cyclic-AMP under 0.7% agarose; again a CRAC/PhdA double mutant is severely affected. The newly-created CRAC and PhdA mutant strains, HM1649, HM1650 and HM1659 were used in the experiments. Cells were starved and pulsed with cyclic-AMP to bring them to aggregation competence in all experiments. Bar = 10 µm.

three strains showed chemotactic defects, and confirming the genetic screen, both single mutants are significantly impaired in blebbing in response to a cyclic-AMP shock, and can be substantially rescued by over-expressing the corresponding GFP-fusion protein (*Figure 6.3-A,B*). The double mutant has an even stronger defect, producing fewer than 20% as many blebs as the wild-type in the cyclic-AMP shock assay, and moving under agarose at only a third of the wild-type speed, without visible blebs (*Figure 6.3-A,C*). Generally, the PhdA/CRAC double null cells are very immotile, unpolarised and flattened compared to the wild-type (*Figure 6.4-B*). It is notable that this phenotype is only apparent in starved cells, whereas vegetative mutant cells are indistinguishable from the wild-type (*Figure 6.4-C*), consistent with the lack of expression of PhdA and CRAC in vegetative cells (*Figure 6.4-A*).

It is known that besides blebbing, a uniform stimulation of wild-type *Dictyostelium* cells with cyclic-AMP induces a rapid and transient actin polymerization, which peaks at about 10 seconds. In contrast to blebbing, this actin response is not impaired in the PI3-kinase quintuple mutant (Hoeller and Kay, 2007), nor in the PhdA/CRAC double mutant (*Figure 6.5*). So, we can conclude that a distinct branch of the cyclic-AMP signal transduction system controls blebbing compared to actin polymerization.

Consistent with the role of blebbing in cell reorientation and migration through resistive environments, both PI3K1-5 quintuple null and PhdA/CRAC double null strains are defective in under-agarose and micropipette reorientation experiments. The PI3K1-5 null cells, being unable to form blebs, move under agarose by pseudopodia and filopodia projections (*Figure 6.2-B*). And, although at low agarose concentrations their motility still remains quite efficient, since these cells are smaller that the wild-type ones, yet at higher concentrations of agarose (above 2%) they often slow down or stall. In reorientation experiments, PI3K1-5 null cells usually turn using a pre-existing pseudopod rather then form a new one, and this process on the average takes them 1.5 times longer than the wild-type cells.

In the PhdA/CRAC double null strain only few cells can get under agarose, they have a poorly polarised morphology and move very slowly, mainly

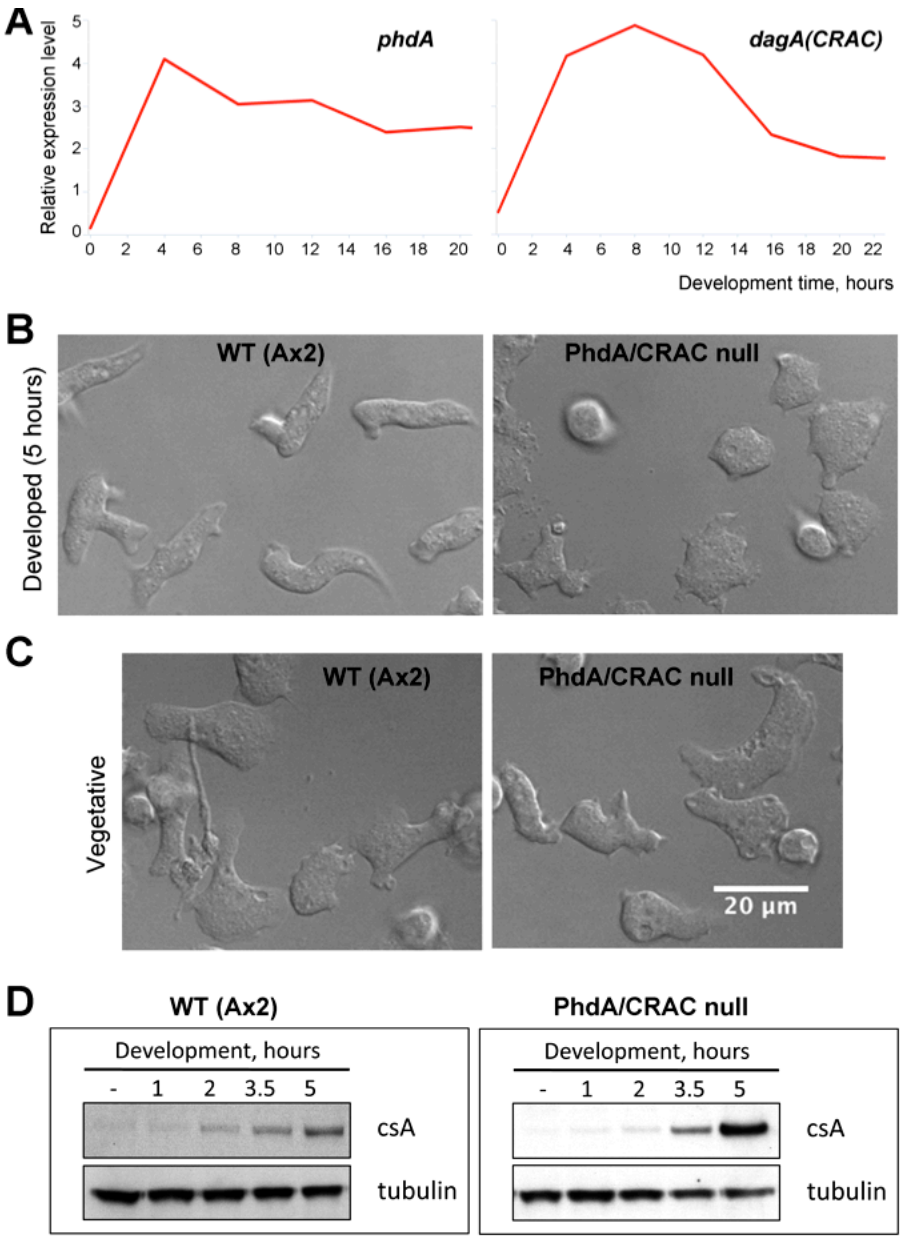

Figure 6.4. **PhdA/CRAC null phenotype becomes apparent only in aggregation competent cells.**

(A) Expression profiles of the *phdA* and *dagA* (*CRAC*) genes. In vegetative cells these genes are expressed at very low levels, and their expression strongly increases during development. (B) After 5 hours development the PhdA/CRAC double null cells demonstrate very unpolarised and flattened morphology compared to the wild-type cells; they also become quite immotile. (C) Vegetative PhdA/CRAC null cells are indistinguishable from the wild-type parent. (D) The phenotype of the PhdA/CRAC null cells in not due to the lack of development. The developmental marker csA is induced in these cells at least as efficiently as in the wild-type, according to the Western blotting experiment.

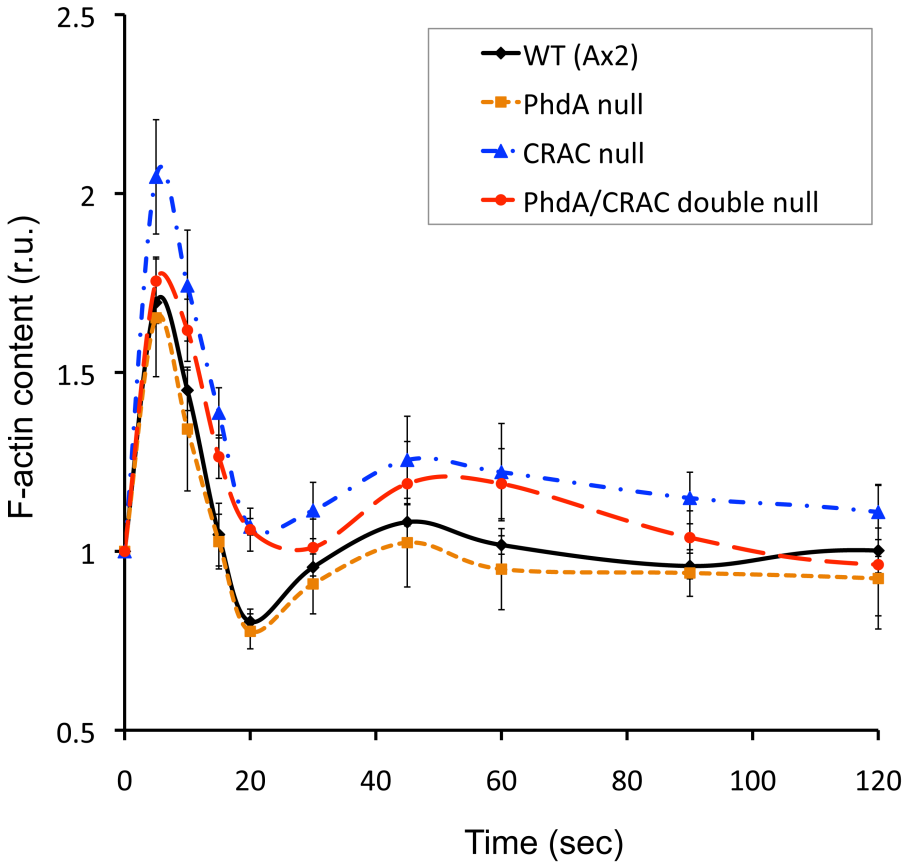

Figure 6.5. **F-actin polymerisation response in unimpaired in the PhdA and CRAC null cells.**

Wild-type and mutant cells were starved for 4.5 hr with pulsing by cyclic-AMP, then washed and shaken with caffeine for 30 min to stop cyclic-AMP secretion. After that, cells were stimulated with 1 μM cyclic-AMP, and F-actin associated with the cytoskeleton was determined at the indicated times after cyclic-AMP addition. Experiment was performed in a triplicate. The data are presented as mean ± S.E.M.

forming lamellipodia-like structures and membrane ruffles. In reorientation experiments they re-orient with a delay, slowly, attempting to gradually turn the front edge by broadening the leading pseudopod towards cell flank and then stopping its progression in the old direction and maintaining the new direction. This takes them 2-3 times longer than the reorientation of wild-type cells.

6.7. Discussion.

Overall, the applied targeted genetic screen approach allowed us to explore the possible molecular regulators of blebbing in *Dictyostelium*. As expected, blebbing appeared to be absolutely dependent on myosin II activity. Formation of blebs is driven by myosin-dependent cortical contraction leading to increased intracellular pressure (Charras et al., 2008). It has been shown in the literature that blebbing can be controlled through the modulation of myosin II activity. For instance, in zebrafish primordial germ cells (Blaser et al., 2006) and antigen-activated mast cells (Yanase et al., 2010), activation of bleb-initiating contractile activity occurred through a local increase in Ca^{2+} concentration. In addition, mammalian cells can regulate myosin II activity through the RhoA GTPase and Rho-associated protein kinase ROCK. (Sahai and Marshall, 2003; Takesono et al., 2010; Petrie et al., 2012) *Dictyostelium* cells do not have clear homologues of the mammalian GTPase RhoA, and according to our genetic screen, calcium signalling does not seem to play a significant role in cell contractility either. However, our experiments confirm that in *Dictyostelium* cells, myosin II activity and consecutive blebbing can be regulated through the cyclic-GMP-dependent phosphorylation of the myosin regulatory light chain by the MlckA kinase (De la Roche et al., 2002).

It has been described in the literature that blebbing can be induced in cells by weakening the membrane-to-cortex binding through the modulation of proteins that link the membrane and cytoskeleton, such as FERM-domain proteins (Diz-Munoz et al., 2010; Takesono et al., 2010), or through regulation of $PI(4,5)P_2$ content in the membrane (Raucher et al., 2000; Niebuhr et al., 2002; Wang et al., 2008; Hao et al., 2009). Here we have demonstrated that in

Dictyostelium, knock-out of membrane-to-cortex linking proteins – talins and ponticulin – also stimulates blebbing. And disruption of the genes involved in $PI(4,5)P_2$ metabolism – such as PI3-kinases, PTEN phosphatase and PI4P5-kinase – dramatically affects blebbing, supporting the idea that $PI(4,5)P_2$ can act as a second messenger in blebbing, regulating membrane-to-cortex adhesion and cytoskeleton reorganization (Sheetz et al., 2006). This accords with the previous observations that occurrence of blebs (Yanase et al., 2010) and the speed of migration for blebbing cells (Dumstrei et al., 2004) depend on PI3-kinase activity. But besides $PI(4,5)P_2$ depletion, the PI3-kinases can also modulate blebs formation through the recruitment of certain $PI(3,4,5)P_3$-binding proteins to the membrane. Accordingly, I have shown that two of such PH-domain containing proteins – PhdA and CRAC – play a critical role in blebbing in *Dictyostelium*.

My genetic screen also revealed that loss of other components of chemotactic signaling – PLA_2, Erk2, PLC, TORC2 – had no serious effect on blebbing. Interestingly, we have found that knock-out of the small GTPase RacE causes constitutively elevated blebbing in *Dictyostelium* cells. This suggests that some RacE-dependent pathways may act as negative regulators of blebbing. There is no detailed information on what RacE does in the cells. So far it is only known that RacE is as a small GTPase similar to mammalian Rho and Rac proteins that exerts its function at the plasma membrane. Measurements of the cortical tension and observations of live cells in suspension revealed that RacE is involved in the regulation of cortical tension and actin organization at cell cortex (Larochelle et al., 2000).

The results described here also go some way towards rationalizing the complexity of the chemotactic signalling system revealed by genetic analysis in *Dictyostelium* (Kay et al., 2008; Veltman et al., 2008; Swaney et al., 2010). They indicate that there are two motors under chemotactic control – actin polymerization and fluid pressure leading to blebs – whose regulation can be genetically separated, at least partially.

CHAPTER 7. Discussion

7.1. Significance of bleb driven motility in *Dictyostelium* and other organisms.

In this study I have shown that migrating *Dictyostelium* cells can switch from F-actin driven mode of locomotion completely to a blebbing mode when facing an increased resistance to their movement. In addition, I have found that *Dictyostelium* cells become more inclined to blebbing as they progress through the developmental program and approach the multicellular state. It seems that mechanical parameters of the environment can dictate the mode of cell migration.

There are several examples in the literature demonstrating that the mechanical properties of the environment can affect the behaviour of cells including their mode of migration. For example, primary fibroblasts can switch their migratory behaviour depending on the elastic properties of the extracellular matrix: when placed into 3D collagen lattice or onto 2D surface they move using F-actin driven lamellipodia, whereas inside dermal explants and in cell-derived matrices (which in contrast with collagen are characterized by non-linear elasticity) they form lobopodia that are dependent on myosin II and cytoplasmic flow (Petrie et al., 2012).

Interestingly, most published examples of bleb-driven amoeboid migration occur when cells are moving through natural (tissues) or artificial (gels and cell-derived matrices) three-dimensional environments (Keller and Eggli, 1998; Sahai and Marshall, 2003; Blaser et al., 2006; Fink, 2007; Tarbashevich et al., 2011). Thus, a blebbing mode of locomotion may be more natural for some cells than F-actin driven migration, which is most often studied on cells moving on solid planar surfaces.

There is an indication that blebbing may be used by cells as a “high-power” mode of migration in conditions where F-actin driven protrusions cannot provide enough force for migration. In bleb mode, cells may be able to find a weak place in the extracellular matrix, fill it with a bleb, and then squeeze through a small gap. It has been shown that cells from the same population can

change their phenotype from elongated mesenchymal to rounded and blebby depending on whether they are moving at the edge or in the middle of the cell mass (Lorentzen et al., 2011). Blebbing is able to increase the invasiveness of the cells. For instance, in MDCK kidney cells transformed with Moloney sarcoma virus, spontaneous activation of Rho/ROCK pathway causes the enhanced invasive capacity through the induction of blebby pseudopodia, where both F-actin and blebs are present (Jia et al., 2006). Certain cancers can exploit this mechanism as an alternative to F-actin driven mesenchymal mode of migration in situations when they cannot destroy the extracellular matrix through proteolysis (Sahai and Marshall, 2003). It has been shown that in invasive fibrosarcoma and carcinoma cells migrating through 3D collagen matrices or mouse dermis, inhibition of MMPs, serine proteases, cathepsins, and other proteases, induced their conversion toward spherical and blebby morphology, meanwhile the speed of their migration remains undiminished (Wolf et al., 2003). Therefore, such transition from proteolytic mesenchymal toward non-proteolytic amoeboid migration represents an escape mechanism for tumor cell dissemination in case of blocked pericellular proteolysis. And it has been shown that the combined inhibition of extracellular proteases and myosin II regulator ROCK negates the ability of tumour cells to switch between modes of motility and synergises to prevent tumour cell invasion (Sahai and Marshall, 2003).

In normal, non-tumorous, cells, blebbing also can enhance their migratory activity. So, during skeletal muscle regeneration, satellite stem cells migrate through the basal lamina to the site of myofiber repair by blebbing. They can switch from lamellipodia based to bleb driven migration to significantly increase the speed of movement. If blebbing is inhibited, their speed drops about 2.4-fold. When these cells move on a myofiber or on a planar plastic surface they don't produce blebs but migrate by lamellipodia extension at lower velocities (Otto et al., 2011).

For *Dictyostelium* cells it has been also shown that their motility within 3D multicellular structures is different from migration of planar surfaces. It requires cortical rigidity and force generation by actomyosin. Cells lacking myosin light chains (MlcE or MlcR) get excluded from aggregating streams when mixed with wild-type cells; and on their own, these mutant cells form aggregates

that get arrested in development at the mound stage, although their cortical integrity is intact (Tsujioka, 2011).

Another factor that can affect the mode of cell migration is adhesion to the substrate. So, neutrophils, lymphocytes (Malawista et al., 2000) and certain cancer cells (Sroka et al., 2002) can switch to blebbing migration when adhesion to the substrate is reduced. Human melanoma cells move with a mesenchymal F-actin driven phenotype on the rigid surface of plastic dishes, but change to a round, blebbing morphology when contacting matrigel (Kitzing et al., 2007). T lymphocytes also can move in two different modes: amoeboid-like and mesenchymal-like. In amoeboid mode they make sequential discontinuous adhesion contacts to the substrate ("walking"), whereas in mesenchymal mode they use a single continuously translating adhesion ("sliding"). The mode of migration depends on the nature of the substrate: on a high adhesion strength substrate (coated with ICAM-1) T cells form broader adhesion contact areas and typically switch to the sliding (mesenchymal) mode, but on non-adhesive substrates they switch to the walking (blebbing) mode. The walking mode provides a faster migration speed than the sliding mode (on average, 1.6 times faster) (Jacobelli et al., 2009).

In my experiments I found that the stiffness of the extracellular matrix and, potentially, the spatial constraints applied on cells moving under the layer of agarose or embedded inside the 3D agarose or polyacrylamide gel, can switch the balance between the F-actin versus bleb driven locomotion. The detailed mechanisms orchestrating this switch are still to be investigated. It is possible that mechanical resistance of the extracellular matrix may inhibit F-actin polymerization in a way similar to the effect of membrane tension: it was shown that when an F-actin protrusion meets the resistance of a tense plasma membrane, polymerization of F-actin is suppressed through the inhibition of polymerization-inducing activity of SCAR/WAVE complex (Houk et al., 2012). Similar events may happen when an F-actin projection meets a resistant environment, thus, switching the cell to the blebbing mode of migration.

7.2. Interplay between F-actin projections and blebs.

As we demonstrated, blebs and F-actin protrusions – such as pseudopodia and filopodia – can co-exist in the same cell, and under certain condition the cell can favour one or another of them. The question here is how these two types of cell projections interact with each other: are they competing, or synergizing, or just regulated independently?

7.2.1. Co-operation

On one hand, we have found that blebs often occur at the edges of existing pseudopodia, as well as on top of them. Moreover, in reorientation experiments F-actin microspikes directly precede bleb formation. Both these observations suggest a possibility that F-actin driven projections may facilitate bleb initiation through the application of local membrane strain caused by curvature. Blebs, in turn, also can induce pseudopodia growth as we have shown in our experiments: when a new cortex is rebuilt in a bleb, the actin polymerization often continues leading to the formation of a F-actin driven protrusion. Similar observations on *Dictyostelium* cells have been earlier described by Yoshida and Soldati (Yoshida and Soldati, 2006). They have found that in their strain, when cells were moving on a glass surface, blebs often appeared between pre-existing or still-growing pseudopodia. Furthermore, blebbing was often followed by the emergence of F-actin rich filopodia growing from the blebs. This supports the idea that blebs and F-actin projections may facilitate each other creating a hybrid motor of cell locomotion. It was also shown that myosin-II null *Dictyostelium* cells, which cannot bleb, also have defects in pseudopodia extension: the rate of extension and the final area of pseudopodia are reduced by about 50% in these cells compared to wild-type (Wessels et al., 1988; Yoshida and Soldati, 2006).

Blebs and F-actin driven protrusions have been shown to co-exist and interchange on the surface of other motile cell types as well. In *Fundulus heteroclitus* killifish embryo deep cells, phases of lamelipodium-based migration

often interchange with blebbing (Fink, 2007). Zebrafish mesoderm and endoderm germ layer progenitor cells also move using a combination of lamellipodia, filopodia and blebs, thus demonstrating another example of a hybrid motor (Diz-Munoz et al., 2010).

Therefore, there may exist some common regulators for both of these types of protrusions in the cells. As an example of such a common activator of both blebbing and actin polymerization, it has been reported that the formin protein FMNL1, which is known to be expressed in blood lineage cells and overexpressed in malignant cells of different origin, besides actin polymerization, also induces a non-apoptotic polarized blebbing, which also might contribute towards the regulation of the hybrid migration mechanism (Han et al., 2009).

7.2.2. Competition

On the other hand, our mutants screen has demonstrated that mutations impairing F-actin polymerization in *Dictyostelium* favour bleb-driven migration, whereas chemical or physical inhibition of blebbing (Yoshida and Soldati, 2006) or knocking-out of myosin II genes and their activators switches cells into F-actin driven mode of migration. In other cell types it has also been shown that cells often switch to blebbing mode of migration when F-actin polymerization is inhibited. So, for example, dendritic cells treated with latrunculin B (Lammermann and Sixt, 2009) move through 3D matrices by blebbing. Antigen-stimulated mast cells after stimulation with cytochalasin D also produce blebs instead of lamellipodia, and this happens in an actin-depolymerisation dependent manner (Yanase et al., 2010). This accords with the observation that blebs form when the actin cortex ruptures locally or detaches from plasma membrane (Keller and Eggli, 1998; Charras, 2008). Moreover, there is evidence that increased actin polymerization strengthens the membrane-to-cortex adhesion, whereas partial disassembly of F-actin weakens this adhesion (Raucher et al., 2000), and local weakening of the cell cortex can cause bleb formation (Boulbitch et al., 2000). Nevertheless, a certain level of F-actin

remodeling is still required to enable blebbing: in motile muscular satellite cells, cytochalasin D treatment completely disrupts blebbing motility (Otto et al., 2011).

Conversely, in various blebbing cells, chemical inhibition of myosin II or its activator – ROCK kinase – leads to the suppression of blebbing and formation of F-actin driven lamellipodia and filopodia (Sahai and Marshall, 2003; Takesono et al., 2010; Otto et al., 2011); whereas in cells moving by a combination of lamellipodia, filopodia and blebs, increasing the intracellular pressure or weakening the membrane-to-cortex association through depletion of FERM linker proteins increases the proportion of blebs and their size (Diz-Munoz et al., 2010).

In *Dictyostelium* cells, which use a mixed mode of migration, environmental conditions also can shift the balance between these two types of protrusions: high osmolarity and myosin II inhibition favouring F-actin protrusions (Yoshida and Soldati, 2006), whereas mechanical resistance shifting cells into the blebbing mode. Mechanisms controlling this balance between the blebs and F-actin projections are unknown. This could be a simple passive competition: in high-osmolarity buffer or in the presence of myosin II inhibitors the intracellular pressure is not high enough to effectively produce blebs for cell migration, whereas in highly resistive environment F-actin branches may not be able to effectively push against the matrix, meanwhile blebbing allows a locally higher hydrostatic force to be applied. This would explain a gradual switch from F-actin driven protrusions to blebs and backwards.

Besides absolute F-actin levels, we have found that the crosslinking and organization of F-actin filaments also affects *Dictyostelium* cells' ability to bleb. Similarly, human melanoma cells deficient in actin filament cross-linking protein ABP-280 are characterized by a constitutive blebbing (Cunningham, 1995). Interestingly, blebs' speed of expansion, size and occurrence in these cells decreases as the F-actin concentration increases over time after plating. Authors of the cited article hypothesize that blebs occur when a fluid driven membrane expansion is sufficiently rapid to outpace the local rate of actin polymerization (Cunningham, 1995). Even though this may be not completely true, yet the

described observations definitely suggest the existence of some competition between blebbing and F-actin polymerization.

As an alternative to a passive competition between hydrostatic pressure and actin polymerisation, there may exist an active molecular switch with feedback loops that facilitates the formation of one type of protrusion and inhibits the other. Such a mechanism could provide a trigger-like switch between the two modes of migration. Similar switching has been described for several different types of mammalian cells. For example, as mentioned above, primary fibroblasts can either form hydrostatically driven lobopodia, and this process is dependent on RhoA, ROCK and myosin II activation, or project F-actin driven lamellipodia, dependent on Rac1 and Cdc42 activation (Petrie et al., 2012). Certain cancer cell lines can also switch abruptly between Rho/ROCK-dependent rounded bleb-associated mode of motility and Rac1/Cdc42-dependent F-actin driven mesenchymal migration (Sahai and Marshall, 2003). In T-cells, RhoA/ROCK signaling also regulates migration by affecting both actomyosin contractility and microtubules stability to switch their mode of migration from lamellipodia driven to bleb-based motility (Takesono et al., 2010).

Hence, it is possible that depending on extracellular chemical signals and physical conditions, cells can activate alternative small GTPases – either RhoA to activate myosin and stimulate blebbing, or Rac1 and Cdc42 to induce actin polymerization and drive filopodia/lamellipodia growth. But how this choice is made is absolutely unknown. It is possible that, for example, $PI(4,5)P_2$ signalling might contribute towards both branches of this mechanism, since it can both affect membrane-to-cortex adhesion through binding with FERM-domain proteins and cause cytoskeletal remodeling through the modulation of Cdc42 and Rac1 activities and interaction with actin-binding proteins (Niebuhr et al., 2002; Sheetz et al., 2006). Accordingly, I have found that in *Dictyostelium* cells, disruption or inhibition of PI3-kinases (which convert $PI(4,5)P_2$ into $PI(3,4,5)P_3$) and disruption of the PIP5-kinase (which synthesizes $PI(4,5)P_2$ from PI(4)P) have severe and opposite effects on a cell's ability to produce blebs.

Nevertheless, signalling underlying the switch is probably more complex. Muscle satellite stem cells also can trigger a switch between blebs and

lamellipodia, but there it depends on non-canonical Wnt and nitric oxide signaling, as well as ROCK1 kinase (Otto et al., 2011). At the same time, in antigen-stimulated mast cells switch from lamellipodia formation to blebbing is induced through myosin II activation that is dependent mainly on Ca^{2+} - calmodulin signaling with a small contribution from Rho kinase. It is also dependent on PI3K activity and PLC, as well as small GTPase - ARF6 (ADP-ribosylation factor 6), which is localized to the plasma membrane and strongly enriched in the rim of the blebs (Yanase et al., 2010). In fact, ARF6 may also contribute towards the regulation of $PI(4,5)P_2$ synthesis through the activation of PIP5K activity (Yanase et al., 2010), and therefore may act through $PI(4,5)P_2$-dependent modulation of membrane-to-cortex adhesion and actin remodelling, as discussed above.

7.2.3. A complex interaction

Analysis of blebs and pseudopodia distribution over the cell perimeter in *Dictyostelium* cells moving under 0.7% agarose suggests a combined model of interactions between these two types of protrusions. Under these conditions, chemotaxing cells produce both types of projections, and directionality graphs (*Figure 7.1-B*) show that F-actin driven protrusions have a uni-modal symmetric distribution over the cell perimeter with a peak at the cell front (the side of the cell closest to the source of chemoattractant), whereas blebs group at the edges of this peak, producing a symmetric bi-modal distribution with the maxima around +35° and -35° relative to the chemoattractant gradient (*Figure 7.1-A*).

We propose that the following physical interaction between these two types of protrusions takes place. F-actin structures will deform the plasma membrane and therefore produce strain, which will facilitate membrane detachment from the underlying cortex and consecutive blebs formation at the edges of the pseudopod, where the membrane is more concave (in accordance with the data from our automated protrusions tracking, which shows that blebs

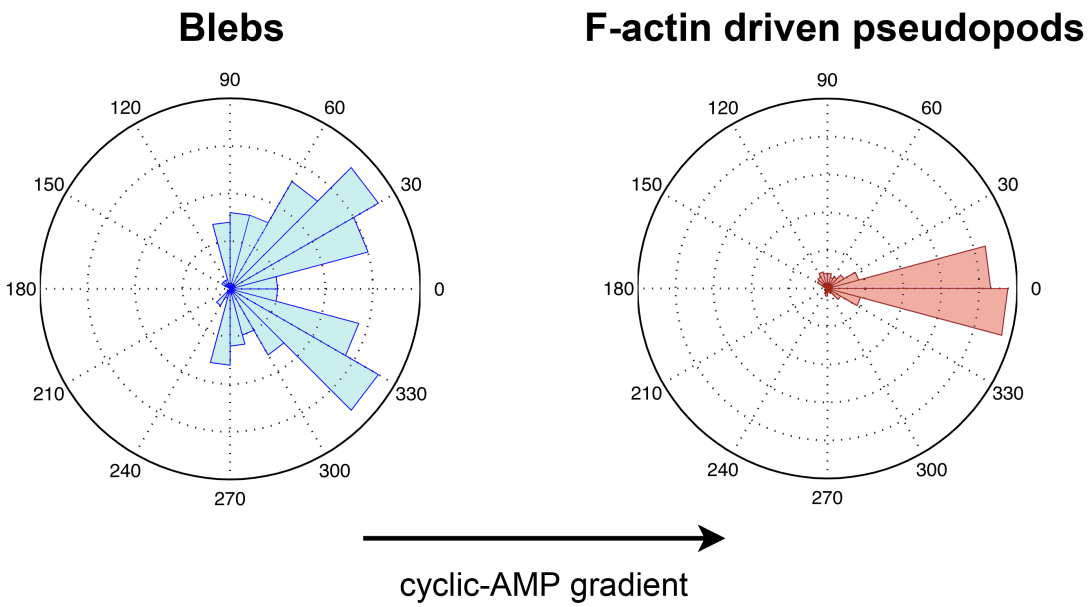

Figure 7.1. **Chemotactic orientation of blebs and pseudopodia in the under-agarose assay.**

Directionality plots demonstrate the chemotactic orientation of blebs and F-atin driven protrusions in *Dictyostelium* cells steadily chemotaxing under 0.7% agarose towards cyclic-AMP. F-actin driven protrusions have a uni-modal symmetric distribution over the cell perimeter with a peak at the cell front, whereas blebs group at the edges of this peak, producing a symmetric bi-modal distribution with the maxima around +35° and -35° relative to the chemoattractant gradient. 144 blebs and 304 pseudopods were analysed.

preferentially appear at the sites with negative membrane curvature). Accordingly, blebs rarely form at the tip of the leading edge because there blebbing is suppressed by a thick layer of F-actin and positive membrane curvature, but they appear at the sides of the leading edge. Besides, blebs presumably contribute towards the restriction of F-actin expansion by increasing the plasma membrane tension (Dai and Sheetz, 1999): it has been shown that formation of a cell protrusion significantly increases the membrane tension, and this tension can serve as a long-range inhibitor of F-actin assembly and pseudopodia formation through the inhibition of Rac activation and SCAR/WAVE recruitment (Houk et al., 2012). So, this may act as a feedback loop regulating the ratio between filopodia/lamellipodia and blebs.

Additionally, we have shown here that in reorientating *Dictyostelium* cells, blebbing precedes pseudopodia formation, and therefore blebs may facilitate pseudopodia growth, providing an additional feedback mechanism to the one just described.

7.3. Mechanisms of bleb initiation and orientation.

For blebs to drive cell migration, their formation must be polarized towards one side of the cell (Charras and Paluch, 2008; Fackler and Grosse, 2008). For this migration to be directional and chemotactic, the site of bleb formation must be defined by the chemoattractant gradient. Here I have proved that blebbing in *Dictyostelium* cells is regulated by the gradient of cyclic-AMP, both in cells migrating in a stable gradient under agarose and in reorientating cells. I investigated how chemoattractant may initiate bleb formation on the up-gradient side of the cells and envision several possible mechanisms.

Basically, bleb nucleation is normally initiated either by local rupture of the actin cortex (Paluch et al., 2005) or by the detachment of plasma membrane from its underlying cortex (Charras et al., 2005). In my experiments the cell cortex remains intact and for a while can be visualized as F-actin scar in the base of blebs. This argues against the mechanism based on cortical fragmentation.

Therefore, I consider mainly the latter possibility – cortex detachment – as the main mechanism of bleb nucleation in *Dictyostelium*.

One can envision several plausible models explaining local delamination of the cell membrane from the underlying cortex, namely:

- local pressure surge;
- chemical modification of cortex or membrane that weakens their interaction;
- local stress in the membrane caused by negative curvature.

These mechanisms are not mutually exclusive, and are discussed in more detail below.

7.3.1. Bleb initiation through a local pressure surge

The first possible mechanism of polarised bleb induction is through a local intracellular pressure increase, which could be provided by local myosin II contraction. It has been shown that a non-equilibration of pressure can exist in animal cells on the scales of about 10 micrometers and several seconds (Charras et al., 2005; Charras et al., 2009), which should be sufficient for local bleb nucleation. A few examples have been described supporting this model. For instance, in zebrafish primordial germ cells, which move through the tissues by forming blebs at the leading edge, local blebbing may be mediated by chemoattractant through the Ca^{2+}-induced activation of myosin II at the cell front (Blaser et al., 2006)). Walker carcinoma cells also can migrate by polarized blebbing (Keller and Eggli, 1998), and myosin is similarly localized at the front edge of these cells (Rossy et al., 2007).

Although in *Dictyostelium* we observe the accumulation of acto-myosin cortex mainly at the back of the cells migrating under agarose (Laevsky and Knecht, 2003), it is still feasible that local activation of myosin II contractility may occur at the cell front through the phosphorylation of the myosin regulatory light chain (De la Roche et al., 2002). It is also possible that when cells are moving in less restricted conditions, myosin may have a different intracellular distribution compared to under-agarose migration. Anyway, this model requires

further testing and investigation. So far we have not obtained any experimental data supporting this mechanism.

7.3.2. Bleb initiation through membrane or cortical modifications

Local cortex-membrane detachment may well be induced by the weakening of membrane-to-cortex adhesion or local cortical softening (Keller and Eggli, 1998; Boulbitch et al., 2000; Paluch et al., 2005). This can be achieved through chemical modification of membrane or cortical components. As a consequence, polarized distribution of membrane-to-cortex linking proteins could provide localized blebbing.

Often the function of such membrane-cortex linkers is performed by FERM-domain proteins, which interact both with F-actin in the cortex and $PI(4,5)P_2$ lipid in the plasma membrane (Sheetz, 2001). It is known that $PI(4,5)P_2$ can regulate cytoskeleton-plasma membrane adhesion. For example, sequestration of $PI(4,5)P_2$ by expression of $PI(4,5)P_2$-specific PH-domain proteins or $PI(4,5)P_2$ hydrolysis by specific phosphatase specifically weakens the membrane-to-cortex adhesion and induces blebbing in NIH-3T3 fibroblasts. Importantly, such a decrease in membrane-to-cortex adhesion could be induced by stimulating certain cell surface receptors (Raucher et al., 2000). Thus the density of membrane-cortex linkers across the cell depends on the $PI(4,5)P_2$ distribution in the membrane, and local depletion of $PI(4,5)P_2$ could cause the release of FERM proteins from the membrane and initiate localized blebbing (Hao et al., 2009). In support of this, melanoma cells moving in a three-dimensional matrix can switch to the bleb-driven amoeboid-like migration, with a stable cell rear, enriched in $PI(4,5)P_2$, FERM protein ezrin, F-actin and myosin (Lorentzen et al., 2011). Alternatively, FERM protein activity can be modulated through post-translational modifications. For instance, in polarized rat Walker carcinoma cells, the FERM proteins ezrin and moesin also co-localise with F-actin at the contracted tail, and the cell's motility can be modulated through C-terminal phosphorylation of ezrin and moesin (Rossy et al., 2007).

Our genetic screen has shown that knock-out of $PI(4,5)P_2$ synthesizing enzyme PI4P5-kinase in *Dictyostelium* cells causes a dramatic increase in blebbing, similarly to murine megakaryocytes where loss of $PI(4,5)P_2$ synthesizing enzyme PIP5KIγ also has been found to cause plasma membrane blebbing accompanied by a decreased association of the membrane with cytoskeleton (Wang et al., 2008). Conversely, disruption of PI3-kinases, which convert $PI(4,5)P_2$ into $PI(3,4,5)P_3$ and are enriched at the leading edge of chemotaxing cells (Merlot and Firtel, 2003; Janetopoulos et al., 2004), suppresses blebbing, therefore suggesting that $PI(4,5)P_2$ interaction with FERM domain proteins indeed might play a role in chemotactic blebs regulation in *Dictyostelium*.

Accordingly, knock-out of the *Dictyostelium* talins – TalA and TalB (Tsujioka et al., 2008), which belong to the family of FERM proteins, elevates blebbing, similarly to the zebrafish germ cells, where depletion of FERMs has also been shown to increase the proportion of blebs among other cell projections and their size (Diz-Munoz et al., 2010). But the phenotype of $PI(4,5)P_2$-deficient PI4P5-kinase null cells is more severe than that of the TalA/TalB null cells. This may be explained by the presence of other $PI(4,5)P_2$-binding linker proteins or by the fact that changes in $PI(4,5)P_2$ concentration can modulate blebbing both through changes in membrane-to-cytoskeleton adhesion and through the local cortical reorganization (Sheetz et al., 2006). Similarly, expression of bacterial inositol 4-phosphatase, that specifically dephosphorylates $PI(4,5)P_2$ into PI(5)P causing decrease in $PI(4,5)P_2$ levels, in mammalian cells weakens the membrane-to-cortex adhesion and stimulates cytoskeletal remodeling through the modulation of Cdc42 and Rac activities causing plasma membrane blebbing (Niebuhr et al., 2002).

It is also important to notice that PI3-kinases knock-out has much more severe effect on blebbing than on F-actin polymerization, and accordingly, the motility of PI3K1-5 null *Dictyostelium* cells is significantly impaired in under-agarose conditions, whereas remains nearly intact in standard conditions under buffer (Hoeller and Kay, 2007). This is consistent with literature data on other organisms. It was shown that *Xenopus* primordial germ cells (PGC) during migration form bleb-like protrusions enriched in $PI(3,4,5)P_3$, and interference

with PI(3,4,5)P_3 synthesis leads to PGC mismigration (Tarbashevich et al., 2011). Inhibition of PI3-kinase also slows down the migration of zebrafish embryonic cells (Dumstrei et al., 2004), which move by blebbing (Blaser et al., 2006).

As mentioned above, our genetic analysis indicates that PI3-kinases can control blebbing in *Dictyostelium* not only by PI(4,5)P_2 depletion but also through two PI(3,4,5)P_3-binding proteins – CRAC (Insall, Kuspa, et al., 1994; Wang et al., 1999) and PhdA (Funamoto et al., 2001). They are recruited to the plasma membrane within 5-10 seconds after cyclic-AMP shock and leave again before blebbing starts at around 25 seconds; they are also recruited to the up-gradient side of cells in cyclic-AMP gradients (Parent et al., 1998). It is thus possible that recruitment of CRAC and PhdA triggers bleb formation, though the mechanism that remains to be discovered. Current knowledge of CRAC and PhdA throws little light on this, since, apart from their N-terminal PH-domains, neither protein has any domains recognizable by standard searches, and no binding partners have yet been identified for either of them. Thus, it possible that these proteins may act as scaffolds to recruit lipid- or protein-modifying enzymes to the membrane at the leading edge of chemotaxing cells and so affect membrane-to-cortex interactions. Alternatively, they may compete with linker proteins displacing them from the leading edge. Potentially we may speculate that these proteins (by themselves or through the recruitment of additional participants) could be involved in the two other mechanisms of bleb nucleation described here – by either activating local myosin surge or provoking membrane deformation.

7.3.3. Bleb initiation by local membrane strain

Our most direct experimental evidence for chemoattractant-induced polarization of blebs came from the reorientation experiments with a cyclic-AMP filled micropipette. In the original paper from 1982 describing such abrupt cell turns in strong gradients (Swanson and Taylor, 1982), the authors found that the first response of cells to a change in gradient direction was a locally generated extension of a “hyaline pseudopod” from the region of the surface

nearest the stimulus. These hyaline pseudopodia were described as having a smooth surface and not to contain any vesicles, granules or organelles visible under the DIC microscope. Therefore, they looked very similar to what we would describe as blebs or bleb-containing pseudopodia. These protrusions were later followed by cell re-polarisation and vesicle flow into the pseudopod. Interestingly, the authors also observed that *Dictyostelium* cells at later stages of development were more elongated and their polarity was more plastic: they more easily formed new hyaline extensions when forced to reorient (Swanson and Taylor, 1982). This is consistent with my observation that cells at later stages of development are more active in making blebs.

My own experiments on cells making an abrupt turn following the rapid change in cyclic-AMP gradient confirm that usually they form a new leading edge in their flank, and, surprisingly, this process often starts from the rapid formation of transient F-actin microspikes, which are then frequently followed by bleb formation and later by an actin-driven pseudopod. This strictly temporal sequence of events provokes the speculation that there may be a mechanistic link between the successive structures, with microspikes triggering blebs, and blebs initiating F-actin-driven pseudopodia.

I propose that F-actin microspikes may impose a curvature strain on the plasma membrane, which could be relieved by separating membrane and cortex, and forming a bleb; continued actin polymerization in the bleb would then transform it into an F-actin-driven pseudopod (*Figure 7.2*). Additionally, microspikes might also weaken the membrane links with the cytoskeleton by tearing the membrane forward from the underlying cortex.

In this scheme blebs are initiated by actin microspikes, and the chemotactic gradient would determine where blebs form indirectly, through the polarization of F-actin polymerization events. Spiky actin polymerization is often nucleated by formin proteins. In support of the hypothesis, it was shown that in certain mammalian cells, the formin protein FMNL1 induces non-apoptotic polarized blebbing (Han et al., 2009). However, in our

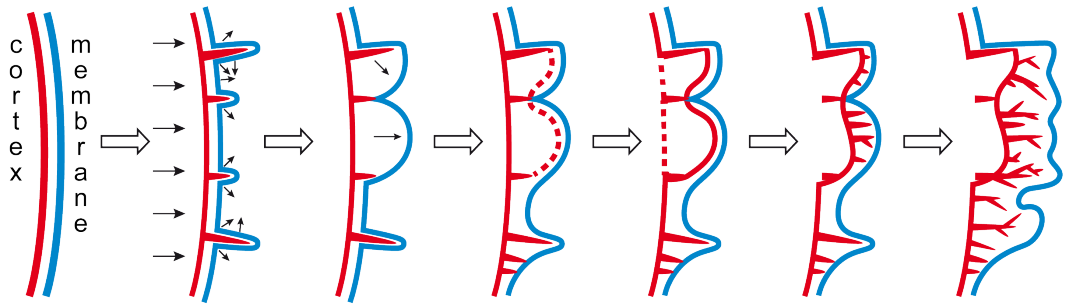

Figure 7.2. **Model for bleb formation and transformation into an actin-driven pseudopod.**

In this model, F-actin spikes form first, imposing bending stress on the plasma membrane and possibly weakening the membrane-cortex attachment; these physical effects then provoke formation of a bleb, the bare membrane of which becomes a site of actin polymerization; continued actin polymerization leads to the formation of an F-actin driven pseudopod.

experiments the knock-out of the best studied *Dictyostelium* formin dDia2 (Schirenbeck et al., 2005) neither impaired blebbing nor interfered with cell reorientation. It seems that some other actin-polymerising proteins may induce the described process, since microspikes remained intact in the dDia2 null cells. In principle, one could speculate that CRAC and PhdA proteins may be somehow involved in microspikes formation since we observe that temporarily this event coincides with their recruitment to the membrane.

An argument against spike-induced bleb initiation is that we do not observe F-actin microspikes in *Dictyostelium* cells moving under the agarose, although they produce multiple blebs. But this may be explained by the assumption that under these conditions, where the cells are exposed to a stable gradient of chemoattractant, they may require a bleb-polarising factor only at the earliest stages when a stable overall cell polarity is established. Further, a self-maintaining mechanism, provided by a positive feedback loop, would sustain the blebbing process at cell front.

Such a feedback mechanism might rely on the fact that when blebs appear, they form a steep landscape of positive and negative membrane curvatures at the leading edge of the cell (positive curvature on the top of the bleb and negative at its edges). And therefore, blebs could induce new blebs on their flanks through the membrane strain release mechanism, in accordance with our observation that blebs preferentially form in concave regions at the leading edge of the cells migrating under agarose.

Another possibility is based on the observation that in cells migrating under agarose, F-actin cortex at the front is much thinner than at the back and it is constantly rebuilt as new blebs form. And therefore, it is reasonable to assume that this long-term polarisation can indeed localise blebs to the leading edge. As long as cortex at the front edge of the cell remains thinner and younger than at the back, it should supposedly be more fragile and could have had less time to recruit membrane-to-cytoskeleton linking proteins. Therefore, it would more easy to rupture and detach from the membrane to produce blebs, further reproducing the situation where a new weak layer of F-actin in rebuilt at the front.

The literature also suggests another possible mechanism of bleb regulation involving microtubules that yet remains to be investigated in *Dictyostelium*. It was found that destabilisation of microtubules with nocodazole switches T cells from lamellipodia- to bleb-driven migration in a RhoA/ROCK-dependent manner (Takesono et al., 2010). This finding is in concordance with the observation that cell contractility can be enhanced by disassembly of the microtubules (Danowski, 1989; Paluch et al., 2005). Furthermore, in *Xenopus* primordial germ cells (PGC), which form bleb-like protrusions enriched with $PI(3,4,5)P_3$, a specific kinesin KIF13B (plus-ended motor protein) has been shown to be crucial for the directional migration. Knockdown of xKIF13B causes inhibition of both $PI(3,4,5)P_3$ accumulation at the front edge and blebbing, and impairs cell migration (Tarbashevich et al., 2011). It is supposed that KIF13B functions in the directional transport of $PI(3,4,5)P_3$-loaded vesicles via interaction with $PI(3,4,5)P_3$-binding proteins, thereby promoting cell polarity (Horiguchi et al., 2006). Thus, there might exist an additional microtubule-dependent pathway for the regulation of blebbing through the control of cell contractility and membrane composition.

We suppose that all or at least some of the described mechanisms may act together in co-ordination to assure proper chemoattractant-dependent polarized blebbing.

7.4. Future directions.

The fact that *Dictyostelium* cells can move both by F-actin polymerization and by blebbing, introduces this organism as a perspective model to study the mechanics and biochemistry of blebs formation and regulation. The accessibility of blebbing motility to experimental manipulation in *Dictyostelium* gives researchers an unparalleled opportunity for detailed study of this mode of cell motility.

Our finding that cells can be forced to switch completely to the blebbing mode of migration when facing the resistive environment raises the questions concerning the mechanics of blebbing and forces produced during bleb-driven

migration. Furthermore, more accurate and controllable studies of the switching process could provide some insight into the biomechanical aspects of this process. A question about the molecular mechanisms executing this switch is also very intriguing.

Molecular pathways that control blebbing also remain to be investigated in more detail. Here we have suggested several possible models of bleb initiation but the molecular basis of these processes is still largely unknown. It would be interesting to test whether the F-actin microspikes indeed can facilitate bleb formation as well as to identify the mechanisms of PhdA and CRAC involvement in blebbing regulation.

Moreover, the results obtained on *Dictyostelium* cells may well be applicable to other cell types. For instance, it would be interesting to know whether neutrophils and other motile mammalian cells can be forced mechanically to change their mode of migration and start blebbing. If so and if blebbing can be used for chemotactic movement of certain cell types in higher eukaryotes, then *Dictyostelium discoideum* may be used as a convenient model for genetic and biochemical studies in this field.

CHAPTER 8. References

Abercrombie, M., G. A. Dunn, et al. (1977). "The shape and movement of fibroblasts in culture." Society of General Physiologists series **32**: 57-70.

Abercrombie, M., J. E. Heaysman, et al. (1970). "The locomotion of fibroblasts in culture. I. Movements of the leading edge." Experimental cell research **59**(3): 393-398.

Andrew, N. and R. H. Insall (2007). "Chemotaxis in shallow gradients is mediated independently of PtdIns 3-kinase by biased choices between random protrusions." Nature cell biology **9**(2): 193-200.

Annesley, S. J. and P. R. Fisher (2009). "Dictyostelium discoideum--a model for many reasons." Molecular and cellular biochemistry **329**(1-2): 73-91.

Armstrong, P. B. (1985). "The control of cell motility during embryogenesis." Cancer metastasis reviews **4**(1): 59-79.

Asano, Y., T. Mizuno, et al. (2004). "Keratocyte-like locomotion in amiB-null Dictyostelium cells." Cell motility and the cytoskeleton **59**(1): 17-27.

Balgude, A. P., X. Yu, et al. (2001). "Agarose gel stiffness determines rate of DRG neurite extension in 3D cultures." Biomaterials **22**(10): 1077-1084.

Barry, N. P. and M. S. Bretscher (2010). "Dictyostelium amoebae and neutrophils can swim." Proceedings of the National Academy of Sciences of the United States of America **107**(25): 11376-11380.

Blagg, S. L., M. Stewart, et al. (2003). "PIR121 regulates pseudopod dynamics and SCAR activity in Dictyostelium." Current biology : CB **13**(17): 1480-1487.

Blaser, H., M. Reichman-Fried, et al. (2006). "Migration of zebrafish primordial germ cells: a role for myosin contraction and cytoplasmic flow." Developmental cell **11**(5): 613-627.

Bloomfield, G., J. Skelton, et al. (2010). "Sex determination in the social amoeba Dictyostelium discoideum." Science **330**(6010): 1533-1536.

Bloomfield, G., Y. Tanaka, et al. (2008). "Widespread duplications in the genomes of laboratory stocks of Dictyostelium discoideum." Genome biology **9**(4).

Bominaar, A. A., F. Kesbeke, et al. (1994). "Phospholipase C in Dictyostelium discoideum. Cyclic AMP surface receptor and G-protein-regulated activity in vitro." The Biochemical journal **297 (Pt 1)**: 181-187.

Bosgraaf, L., H. Russcher, et al. (2002). "A novel cGMP signalling pathway mediating myosin phosphorylation and chemotaxis in Dictyostelium." The EMBO journal **21**(17): 4560-4570.

Bosgraaf, L., A. Waijer, et al. (2005). "RasGEF-containing proteins GbpC and GbpD have differential effects on cell polarity and chemotaxis in Dictyostelium." Journal of cell science **118**(Pt 9): 1899-1910.

Boulbitch, A., R. Simson, et al. (2000). "Shape instability of a biomembrane driven by a local softening of the underlying actin cortex." Physical review. E, Statistical physics, plasmas, fluids, and related interdisciplinary topics **62**(3 Pt B): 3974-3985.

Bray, D. and J. G. White (1988). "Cortical flow in animal cells." Science **239**(4842): 883-888.

Bretscher, M. S. (1976). "Directed lipid flow in cell membranes." Nature **260**(5546): 21-23.

Bretscher, M. S. (1984). "Endocytosis: relation to capping and cell locomotion." Science **224**(4650): 681-686.

Calle, Y., N. O. Carragher, et al. (2006). "Inhibition of calpain stabilises podosomes and impairs dendritic cell motility." Journal of cell science **119**(Pt 11): 2375-2385.

Campellone, K. G. and M. D. Welch (2010). "A nucleator arms race: cellular control of actin assembly." Nature reviews. Molecular cell biology **11**(4): 237-251.

Carrin, I., I. Murgia, et al. (1996). "A mutational analysis of Dictyostelium discoideum multicellular development." Microbiology-Uk **142**: 993-1003.

Charest, P. G., Z. Shen, et al. (2010). "A Ras signaling complex controls the RasC-TORC2 pathway and directed cell migration." Developmental cell **18**(5): 737-749.

Charras, G. and E. Paluch (2008). "Blebs lead the way: how to migrate without lamellipodia." Nature reviews. Molecular cell biology **9**(9): 730-736.

Charras, G. T. (2008). "A short history of blebbing." Journal of microscopy **231**(3): 466-478.

Charras, G. T., M. Coughlin, et al. (2008). "Life and times of a cellular bleb." Biophysical journal **94**(5): 1836-1853.

Charras, G. T., C. K. Hu, et al. (2006). "Reassembly of contractile actin cortex in cell blebs." The Journal of cell biology **175**(3): 477-490.

Charras, G. T., T. J. Mitchison, et al. (2009). "Animal cell hydraulics." Journal of cell science **122**(Pt 18): 3233-3241.

Charras, G. T., J. C. Yarrow, et al. (2005). "Non-equilibration of hydrostatic pressure in blebbing cells." Nature **435**(7040): 365-369.

Chen, L., M. Iijima, et al. (2007). "PLA2 and PI3K/PTEN pathways act in parallel to mediate chemotaxis." Developmental cell **12**(4): 603-614.

Christensen, J. E. and A. R. Thomsen (2009). "Co-ordinating innate and adaptive immunity to viral infection: mobility is the key." APMIS : acta pathologica, microbiologica, et immunologica Scandinavica **117**(5-6): 338-355.

Comer, F. I., C. K. Lippincott, et al. (2005). "The PI3K-mediated activation of CRAC independently regulates adenylyl cyclase activation and chemotaxis." Current biology : CB **15**(2): 134-139.

Condeelis, J., R. H. Singer, et al. (2005). "The great escape: when cancer cells hijack the genes for chemotaxis and motility." Annual review of cell and developmental biology **21**: 695-718.

Cooper, M. S. and M. Schliwa (1986). "Motility of cultured fish epidermal cells in the presence and absence of direct current electric fields." The Journal of cell biology **102**(4): 1384-1399.

Coudrier, E., F. Amblard, et al. (2005). "Myosin II and the Gal-GalNAc lectin play a crucial role in tissue invasion by Entamoeba histolytica." Cellular microbiology **7**(1): 19-27.

Cunningham, C. C. (1995). "Actin polymerization and intracellular solvent flow in cell surface blebbing." The Journal of cell biology **129**(6): 1589-1599.

Currie, R. A., K. S. Walker, et al. (1999). "Role of phosphatidylinositol 3,4,5-trisphosphate in regulating the activity and localization of 3-phosphoinositide-dependent protein kinase-1." The Biochemical journal **337 (Pt 3)**: 575-583.

Dai, J. and M. P. Sheetz (1999). "Membrane tether formation from blebbing cells." Biophysical journal **77**(6): 3363-3370.

Danowski, B. A. (1989). "Fibroblast contractility and actin organization are stimulated by microtubule inhibitors." Journal of cell science **93 (Pt 2)**: 255-266.

De la Roche, M. A., J. L. Smith, et al. (2002). "Signaling pathways regulating Dictyostelium myosin II." Journal of muscle research and cell motility **23**(7-8): 703-718.

Diz-Munoz, A., M. Krieg, et al. (2010). "Control of directed cell migration in vivo by membrane-to-cortex attachment." PLoS biology **8**(11): e1000544.

Drayer, A. L. and P. J. van Haastert (1992). "Molecular cloning and expression of a phosphoinositide-specific phospholipase C of Dictyostelium discoideum." The Journal of biological chemistry **267**(26): 18387-18392.

Dumstrei, K., R. Mennecke, et al. (2004). "Signaling pathways controlling primordial germ cell migration in zebrafish." Journal of cell science **117**(Pt 20): 4787-4795.

Eichinger, L., J. A. Pachebat, et al. (2005). "The genome of the social amoeba Dictyostelium discoideum." Nature **435**(7038): 43-57.

Eisenbach, M. and J. W. Lengeler (2004). Chemotaxis. London, UK, Imperial College Press.

Euteneuer, U. and M. Schliwa (1984). "Persistent, directional motility of cells and cytoplasmic fragments in the absence of microtubules." Nature **310**(5972): 58-61.

Fackler, O. T. and R. Grosse (2008). "Cell motility through plasma membrane blebbing." The Journal of cell biology **181**(6): 879-884.

Fink, R. (2007). ASCB Image & Video library, American Society for Cell Biology.

Franco, S. J., M. A. Rodgers, et al. (2004). "Calpain-mediated proteolysis of talin regulates adhesion dynamics." Nature cell biology **6**(10): 977-983.

Friedl, P. and B. Weigelin (2008). "Interstitial leukocyte migration and immune function." Nature immunology **9**(9): 960-969.

Friedl, P. and K. Wolf (2003). "Proteolytic and non-proteolytic migration of tumour cells and leucocytes." Biochemical Society symposium(70): 277-285.

Funamoto, S., R. Meili, et al. (2002). "Spatial and temporal regulation of 3-phosphoinositides by PI 3-kinase and PTEN mediates chemotaxis." Cell **109**(5): 611-623.

Funamoto, S., K. Milan, et al. (2001). "Role of phosphatidylinositol 3' kinase and a downstream pleckstrin homology domain-containing protein in controlling chemotaxis in dictyostelium." The Journal of cell biology **153**(4): 795-810.

Gerald, N., J. Dai, et al. (1998). "A role for Dictyostelium racE in cortical tension and cleavage furrow progression." The Journal of cell biology **141**(2): 483-492.

Grebecki, A. (1994). "Membrane and Cytoskeleton Flow in Motile Cells with Emphasis an the Contribution of Free-Living Amebas." International Review of Cytology - a Survey of Cell Biology, Vol 148 **148**: 37-80.

Haas, P. and D. Gilmour (2006). "Chemokine signaling mediates self-organizing tissue migration in the zebrafish lateral line." Developmental cell **10**(5): 673-680.

Hall, A. L., A. Schlein, et al. (1988). "Relationship of pseudopod extension to chemotactic hormone-induced actin polymerization in amoeboid cells." Journal of cellular biochemistry **37**(3): 285-299.

Han, Y., E. Eppinger, et al. (2009). "Formin-like 1 (FMNL1) is regulated by N-terminal myristoylation and induces polarized membrane blebbing." The Journal of biological chemistry **284**(48): 33409-33417.

Hao, J. J., Y. Liu, et al. (2009). "Phospholipase C-mediated hydrolysis of PIP2 releases ERM proteins from lymphocyte membrane." The Journal of cell biology **184**(3): 451-462.

Haston, W. S. and J. M. Shields (1984). "Contraction waves in lymphocyte locomotion." Journal of cell science **68**: 227-241.

Haugwitz, M., A. A. Noegel, et al. (1994). "Dictyostelium amoebae that lack G-actin-sequestering profilins show defects in F-actin content, cytokinesis, and development." Cell **79**(2): 303-314.

Hitt, A. L., J. H. Hartwig, et al. (1994). "Ponticulin is the major high affinity link between the plasma membrane and the cortical actin network in Dictyostelium." The Journal of cell biology **126**(6): 1433-1444.

Hoeller, O. and R. R. Kay (2007). "Chemotaxis in the absence of PIP3 gradients." Current biology : CB **17**(9): 813-817.

Horiguchi, K., T. Hanada, et al. (2006). "Transport of PIP3 by GAKIN, a kinesin-3 family protein, regulates neuronal cell polarity." The Journal of cell biology **174**(3): 425-436.

Houk, A. R., A. Jilkine, et al. (2012). "Membrane tension maintains cell polarity by confining signals to the leading edge during neutrophil migration." Cell **148**(1-2): 175-188.

Huang, X., E. Czerwinski, et al. (2003). "Purification and properties of the Dictyostelium calpain-like protein, Cpl." Biochemistry **42**(6): 1789-1795.

Hwang, S. M., N. Y. Koo, et al. (2009). "P2X7 Receptor-mediated Membrane Blebbing in Salivary Epithelial Cells." The Korean journal of physiology & pharmacology : official journal of the Korean Physiological Society and the Korean Society of Pharmacology **13**(3): 175-179.

Iijima, M. and P. Devreotes (2002). "Tumor suppressor PTEN mediates sensing of chemoattractant gradients." Cell **109**(5): 599-610.

Insall, R., A. Kuspa, et al. (1994). "CRAC, a cytosolic protein containing a pleckstrin homology domain, is required for receptor and G protein-mediated activation of adenylyl cyclase in Dictyostelium." The Journal of cell biology **126**(6): 1537-1545.

Insall, R. H. (2010). "Understanding eukaryotic chemotaxis: a pseudopod-centred view." Nature reviews. Molecular cell biology **11**(6): 453-458.

Insall, R. H. and L. M. Machesky (2009). "Actin dynamics at the leading edge: from simple machinery to complex networks." Developmental cell **17**(3): 310-322.

Insall, R. H., R. D. Soede, et al. (1994). "Two cAMP receptors activate common signaling pathways in Dictyostelium." Molecular biology of the cell **5**(6): 703-711.

Jacobelli, J., F. C. Bennett, et al. (2009). "Myosin-IIA and ICAM-1 regulate the interchange between two distinct modes of T cell migration." Journal of immunology **182**(4): 2041-2050.

Jaglarz, M. K. and K. R. Howard (1995). "The active migration of Drosophila primordial germ cells." Development **121**(11): 3495-3503.

Jalink, K., W. H. Moolenaar, et al. (1993). "Lysophosphatidic acid is a chemoattractant for Dictyostelium discoideum amoebae." Proceedings of the National Academy of Sciences of the United States of America **90**(5): 1857-1861.

Janetopoulos, C., T. Jin, et al. (2001). "Receptor-mediated activation of heterotrimeric G-proteins in living cells." Science **291**(5512): 2408-2411.

Janetopoulos, C., L. Ma, et al. (2004). "Chemoattractant-induced phosphatidylinositol 3,4,5-trisphosphate accumulation is spatially amplified and adapts, independent of the actin cytoskeleton." Proceedings of the National Academy of Sciences of the United States of America **101**(24): 8951-8956.

Jay, P. Y., P. A. Pham, et al. (1995). "A mechanical function of myosin II in cell motility." Journal of cell science **108 (Pt 1)**: 387-393.

Jia, Z., J. Vadnais, et al. (2006). "Rho/ROCK-dependent pseudopodial protrusion and cellular blebbing are regulated by p38 MAPK in tumour cells exhibiting autocrine c-Met activation." Biology of the cell / under the auspices of the European Cell Biology Organization **98**(6): 337-351.

Jin, T., N. Zhang, et al. (2000). "Localization of the G protein betagamma complex in living cells during chemotaxis." Science **287**(5455): 1034-1036.

Kamimura, Y. and P. N. Devreotes (2010). "Phosphoinositide-dependent protein kinase (PDK) activity regulates phosphatidylinositol 3,4,5-trisphosphate-dependent and -independent protein kinase B activation and chemotaxis." The Journal of biological chemistry **285**(11): 7938-7946.

Kamimura, Y., Y. Xiong, et al. (2008). "PIP3-independent activation of TorC2 and PKB at the cell's leading edge mediates chemotaxis." Current biology : CB **18**(14): 1034-1043.

Kay, R. R., P. Langridge, et al. (2008). "Changing directions in the study of chemotaxis." Nature reviews. Molecular cell biology **9**(6): 455-463.

Kay, R. R. and C. R. Thompson (2009). "Forming patterns in development without morphogen gradients: scattered differentiation and sorting out." Cold Spring Harbor perspectives in biology **1**(6): a001503.

Keller, H. and P. Eggli (1998). "Protrusive activity, cytoplasmic compartmentalization, and restriction rings in locomoting blebbing Walker carcinosarcoma cells are related to detachment of cortical actin from the plasma membrane." Cell motility and the cytoskeleton **41**(2): 181-193.

Keren, K., Z. Pincus, et al. (2008). "Mechanism of shape determination in motile cells." Nature **453**(7194): 475-480.

Kessin, R. H. (2001). Dictyostelium: Evolution, Cell Biology, and the Development of Multicellularity. Cambridge, UK, Cambridge University Press.

Kitzing, T. M., A. S. Sahadevan, et al. (2007). "Positive feedback between Dia1, LARG, and RhoA regulates cell morphology and invasion." Genes & development **21**(12): 1478-1483.

Knecht, D. and K. M. Pang (1995). "Electroporation of Dictyostelium discoideum." Methods in molecular biology **47**: 321-330.

Kotecki, M., A. S. Zeiger, et al. (2010). "Calpain- and talin-dependent control of microvascular pericyte contractility and cellular stiffness." Microvascular research **80**(3): 339-348.

Kumagai, A., J. A. Hadwiger, et al. (1991). "Molecular genetic analysis of two G alpha protein subunits in Dictyostelium." The Journal of biological chemistry **266**(2): 1220-1228.

Kuspa, A. (2006). "Restriction enzyme-mediated integration (REMI) mutagenesis." Methods in molecular biology **346**: 201-209.

Laevsky, G. and D. A. Knecht (2001). "Under-agarose folate chemotaxis of Dictyostelium discoideum amoebae in permissive and mechanically inhibited conditions." BioTechniques **31**(5): 1140-1142, 1144, 1146-1149.

Laevsky, G. and D. A. Knecht (2003). "Cross-linking of actin filaments by myosin II is a major contributor to cortical integrity and cell motility in restrictive environments." Journal of cell science **116**(Pt 18): 3761-3770.

Lammermann, T., B. L. Bader, et al. (2008). "Rapid leukocyte migration by integrin-independent flowing and squeezing." Nature **453**(7191): 51-55.

Lammermann, T. and M. Sixt (2009). "Mechanical modes of 'amoeboid' cell migration." Current opinion in cell biology **21**(5): 636-644.

Langridge, P. D. and R. R. Kay (2006). "Blebbing of Dictyostelium cells in response to chemoattractant." Experimental cell research **312**(11): 2009-2017.

Larochelle, D. A., N. Gerald, et al. (2000). "Molecular analysis of racE function in Dictyostelium." Microscopy research and technique **49**(2): 145-151.

Lauffenburger, D. A. and A. F. Horwitz (1996). "Cell migration: a physically integrated molecular process." Cell **84**(3): 359-369.

Lee, S., F. I. Comer, et al. (2005). "TOR complex 2 integrates cell movement during chemotaxis and signal relay in Dictyostelium." Molecular biology of the cell **16**(10): 4572-4583.

Lorentzen, A., J. Bamber, et al. (2011). "An ezrin-rich, rigid uropod-like structure directs movement of amoeboid blebbing cells." Journal of cell science **124**(Pt 8): 1256-1267.

Luster, A. D. (1998). "Chemokines--chemotactic cytokines that mediate inflammation." The New England journal of medicine **338**(7): 436-445.

Malawista, S. E., A. de Boisfleury Chevance, et al. (2000). "Random locomotion and chemotaxis of human blood polymorphonuclear leukocytes from a patient with leukocyte adhesion deficiency-1: normal displacement in close quarters via chimneying." Cell motility and the cytoskeleton **46**(3): 183-189.

Martin, P. and S. M. Parkhurst (2004). "Parallels between tissue repair and embryo morphogenesis." Development **131**(13): 3021-3034.

Mato, J. M., A. Losada, et al. (1975). "Signal input for a chemotactic response in the cellular slime mold Dictyostelium discoideum." Proceedings of the National Academy of Sciences of the United States of America **72**(12): 4991-4993.

Maugis, B., J. Brugues, et al. (2010). "Dynamic instability of the intracellular pressure drives bleb-based motility." Journal of cell science **123**(Pt 22): 3884-3892.

Meili, R., C. Ellsworth, et al. (2000). "A novel Akt/PKB-related kinase is essential for morphogenesis in Dictyostelium." Current biology : CB **10**(12): 708-717.

Meili, R., C. Ellsworth, et al. (1999). "Chemoattractant-mediated transient activation and membrane localization of Akt/PKB is required for efficient chemotaxis to cAMP in Dictyostelium." The EMBO journal **18**(8): 2092-2105.

Mellor, H. (2010). "The role of formins in filopodia formation." Biochimica et biophysica acta **1803**(2): 191-200.

Merlot, S. and R. A. Firtel (2003). "Leading the way: Directional sensing through phosphatidylinositol 3-kinase and other signaling pathways." Journal of cell science **116**(Pt 17): 3471-3478.

Mitchison, T. J. and L. P. Cramer (1996). "Actin-based cell motility and cell locomotion." Cell **84**(3): 371-379.

Mogilner, A. and K. Keren (2009). "The shape of motile cells." Current biology : CB **19**(17): R762-771.

Mogilner, A. and G. Oster (1996). "Cell motility driven by actin polymerization." Biophysical journal **71**(6): 3030-3045.

Mohandas, N. and E. Evans (1994). "Mechanical properties of the red cell membrane in relation to molecular structure and genetic defects." Annual review of biophysics and biomolecular structure **23**: 787-818.

Morelli, A., P. Chiozzi, et al. (2003). "Extracellular ATP causes ROCK I-dependent bleb formation in P2X7-transfected HEK293 cells." Molecular biology of the cell **14**(7): 2655-2664.

Mortimer, D., T. Fothergill, et al. (2008). "Growth cone chemotaxis." Trends in neurosciences **31**(2): 90-98.

Nguyen, T. N., H. J. Wang, et al. (2000). "Purification and characterization of beta-actin-rich tumor cell pseudopodia: role of glycolysis." Experimental cell research **258**(1): 171-183.

Niebuhr, K., S. Giuriato, et al. (2002). "Conversion of PtdIns(4,5)P(2) into PtdIns(5)P by the S.flexneri effector IpgD reorganizes host cell morphology." The EMBO journal **21**(19): 5069-5078.

Norman, L. L., J. Brugues, et al. (2010). "Cell blebbing and membrane area homeostasis in spreading and retracting cells." Biophysical journal **99**(6): 1726-1733.

Otto, A., H. Collins-Hooper, et al. (2011). "Adult Skeletal Muscle Stem Cell Migration Is Mediated by a Blebbing/Amoeboid Mechanism." Rejuvenation research.

Paluch, E., M. Piel, et al. (2005). "Cortical actomyosin breakage triggers shape oscillations in cells and cell fragments." Biophysical journal **89**(1): 724-733.

Pang, K. M., E. Lee, et al. (1998). "Use of a fusion protein between GFP and an actin-binding domain to visualize transient filamentous-actin structures." Current biology : CB **8**(7): 405-408.

Panupinthu, N., L. Zhao, et al. (2007). "P2X7 nucleotide receptors mediate blebbing in osteoblasts through a pathway involving lysophosphatidic acid." The Journal of biological chemistry **282**(5): 3403-3412.

Parent, C. A., B. J. Blacklock, et al. (1998). "G protein signaling events are activated at the leading edge of chemotactic cells." Cell **95**(1): 81-91.

Parent, C. A. and P. N. Devreotes (1996). "Molecular genetics of signal transduction in Dictyostelium." Annual review of biochemistry **65**: 411-440.

Parikh, A., E. R. Miranda, et al. (2010). "Conserved developmental transcriptomes in evolutionarily divergent species." Genome biology **11**(3): R35.

Petrie, R. J., N. Gavara, et al. (2012). "Nonpolarized signaling reveals two distinct modes of 3D cell migration." The Journal of cell biology **197**(3): 439-455.

Pollard, T. D. and G. G. Borisy (2003). "Cellular motility driven by assembly and disassembly of actin filaments." Cell **112**(4): 453-465.

Postma, M. and P. J. van Haastert (2009). "Mathematics of experimentally generated chemoattractant gradients." Methods in molecular biology **571**: 473-488.

Rappel, W. J. and W. F. Loomis (2009). "Eukaryotic chemotaxis." Wiley interdisciplinary reviews. Systems biology and medicine **1**(1): 141-149.

Raucher, D., T. Stauffer, et al. (2000). "Phosphatidylinositol 4,5-bisphosphate functions as a second messenger that regulates cytoskeleton-plasma membrane adhesion." Cell **100**(2): 221-228.

Raz, E. (2003). "Primordial germ-cell development: the zebrafish perspective." Nature reviews. Genetics **4**(9): 690-700.

Richardson, B. E. and R. Lehmann (2010). "Mechanisms guiding primordial germ cell migration: strategies from different organisms." Nature reviews. Molecular cell biology **11**(1): 37-49.

Ridley, A. J. (2011). "Life at the leading edge." Cell **145**(7): 1012-1022.

Ridley, A. J., M. A. Schwartz, et al. (2003). "Cell migration: integrating signals from front to back." Science **302**(5651): 1704-1709.

Riedl, J., A. H. Crevenna, et al. (2008). "Lifeact: a versatile marker to visualize F-actin." Nature methods **5**(7): 605-607.

Roelofs, J. and P. J. Van Haastert (2002). "Characterization of two unusual guanylyl cyclases from dictyostelium." The Journal of biological chemistry **277**(11): 9167-9174.

Roger, S., P. Pelegrin, et al. (2008). "Facilitation of P2X7 receptor currents and membrane blebbing via constitutive and dynamic calmodulin binding." The Journal of neuroscience : the official journal of the Society for Neuroscience **28**(25): 6393-6401.

Rossy, J., M. C. Gutjahr, et al. (2007). "Ezrin/moesin in motile Walker 256 carcinosarcoma cells: signal-dependent relocalization and role in migration." Experimental cell research **313**(6): 1106-1120.

Roussos, E. T., J. S. Condeelis, et al. (2011). "Chemotaxis in cancer." Nature reviews. Cancer **11**(8): 573-587.

Sahai, E. and C. J. Marshall (2003). "Differing modes of tumour cell invasion have distinct requirements for Rho/ROCK signalling and extracellular proteolysis." Nature cell biology **5**(8): 711-719.

Sasaki, A. T., C. Chun, et al. (2004). "Localized Ras signaling at the leading edge regulates PI3K, cell polarity, and directional cell movement." The Journal of cell biology **167**(3): 505-518.

Schaap, P. (2011). "Evolutionary crossroads in developmental biology: Dictyostelium discoideum." Development **138**(3): 387-396.

Schirenbeck, A., T. Bretschneider, et al. (2005). "The Diaphanous-related formin dDia2 is required for the formation and maintenance of filopodia." Nature cell biology **7**(6): 619-U624.

Schneider, I. C. and J. M. Haugh (2006). "Mechanisms of gradient sensing and chemotaxis: conserved pathways, diverse regulation." Cell cycle **5**(11): 1130-1134.

Sheetz, M. P. (2001). "Cell control by membrane-cytoskeleton adhesion." Nature reviews. Molecular cell biology **2**(5): 392-396.

Sheetz, M. P., J. E. Sable, et al. (2006). "Continuous membrane-cytoskeleton adhesion requires continuous accommodation to lipid and cytoskeleton dynamics." Annual review of biophysics and biomolecular structure **35**: 417-434.

Shina, M. C., A. Muller-Taubenberger, et al. (2011). "Redundant and unique roles of coronin proteins in Dictyostelium." Cellular and molecular life sciences : CMLS **68**(2): 303-313.

Shu, S., X. Liu, et al. (2012). "Actin cross-linking proteins cortexillin I and II are required for cAMP signaling during Dictyostelium chemotaxis and development." Molecular biology of the cell **23**(2): 390-400.

Solnica-Krezel, L. and D. S. Sepich (2012). "Gastrulation: Making and Shaping Germ Layers." Annual review of cell and developmental biology.

Sroka, J., M. von Gunten, et al. (2002). "Phenotype modulation in non-adherent and adherent sublines of Walker carcinosarcoma cells: the role of cell-substratum contacts and microtubules in controlling cell shape, locomotion and cytoskeletal structure." The international journal of biochemistry & cell biology **34**(7): 882-899.

Strassmann, J. E., Y. Zhu, et al. (2000). "Altruism and social cheating in the social amoeba Dictyostelium discoideum." Nature **408**(6815): 965-967.

Swaney, K. F., C. H. Huang, et al. (2010). "Eukaryotic chemotaxis: a network of signaling pathways controls motility, directional sensing, and polarity." Annual review of biophysics **39**: 265-289.

Swanson, J. A. and D. L. Taylor (1982). "Local and spatially coordinated movements in Dictyostelium discoideum amoebae during chemotaxis." Cell **28**(2): 225-232.

Takesono, A., S. J. Heasman, et al. (2010). "Microtubules regulate migratory polarity through Rho/ROCK signaling in T cells." PloS one **5**(1): e8774.

Tarbashevich, K., A. Dzementsei, et al. (2011). "A novel function for KIF13B in germ cell migration." Developmental biology **349**(2): 169-178.

Tessier-Lavigne, M. and M. Placzek (1991). "Target attraction: are developing axons guided by chemotropism?" Trends in neurosciences **14**(7): 303-310.

Tinevez, J. Y., U. Schulze, et al. (2009). "Role of cortical tension in bleb growth." Proceedings of the National Academy of Sciences of the United States of America **106**(44): 18581-18586.

Traynor, D., J. L. Milne, et al. (2000). "Ca(2+) signalling is not required for chemotaxis in Dictyostelium." The EMBO journal **19**(17): 4846-4854.

Trinkaus, J. P. (1973). "Surface activity and locomotion of Fundulus deep cells during blastula and gastrula stages." Developmental biology **30**(1): 69-103.

Tsujioka, M. (2011). "Cell migration in multicellular environments." Development, growth & differentiation **53**(4): 528-537.

Tsujioka, M., K. Yoshida, et al. (2008). "Overlapping functions of the two talin homologues in Dictyostelium." Eukaryotic cell **7**(5): 906-916.

Tyson, R. A., D. B. A. Epstein, et al. (2010). "High Resolution Tracking of Cell Membrane Dynamics in Moving Cells: an Electrifying Approach." Mathematical Modelling of Natural Phenomena **5**(1): 34-55.

van Haastert, P. J., I. Keizer-Gunnink, et al. (2007). "Essential role of PI3-kinase and phospholipase A2 in Dictyostelium discoideum chemotaxis." The Journal of cell biology **177**(5): 809-816.

Veltman, D. M., I. Keizer-Gunnik, et al. (2008). "Four key signaling pathways mediating chemotaxis in Dictyostelium discoideum." The Journal of cell biology **180**(4): 747-753.

Wang, B., G. Shaulsky, et al. (1999). "Multiple developmental roles for CRAC, a cytosolic regulator of adenylyl cyclase." Developmental biology **208**(1): 1-13.

Wang, Y., R. I. Litvinov, et al. (2008). "Loss of PIP5KIgamma, unlike other PIP5KI isoforms, impairs the integrity of the membrane cytoskeleton in murine megakaryocytes." The Journal of clinical investigation.

Wessels, D., D. R. Soll, et al. (1988). "Cell motility and chemotaxis in Dictyostelium amebae lacking myosin heavy chain." Developmental biology **128**(1): 164-177.

Wolf, K., I. Mazo, et al. (2003). "Compensation mechanism in tumor cell migration: mesenchymal-amoeboid transition after blocking of pericellular proteolysis." The Journal of cell biology **160**(2): 267-277.

Wu, L., R. Valkema, et al. (1995). "The G protein beta subunit is essential for multiple responses to chemoattractants in Dictyostelium." The Journal of cell biology **129**(6): 1667-1675.

Yanai, M., C. M. Kenyon, et al. (1996). "Intracellular pressure is a motive force for cell motion in Amoeba proteus." Cell motility and the cytoskeleton **33**(1): 22-29.

Yanase, Y., N. Carvou, et al. (2010). "Reversible bleb formation in mast cells stimulated with antigen is Ca2+/calmodulin-dependent and bleb size is regulated by ARF6." The Biochemical journal **425**(1): 179-193.

Yoshida, K. and K. Inouye (2001). "Myosin II-dependent cylindrical protrusions induced by quinine in Dictyostelium: antagonizing effects of actin polymerization at the leading edge." Journal of cell science **114**(Pt 11): 2155-2165.

Yoshida, K. and T. Soldati (2006). "Dissection of amoeboid movement into two mechanically distinct modes." Journal of cell science **119**(Pt 18): 3833-3844.

Zhang, N., Y. Long, et al. (2001). "Ggamma in dictyostelium: its role in localization of gbetagamma to the membrane is required for chemotaxis in shallow gradients." Molecular biology of the cell **12**(10): 3204-3213.

Zhang, P., Y. Wang, et al. (2010). "Proteomic identification of phosphatidylinositol (3,4,5) triphosphate-binding proteins in Dictyostelium discoideum." Proceedings of the National Academy of Sciences of the United States of America **107**(26): 11829-11834.

Zicha, D., G. A. Dunn, et al. (1991). "A new direct-viewing chemotaxis chamber." Journal of cell science **99 (Pt 4)**: 769-775.

Zigmond, S. H. (1977). "Ability of polymorphonuclear leukocytes to orient in gradients of chemotactic factors." The Journal of cell biology **75**(2 Pt 1): 606-616.